



Flavio Luiz Duarte

**Max-Link Relay Selection Techniques for
Multi-Way Cooperative Multi-Antenna Systems**

Tese de Doutorado

Thesis presented to the Programa de Pós-graduação em Engenharia Elétrica of PUC-Rio in partial fulfillment of the requirements for the degree of Doutor em Engenharia Elétrica.

Advisor: Prof. Rodrigo Caiado de Lamare

Rio de Janeiro
March 2020



Flavio Luiz Duarte

Max-Link Relay Selection Techniques for Multi-Way Cooperative Multi-Antenna Systems

Thesis presented to the Programa de Pós-graduação em Engenharia Elétrica of PUC-Rio in partial fulfillment of the requirements for the degree of Doutor em Engenharia Elétrica. Approved by the Examination Committee.

Prof. Rodrigo Caiado de Lamare

Advisor

Centro de Estudos em Telecomunicações – PUC-Rio

Prof. Lukas Tobias Nepomuk Landau

Centro de Estudos em Telecomunicações – PUC-Rio

Prof. João Terêncio Dias

Centro de Estudos em Telecomunicações – PUC-Rio

Dr. Silvio Fernando Bernardes Pinto

Centro de Estudos em Telecomunicações – PUC-Rio

Prof. Maurício Henrique Costa Dias

Centro Federal de Educação Tecnológica Celso Suckow da
Fonseca – CEFET/RJ

Prof. Pedro Vladimir Gonzalez Castellanos

Universidade Federal Fluminense – UFF

Prof. Bartolomeu Ferreira Uchoa Filho

Universidade Federal de Santa Catarina – UFSC

Rio de Janeiro, March the 4th, 2020

All rights reserved.

Flavio Luiz Duarte

The author graduated in Eletronic Engineering from the Universidade Federal do Rio de Janeiro (UFRJ), Rio de Janeiro - RJ, Brasil, 1999, and received an MSc in Electrical Engineering from Instituto Militar de Engenharia (IME), Rio de Janeiro - RJ, Brasil, 2005.

Bibliographic data

Duarte, Flavio Luiz

Max-Link Relay Selection Techniques for Multi-Way Cooperative Multi-Antenna Systems / Flavio Luiz Duarte; advisor: Rodrigo Caiado de Lamare. – Rio de Janeiro: PUC-Rio, Departamento de Engenharia Elétrica, 2020.

v., 153 f: il. color. ; 30 cm

Tese (doutorado) - Pontifícia Universidade Católica do Rio de Janeiro, Departamento de Engenharia Elétrica.

Inclui bibliografia

1. Engenharia Elétrica – Teses. 2. Comunicações Cooperativas;. 3. Seleção de Repetidores;. 4. Princípio de Máxima Verossimilhança;. 5. Princípio do Erro Quadrático Médio Mínimo;. 6. Max-Link.. I. Lamare, Rodrigo Caiado de. II. Pontifícia Universidade Católica do Rio de Janeiro. Departamento de Engenharia Elétrica. III. Título.

CDD: 621.3

To my dear parents and brother.

Acknowledgments

First, I would like to thank God for successfully completing the PhD degree in Electrical Engineering at Pontifícia Universidade Católica do Rio de Janeiro (PUC-Rio), and also for the innovative ideas used in this Thesis, in particular the "Cloud-Driven" framework.

I would like to thank my dear mother, Lucia Maria Ribeiro de Matos Duarte, for giving me all the support and love I needed to study and improve my knowledge, my dear father, Walter Luiz Duarte Filho, and my dear brother, Diogo Luiz Duarte, graduated in Computer Engineering from the Instituto Militar de Engenharia, with whom I also have discussed some innovative ideas of my own.

I would like to thank my advisor, Prof. Rodrigo Caiado de Lamare, who has always enthusiastically contributed to the success of this work. I must emphasize his high intellectual capacity and his ease of teaching and advising, which helped me a lot to fulfill this mission.

I would like to thank Prof. Lukas Landau, Prof. João Terêncio Dias, Dr. Silvio Fernando Bernardes Pinto, Prof. Pedro Vladimir Gonzalez Castellanos, Prof. Maurício Henrique Costa Dias and Prof. Bartolomeu Ferreira Uchoa Filho, for having agreed to participate in the Examination Committee of this Thesis.

I would like to thank Thiago Elias Bitencourt Cunha, my colleague with also high intellectual capacity, who contributed a lot to the success of this work.

I would like to thank all my colleagues and professors in the Centro de Estudos de Telecomunicações (CETUC/ PUC-Rio).

Moreover, I would like to thank the Brazilian Army, in particular the Instituto Militar de Engenharia (IME), for allowing me to study this Doctorate in Electrical Engineering at PUC-Rio.

This study was financed in part by the Coordenação de Aperfeiçoamento de Pessoal de Nível Superior -Brasil (CAPES) -Finance Code 001.

Abstract

Duarte, Flavio Luiz; Lamare, Rodrigo Caiado de (Advisor). **Max-Link Relay Selection Techniques for Multi-Way Cooperative Multi-Antenna Systems**. Rio de Janeiro, 2020. 153p. Tese de doutorado – Departamento de Engenharia Elétrica, Pontifícia Universidade Católica do Rio de Janeiro.

In wireless networks, signal fading caused by multipath propagation can be mitigated through the use of cooperative diversity [1–3]. In this context, relay selection schemes are key because of their high performance [4–6]. Thus, this thesis is focused on developing relay selection techniques, that uses buffers.

In this work, as a first contribution, we present a switched relaying framework for multiple-input multiple-output (MIMO) relay systems where a source node may transmit directly to a destination node or aided by relays equipped with buffers. In particular, we develop a novel relay selection protocol based on switching and the selection of the best link, denoted as Switched Max-Link, that uses the novel Maximum Minimum Distance (MMD) relay selection criterion.

After that, as a second contribution, we present a relay-selection strategy for multi-way cooperative multi-antenna systems that are aided by a central processor node, where a cluster formed by two users is selected to simultaneously transmit to each other with the help of relays. In particular, we present a novel multi-way relay selection strategy based on the selection of the best link, exploiting the use of buffers and physical-layer network coding (PLNC), that is called Multi-Way Buffer-Aided Max-Link (MW-Max-Link). Moreover, as a third contribution, we present a cloud-driven uplink framework for multi-way multiple-antenna relay systems which aids joint symbol detection in the cloud and where users are selected to simultaneously transmit to each other aided by relays. In particular, we develop a novel multi-way relay selection protocol based on the selection of the best link, exploiting the use of cloud buffers and PLNC, denoted as Multi-Way Cloud-Driven Best-User-Link (MWC-Best-User-Link). An analysis of the proposed and existing techniques in terms of computational cost, pairwise error probability, sum-rate and average delay is carried out. Simulations are then employed to evaluate the performance of these techniques.

Keywords

Cooperative Communications; Relay-Selection; Maximum-Likelihood Principle; Minimum Mean Square Error Principle; Max-Link.

Resumo

Duarte, Flavio Luiz; Lamare, Rodrigo Caiado de. **Técnicas Max-Link de Seleção de Repetidores para Sistemas Cooperativos Multi-Way com Múltiplas Antenas**. Rio de Janeiro, 2020. 153p. Tese de Doutorado – Departamento de Engenharia Elétrica, Pontifícia Universidade Católica do Rio de Janeiro.

Em redes sem fio, o desvanecimento do sinal causado pela propagação por caminhos múltiplos pode ser mitigado através do uso de diversidade cooperativa [1–3]. Neste contexto, esquemas de seleção de repetidores são essenciais por causa de seu alto desempenho [4–6]. Esta tese é focada no desenvolvimento de técnicas de seleção de repetidores, que utilizam *buffers*. Como primeira contribuição, apresentamos uma estrutura de chaveamento para sistemas de repetidores MIMO em que um nó de origem pode transmitir diretamente para um nó de destino ou auxiliado por repetidores. Em particular, apresentamos uma nova técnica de seleção de repetidores baseada no chaveamento e seleção do melhor canal, denominada *Switched Max-Link*, que faz uso do critério de seleção *Maximum Minimum Distance* (MMD).

Como segunda contribuição, apresentamos uma estratégia de seleção de repetidores para sistemas cooperativos de múltiplas antenas que são auxiliados por um nó processador central, em que um *cluster* formado por dois usuários é selecionado para transmitir simultaneamente um ao outro com a ajuda de repetidores. Em particular, apresentamos uma nova estratégia de seleção de repetidores *Multi-Way* com base na seleção do melhor *link*, explorando o uso de *buffers* e codificação de rede em camada física (PLNC), denominada *Multi-Way Buffer-Aided Max-Link* (*MW-Max-Link*).

Como terceira contribuição, apresentamos uma estrutura de *uplink* dirigida por nuvem para sistemas de repetidores *Multi-Way* de múltiplas antenas, que ajuda na detecção conjunta de símbolos na nuvem, onde os usuários são selecionados para transmitir simultaneamente uns aos outros auxiliados por repetidores. Em particular, desenvolvemos um novo protocolo de seleção de repetidores *Multi-Way* com base na seleção do melhor *link*, explorando o uso de *buffers* em nuvem e PLNC, denominado *Multi-Way Cloud-Driven Best-User-Link* (*MWC-Best-User-Link*). É realizada uma análise das técnicas propostas e existentes em termos de custo computacional, probabilidade de erro de pareamento, soma das taxas e atraso médio e simulações são empregadas para avaliar o desempenho dessas técnicas.

Palavras-chave

Comunicações Cooperativas; Seleção de Repetidores; Princípio de Máxima Verossimilhança; Princípio do Erro Quadrático Médio Mínimo; Max-Link.

Table of contents

1	Introduction	16
1.1	Motivation and Problems	16
1.1.1	Contributions	18
1.2	Thesis Outline	20
1.3	Publication List	21
2	Literature Review	22
2.1	Introduction	22
2.2	Overview of Cooperative Relaying	22
2.2.1	System Model	22
2.2.2	Protocols	23
2.2.3	Power Allocation	24
2.2.4	Relay Selection	24
2.3	Advanced Relaying Concepts	30
2.3.1	Physical-Layer Network Coding	30
2.3.2	Two-Way and Multi-Way Relay Channels	31
2.4	MIMO Wireless Communication Systems	33
2.4.1	System Model	34
2.4.2	Advantages of MIMO Systems	35
2.4.3	Capacity	36
2.4.3.1	Channel Capacity for MIMO Communications	36
2.4.3.2	Capacity of random MIMO channels	37
2.4.4	Modulation Schemes	38
2.4.5	Precoding and Related Techniques	39
2.4.6	Receiver Design	41
2.4.6.1	Maximum Likelihood receiver	42
2.4.6.2	Zero-forcing receiver	43
2.4.6.3	Minimum Mean Square Error receiver	44
2.4.6.4	Successive Interference Cancellation (SIC) and Decision Feedback (DF)	45
2.4.7	Computational Complexity	47
2.5	Summary	47
3	Switched Max-Link Relay Selection Based on Maximum Minimum Distance for Cooperative MIMO Systems	49
3.1	Introduction	49
3.1.1	Prior and Related Work	50
3.1.2	Contributions	51
3.2	System Description	52
3.2.1	Assumptions	54
3.2.2	System Model	55
3.3	Principles of Switched Max-Link Relay Selection Based on MMD	57
3.3.1	Principles of Switched Max-Link Relay Selection	57
3.3.2	Calculation of relay selection metric	58

3.3.3	Calculation of the metric for direct transmission	59
3.4	Analysis of MMD: Impact on Relay Selection, PEP, Complexity, Sum-rate and Average Delay	60
3.4.1	Impact of the MMD and QN criteria on relay selection	60
3.4.2	Pairwise Error Probability	64
3.4.3	Computational Complexity	66
3.4.4	Sum-Rate	66
3.4.5	States of buffers, outage probability and throughput	69
3.4.6	Average Delay	71
3.5	Numerical Results	73
3.5.1	Analysis accuracy validation: PEP and BER performance	74
3.5.2	Performance under asymmetric channels	76
3.5.3	Performance for Massive MIMO	80
3.6	Summary	81
4	Buffer-Aided Max-Link Relay Selection for Multi-Way Cooperative Multi-Antenna Systems	84
4.1	Introduction	84
4.2	System Description	85
4.2.1	Assumptions	86
4.2.2	System Model	87
4.3	Proposed MW-Max-Link Relay Selection Scheme	88
4.3.1	Relay selection metric	90
4.3.2	Comparison of metrics and choice of transmission mode	91
4.4	Analysis	92
4.4.1	Pairwise Error Probability	92
4.4.2	Sum-Rate	92
4.4.3	Computational Complexity	94
4.5	Simulation Results	94
4.6	Summary	97
5	Cloud-Driven Multi-Way Multiple-Antenna Relay Systems: Joint Detection, Best-User-Link Selection and Analysis	99
5.1	Introduction	99
5.1.1	Prior and Related Work	100
5.1.2	Contributions	101
5.2	System Description	102
5.2.1	Assumptions	103
5.2.2	System Model	104
5.3	Proposed MWC-Best-User-Link Protocol and Relay Selection Algorithms	107
5.3.1	Relay selection metric for MA and BC modes	109
5.3.2	Choice of the transmission mode	111
5.4	Analysis	112
5.4.1	Pairwise Error Probability	112
5.4.2	Sum-Rate	113
5.4.3	Computational Cost	114
5.4.4	Average Delay	116
5.5	Simulation Results	117
5.5.1	PEP and Sum-Rate performances	118

5.5.2	BER and Average Delay performances with the ML receiver	119
5.5.3	BER and Average Delay performances with the MMSE receiver	121
5.5.4	BER and Sum-Rate performances, for heterogeneous path-loss and time-correlated channels	124
5.6	Summary	125
6	Conclusions and Future Work	126
6.1	Conclusions	126
6.2	Future Work	127
6.2.1	Capacity-Constrained Fronthaul Links	127
6.2.2	Physical-Layer Network Coding	128
6.2.3	Channel Estimation	128
6.2.4	Unmanned Aerial Vehicles and time-correlated channels	129
A	Proof of $\mathcal{D}_{\min}^{MMD} \geq \mathcal{D}_{\min}^{QN}$	146
B	Proof of the minimization of the PEP and of the error in the ML receiver - MMD	149
C	Proof of the Sum-Rate Maximization - CNB	151
D	Proof of minimization of the error in the MMSE receiver - CNB	152

List of figures

Figure 1.1	System model of a cooperative relay system.	18
Figure 2.1	System model of a buffer-aided relaying scheme.	26
Figure 2.2	Constellation diagrams of BPSK, QPSK and 16-QAM modulation schemes with unitary average power.	40
2.2(a)	BPSK	40
2.2(b)	QPSK	40
2.2(c)	16-QAM	40
Figure 2.3	MIMO spatial multiplexing linear detection scheme.	42
Figure 2.4	SIC algorithm.	46
Figure 3.1	System Model of the multiple-antenna buffer-aided relay network.	54
Figure 3.2	The frame of each packet.	55
Figure 3.3	MMD-Max-Link and QN-Max-Link a) PEP performance and b) Computational Complexity.	65
Figure 3.4	Switched Max-Link and Max-Link [40] PEP and BER performances.	74
Figure 3.5	Switched Max-Link and Max-Link [40] a) average throughput and b) average delay.	75
Figure 3.6	a) BER performance for BPSK and b) BER performance for QPSK, with perfect and imperfect channel knowledge.	75
Figure 3.7	BER performance, with low power SD links.	76
Figure 3.8	a) Sum-rate and b) average delay performances, with low power SD links.	77
Figure 3.9	BER performance, with high power SD links.	78
Figure 3.10	a) Sum-rate and b) average delay performances, with high power SD links.	78
Figure 3.11	BER performance, with low power SR or RD links.	79
Figure 3.12	a) Sum-rate and b) average delay performances, with low power SR or RD links.	79
Figure 3.13	a) BER and b) sum-rate performances, for massive MIMO.	80
Figure 4.1	System model of a buffer-aided multi-way relay system.	86
Figure 4.2	The frame of each packet.	87
Figure 4.3	TW-Max-Link [14] and TW-Max-Min [82] PEP performance versus SNR, for BPSK and perfect CSI.	95
Figure 4.4	TW-Max-Link [14] and TW-Max-Min [82] BER performance versus SNR, for QPSK and perfect CSI.	96
Figure 4.5	TW-Max-Link [14] and TW-Max-Min [82] BER performance versus SNR, for BPSK, perfect and imperfect CSI.	96
Figure 4.6	MW-Max-Link, TW-Max-Link [14] and TW-Max-Min [82] BER performance versus SNR, for BPSK, perfect and imperfect CSI.	97

Figure 4.7	MW-Max-Link, TW-Max-Link [14] and TW-Max-Min [82] PEP and Sum-Rate performances versus SNR.	97
Figure 5.1	System model of the proposed cloud-driven multi-way relay scheme.	103
Figure 5.2	The frame of each packet.	105
Figure 5.3	Theoretical PEP performance versus SNR.	113
Figure 5.4	Computational cost.	115
Figure 5.5	PEP and Sum-Rate performances versus SNR.	119
Figure 5.6	BER performance versus SNR, for perfect and imperfect CSI, with the ML receiver.	119
Figure 5.7	BER and Average Delay performances versus SNR, for perfect CSI and symmetric channels, with the ML receiver.	120
Figure 5.8	BER and Average Delay performances versus SNR, for perfect CSI, symmetric and asymmetric channels, with the ML receiver.	121
Figure 5.9	BER performance versus SNR, for perfect and imperfect CSI, with the linear MMSE receiver.	122
Figure 5.10	BER and Average Delay performances versus SNR, for perfect CSI and symmetric channels, with the linear MMSE receiver.	122
Figure 5.11	BER and Average Delay performances versus SNR, for perfect CSI, symmetric and asymmetric channels, with the linear MMSE receiver.	123
Figure 5.12	BER and Sum-Rate performances versus SNR, for homogeneous and heterogeneous path-loss, time-correlated and time-uncorrelated channels.	124
Figure 6.1	System model of a cloud-driven multi-clusters relay system.	128

List of tables

Table 2.1	Computational complexity of some matrix calculations	48
Table 3.1	Description of the symbols	53
Table 3.2	Switched Max-Link Pseudo-Code	82
Table 3.3	Computational Complexity of Criteria	83
Table 4.1	MW-Max-Link Pseudo-Code	89
Table 4.2	MW-Max-Link - Computational Complexity	94
Table 5.1	Multi-Way Cloud-Driven Best-User-Link: pseudo-code of the relay selection algorithms	110
Table 5.2	Computational Cost	115

List of Abbreviations

5G – *5th Generation*
AF – *Amplify and Forward*
ARQ – *Automatic Repeat Request*
AWGN – *Additive White Gaussian Noise*
BER – *Bit Error Rate*
BPSK – *Binary Phase Shift Keying*
BA – *Buffer Aided*
BC – *Broadcast Channel*
BS – *Base Station*
CNB – *Channel Norm Based*
CSI – *Channel State Information*
C-RAN – *Cloud Radio Access Network*
DF – *Decode and Forward*
FD – *Full Duplex*
HD – *Half Duplex*
MA – *Multiple Access*
MMD – *Maximum Minimum Distance*
MIMO – *Multiple-Input Multiple-Output*
ML – *Maximum Likelihood*
MMSE – *Minimum Mean Square Error*
mRC – *Multi-Way Relay Channel*
MW – *Multi-Way*
PEP – *Pairwise Error Probability*
PLNC – *Physical-Layer Network Coding*
QAM – *Quadrature Amplitude Modulation*
QN – *Quadratic Norm*
QPSK – *Quadrature Phase Shift Keying*
RRH – *Remote Radio Head*
SIC – *Successive Interference Cancellation*
SNR – *Signal to Noise Ratio*
TW – *Two-Way*
ZF – *Zero Forcing*

*This is what the Lord says - your Redeemer,
the Holy One of Israel: "I am the Lord your
God, who teaches you what is best for you, who
directs you in the way you should go".*

Isaiah 48:17, *The Holy Bible.*

1

Introduction

This chapter presents the research background and the motivations of this thesis. Additionally, the main contributions are also explained. At last, this chapter outlines the thesis structure to provide access to readers of the state of the art.

1.1

Motivation and Problems

Wireless communications technologies have had a fast evolution in the past three decades. Each new generation of wireless devices has brought considerable improvements in terms of communication reliability, data rates, device sizes, battery life and network connectivity. Moreover, the increasing homogenization of traffic transports using Internet Protocols is leading to network topologies that are less centralized [7]. In recent years, ad-hoc and sensor networks have emerged with many new applications, where a source needs the help from other nodes to forward information to a destination. Ad-hoc wireless networks can be used in natural disasters, military battles and scenarios with limitations of data communications infrastructure and electrical infrastructure [8]. Various wireless devices can form a temporary network without the need for any established infrastructure and centralized management. As a result, the devices cooperate with each other in order to enable communication between distant devices. Such a need of cooperation among nodes or users has inspired new ideas for the design of communications systems by asking whether cooperation can be used to improve system performance [7].

In a wireless channel, many nodes or users can receive transmissions from a source and help to relay information if necessary. We know that the wireless channel is quite dynamic and could experience fading (when a channel is in a severe fading, it is likely to stay in this state for a while). So, when a source cannot reach the destination due to severe fading, it might not be effective to spend transmit power by using repetitive transmission protocols such as ARQ. If another node that receives data from the source could help with a link that is independent from the source–destination link, a successful transmission would be more likely, thereby improving the performance. The key for developing

cooperative schemes with improved performances lies in the advances in multiple-input multiple-output (MIMO) communication technologies. MIMO users must be equipped with multiple transceiver antennas [9, 10], but in practice, most users either do not have multiple antennas installed on small-size devices. To overcome the limitations of achieving MIMO gains in future wireless networks, it is necessary to think of new techniques beyond traditional point-to-point communications [7].

A wireless network system is usually considered as a set of nodes trying to communicate with each other. However, due to the broadcast nature of wireless channels, we may consider these nodes as a set of antennas distributed in the wireless system. By considering this, nodes in the network may cooperate together for distributed transmission and processing of information. A cooperating node can be used as a relay for a source node. As such, cooperative communications can generate independent MIMO-like links between a source and a destination by the introduction of relay channels. Indeed, cooperative communications can be thought of as a generalized MIMO concept with different reliabilities in antenna array elements. It draws from the ideas of using the broadcast nature of the wireless channels to make communicating nodes help each other, implementing the communication in a distributed way, and achieving the same advantages of the MIMO systems. This has brought a lot of new communication techniques that improve communication capacity, speed and performance; reduce battery consumption and extend network lifetime; increase the throughput and stability region for multiple access schemes; expand the transmission coverage area; and provide cooperation tradeoff beyond source-channel coding for multimedia communications [7].

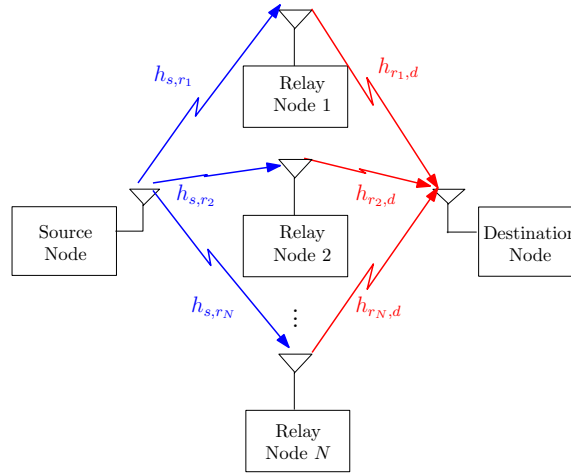


Figure 1.1: System model of a cooperative relay system.

Figure 1.1 shows an example of how cooperative diversity is used in a wireless network. A source node S needs to send messages to a destination node D . The source S needs the assistance of other node(s) (relays), to forward the messages to reach the destination.

1.1.1 Contributions

In this work, we develop in Chapter 3 a switched relaying framework extended for MIMO one-way relay systems that considers direct or cooperative transmissions with Maximum Likelihood (ML) detection and a Switched Max-Link protocol for cooperative MIMO systems, with non reciprocal channels, which selects the best links among N relay nodes and whose preliminary results were reported in [11]. We then consider the novel MMD relay selection criterion [11, 12], which is based on the optimal ML principle and the Pairwise Error Probability (PEP) [11–14], and the existing Quadratic Norm (QN) criterion and devise relay selection algorithms for Switched Max-Link. An analysis of the proposed scheme in terms of PEP, sum-rate, average delay and computational cost is also carried out. Simulations illustrate the excellent performance of the proposed framework, the proposed Switched Max-Link protocol and the MMD-based relay selection algorithm as compared to previously reported approaches.

The main contributions of this work in Chapter 3 can be summarized as:

1. A switched relaying framework extended for MIMO relay systems that considers direct or cooperative transmissions with ML detection;

2. The Switched Max-Link protocol for cooperative MIMO relay systems;
3. The MMD criterion for MIMO relay systems, along with a relay selection algorithm;
4. An analysis of the proposed Switched Max-Link scheme with the MMD relay selection criterion in terms of PEP, sum-rate, average delay and computational cost.

We also propose in Chapter 4 a multi-way Max-Link protocol for buffer-aided cooperative multi-antenna systems (MW-Max-Link) in non reciprocal channels. The proposed MW-Max-Link protocol selects the best channels among Z pairs of users and achieves a diversity gain of $2NZ$. We also extend the MMD criterion [11,12] (used previously in the one-way Switched Max-Link, in Chapter 3) to multi-way systems for selection of relays in the proposed multi-way MW-Max-Link scheme and carry out pairwise error probability (PEP), sum rate and computational complexity analyses.

Therefore, the main contributions in Chapter 4 are:

1. A buffer-aided framework, in which each pair of users has a particular buffer established on demand in the relays;
2. The MW-Max-Link multi-way protocol for cooperative MIMO systems;
3. The MMD relay selection criterion along with a relay selection algorithm;
4. An analysis of the proposed MW-Max-Link scheme in terms of PEP, sum-rate and computational cost.

Moreover, in Chapter 5, with the aim of improving the performance achieved by the multi-way MW-Max-Link protocol (studied previously in Chapter 4) in terms of BER and average delay, we develop a cloud-driven framework and a Multi-Way Best-User-Link (MWC-Best-User-Link) protocol for cooperative MIMO systems, with non reciprocal channels, which selects the best links among K pairs of sources (clusters) and N relay nodes. In order to perform signal detection at the cloud and the nodes, we present maximum likelihood (ML) and linear minimum mean-square error (MMSE) detectors. We then consider the extended MMD [11,12] criterion and a channel-norm based (CNB) criterion and devise relay selection algorithms for MWC-Best-User-Link. Moreover, as MWC-Best-User-Link has only one cloud buffer (instead of buffers in the N relays), its average delay is considerably reduced, keeping a high diversity gain. An analysis of the proposed scheme in terms of PEP, sum-rate, average delay and computational cost is also carried out. Simulations

illustrate the excellent performance of the proposed framework, the proposed MWC-Best-User-Link protocol and the relay selection algorithms as compared to previously reported approaches.

Therefore, the main contributions in Chapter 5 are:

1. A cloud-driven framework with joint detection at the cloud and the nodes;
2. The MWC-Best-User-Link multi-way protocol for cooperative MIMO systems;
3. The MMD and CNB relay selection criteria along with relay selection algorithms;
4. An analysis of the proposed MWC-Best-User-Link scheme in terms of PEP, sum-rate, average delay and computational cost.

1.2

Thesis Outline

The rest of this thesis is structured as follows:

- Chapter 2 presents the literature review.
- Chapter 3 presents the proposed Switched Max-Link relay selection protocol based on Maximum Minimum Distance for One-Way Cooperative MIMO Systems.
- Chapter 4 presents the proposed Buffer-Aided Max-Link relay-selection protocol for Multi-Way Cooperative Multi-Antenna Systems.
- Chapter 5 presents the proposed Cloud-Driven Best-User-Link relay-selection protocol for Multi-Way Cooperative Multi-Antenna Systems.
- Chapter 6 presents the conclusions of this thesis, and suggests directions in which further research could be carried out.

1.3

Publication List

Some of the results in this thesis have been published, or are under review awaiting publication in conferences and journals.

Journal Papers:

1. F. L. Duarte and R. C. de Lamare, "Switched Max-Link Relay Selection Based on Maximum Minimum Distance for Cooperative MIMO Systems," in *IEEE Transactions on Vehicular Technology*, vol. 69, no. 2, pp. 1928-1941, Feb. 2020.
2. F. L. Duarte and R. C. de Lamare, "Buffer-Aided Max-Link Relay Selection for Multi-Way Cooperative Multi-Antenna Systems", in *IEEE Communications Letters*, vol. 23, no. 8, pp. 1423-1426, Aug. 2019.
3. F. L. Duarte and R. C. de Lamare, "Cloud-Driven Multi-Way Multiple-Antenna Relay Systems: Joint Detection, Best-User-Link Selection and Analysis", in *IEEE Transactions on Communications*, 2020, accepted.

Conference Papers:

1. F. L. Duarte and R. C. de Lamare, "Switched Max-Link Buffer-Aided Relay Selection for Cooperative Multiple-Antenna Systems", in SCC 2019; 12th International ITG Conference on Systems, Communications and Coding, Rostock, Germany, 2019, pp. 1-6.
2. F. L. Duarte and R. C. de Lamare, "Cloud-Aided Max-Link Relay Selection for Two-Way Cooperative Multi-Antenna Systems", in 53rd Annual Asilomar Conference on Signals, Systems, and Computers, Asilomar Hotel and Conference Grounds, Pacific Grove, California, 2019, accepted.
3. F. L. Duarte and R. C. de Lamare, "Buffer-Aided Max-Link Relay Selection for Two-Way Cooperative Multi-Antenna Systems", in 16th International Symposium on Wireless Communication Systems (ISWCS), Oulu, Finland, 2019, pp. 288-292.
4. F. L. Duarte and R. C. de Lamare, "Cloud-Driven Multi-Way Multiple-Antenna Relay Systems: Best-User-Link Selection and Joint MMSE Detection", in 45th International Conference on Acoustics, Speech, and Signal Processing (ICASSP 2020), Barcelona, Spain, accepted.
5. F. L. Duarte and R. C. de Lamare, "Cloud-Aided Multi-Way Multiple-Antenna Relaying with Best-User Link Selection and Joint ML Detection", in 24th International ITG Workshop on Smart Antennas (WSA 2020), Hamburg, Germany, accepted.

2

Literature Review

2.1

Introduction

This chapter provides an overview of the research in cooperative communication MIMO systems and the principles and techniques upon which the contents of this thesis are based. We first present some of the main aspects of Cooperative Relaying. Then, system models along with expressions for the capacity of the MIMO system and the sum rates achieved by MIMO systems with deterministic and random channels are also presented. After that, we discuss some system parameters such as modulation schemes and MIMO detection techniques covering the topics of linear filtering, and their computational complexity.

2.2

Overview of Cooperative Relaying

Cooperative relaying is an important technique for wireless communications that increases throughput and extends the coverage of systems. Recently, relays with buffers have been incorporated into cooperative relaying providing extra degrees of freedom in selection and, consequently, improving the outage probability, throughput and reducing the transmit power, at the expense of an increase in packet delay [15]. In this section, we present the system model of a cooperative relay system, review the protocols, power allocation and a number of buffer-aided relay selection strategies and discuss their importance through applications.

2.2.1

System Model

As an example to illustrate the system model of a cooperative relay system, for simplicity, we consider a general relaying scheme with one source node S , one destination node D , and N Half-Duplex relays, R_1, \dots, R_N , as depicted in Fig. 1.1. All nodes are equipped with only one antenna (single-antenna systems). Single relay selection consists of testing all the links and

select the best one, considering a particular criterion. Usually, we may adopt one of three criteria to select the best link: the highest signal to noise ratio, signal to noise and interference ratio or channel power [15]. In a prefixed schedule, in the first time slot, the system operates an uplink transmission (from the source to the selected relay R) and in the consecutive time slot, the system operates a downlink transmission (from the selected relay R to the destination node). Therefore, in the first time slot, the signal sent by S and received at R is given by

$$y_{S,R}[i] = \sqrt{E}h_{S,R}x[i] + n_R[i], \quad (2-1)$$

where E is the average power of the transmitted signal, $x[i]$ is the symbol sent by S , $h_{S,R}$ is the coefficient associated with the propagation effect of the SR channel and n_R is the zero mean additive white complex Gaussian noise (AWGN) at R .

Moreover, in the consecutive time slot the signal sent by R and received at D is given by

$$y_{R,D}[i] = \sqrt{E}h_{R,D}\hat{x}[i] + n_D[i], \quad (2-2)$$

where $\hat{x}[i]$ is a processing information of the symbol sent by S in the early time slot, $h_{R,D}$ is the coefficient associated with the RD channel and n_D is the AWGN at D .

2.2.2 Protocols

Relaying protocols include "amplify-and-forward" (AF), "decode-and-forward" (DF), "compress-and-forward" (CAF) and "compute-and-forward" (CF). The AF strategy allows the relay station to amplify the received signal from the source node and forward it to the destination. By considering AF in (2-2), $\hat{x}[i]$ is an amplification of the the symbol sent by S . On the other hand, relays that follow the DF strategy listen to the source transmissions, decode and forward them to the destination. By considering DF in (2-2), $\hat{x}[i]$ is an estimate of the symbol sent by S . Whenever there are unrecoverable errors in the transmission, the relay can not contribute to cooperative transmission. The CAF strategy allows the relay station to compress the received signal from the source node and forward it to the destination without decoding the signal, in which the Wyner-Ziv encoding can be used for optimum compression.

Moreover, in the CF technique, the relay instead of decoding the transmitted messages from the source, decodes an integer linear combination of these messages and then forwards them to the destination.

2.2.3

Power Allocation

In direct transmissions, all the power is transmitted through the SD channel [7]. On the other hand, in cooperative relaying transmissions with power allocation [16], we determine the optimum powers transmitted by the source and by each relay, which minimize the symbol error rate (SER), minimize the power consumption or maximize the system capacity. The total power transmitted by the source and by the relays is subject to a constraint:

$$E_S + \sum_{n=1}^N E_{R_n} = E. \quad (2-3)$$

Relay selection is the extreme case of power allocation, since the power is allocated to only the source and to the relay selected R_i :

$$E_S + E_{R_i} = E. \quad (2-4)$$

For simplicity, the systems studied and simulated in this work consider the uniform power allocation given by

$$E_S = E_{R_i} = E/2. \quad (2-5)$$

2.2.4

Relay Selection

In wireless networks, signal fading caused by multipath propagation is a channel propagation phenomenon that can be mitigated through the use of cooperative diversity [1–3]. In cooperative communications with multiple relays, where a number of relays help a source in transmitting data packets to a destination, by receiving, processing and forwarding these packets, relay selection schemes are key because of their high performance [4–6]. Relay selection can improve the outage probability and throughput, reduce the transmit power and also extend the coverage of wireless communications systems [15]. In this context, relay schemes have been included in recent/future wireless standards such as Long Term Evolution (LTE) Advanced [17, 18] and 5G standards [19].

In [15], a survey on buffer-aided relay selection is presented, which reviews and classifies various buffer-aided relay selection policies and discuss their importance through applications. Depending on the way a relay performs its reception and transmission, it is called either Full-Duplex (FD) or Half-Duplex (HD). In conventional relaying, using HD and DF protocols, transmission is usually organized in a prefixed schedule with two successive time slots. In the first time slot, the relay receives and decodes the data transmitted from the source, and in the second time slot the relay forwards the decoded data to the destination. Single relay selection schemes use the same relay for reception and transmission, so they are not able to simultaneously exploit the best available source-relay (SR) and relay-destination (RD) channels. The most common schemes are bottleneck based and maximum harmonic mean based best relay selection (BRS) [4]. In this work we only consider the bottleneck based BRS, due to its good performance. To select the best relay, we may consider the highest signal to noise ratio, signal to noise and interference ratio or channel power. Thus, for simplicity, in BRS, considering the highest channel power criterion, the selected relay \hat{R} out of N available relays, has the best bottleneck link, being used for reception and transmission:

$$\hat{R} = \arg \max_{R_i, i \in \{1, \dots, N\}} (\min(|h_{S,R_i}|^2, |h_{R_i,D}|^2)). \quad (2-6)$$

In BRS the source either broadcasts or activates one of the available relays to receive the signal through a selection process that involves the exchange of Channel State Information (CSI) between the relays and the transmitter-receiver pair. After the CSI exchange, an algorithm activates the best relay to help in the end-to-end communication [15]. The selected relay transmits to the destination using one channel, thus reducing the number of channels without losing diversity gain [20]. Thus, a number of BRS protocols have been proposed for optimal relay selection when global (exact or statistical) CSI is available [21,22], or efficient relay selection with a good balance between performance and reduced CSI overhead, when partial CSI is available [23–27].

When a relay is selected to operate in FD, only one channel is used for the end-to-end transmission, as concurrent reception and transmission is performed at the relay [15]. However, the hardware complexity and loop-interference from the relay's output to its input are increased [28–30]. In contrast, by adopting an HD relay, orthogonal channels are used, thus leading to reduced spectral efficiency. Spectral-efficient techniques, as Successive Relaying (SuR), have been proposed to recover the HD loss of conventional relays [31–34]. SuR mimics FD, as while one relay receives the signal transmitted

by the source, another one forwards a previously received signal to the destination [15]. Moreover, SuR suffers from Inter-Relay Interference (IRI) introduced by the simultaneous transmissions. To reduce this degradation and achieve a better performance, efficient IRI mitigation techniques may be adopted [15].

Moreover, the performance of relaying schemes can be improved if the link with the highest power is used in each time slot. This can be achieved via a buffer-aided (BA) relaying protocol, where the relay can accumulate packets in its buffer, before transmitting. Figure 2.1 shows an example of how buffer-aided relaying is used in a wireless network. The use of buffers provides an improved performance and new degrees of freedom for system design [17, 35]. However, it suffers from additional delay that must be well managed for delay-sensitive applications. Buffer-aided relaying protocols require not only the acquisition of CSI, but control of the buffer status. Some possible applications of buffer-aided relaying are: vehicular, cellular, and sensor networks [17].

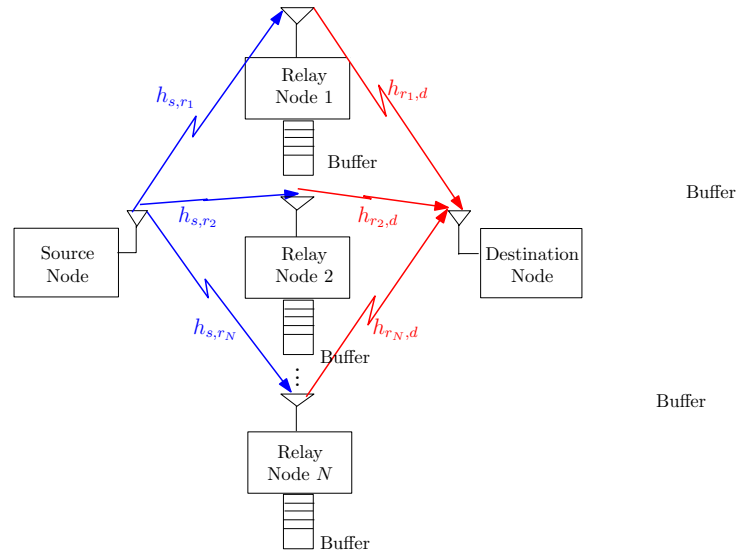


Figure 2.1: System model of a buffer-aided relaying scheme.

Recently, the use of BA relays has been shown to improve the system performance. By storing packets and transmitting them in favorable conditions, the system has its resiliency, throughput and diversity increased [17, 36–38]. In the following, some works on BA relaying are described. In [4] the BRS scheme [20] was extended by using BA relays, leading to more options in the selection process, as relays operate without necessarily having decoded the previous transmitted packet [15]. In Max-Max Relay Selection (MMRS) [4], in the first time slot, the relay selected for reception can store the received packets in its buffer and forward them at a later time when selected for transmission. In

the second time slot, the relay selected for transmission can transmit the first packet in the queue of its buffer, which was received from the source earlier. Thus, in MMRS, considering the highest channel power, the best relay \hat{R}_g for reception is selected based on:

$$\hat{R}_g = \arg \max_{R_i, i \in \{1, \dots, N\}} (|h_{S,R_i}|^2). \quad (2-7)$$

And the best relay \hat{R}_f for transmission is selected according to:

$$\hat{R}_f = \arg \max_{R_i, i \in \{1, \dots, N\}} (|h_{R_i,D}|^2). \quad (2-8)$$

The MMRS protocol assumes infinite buffer sizes. However, considering finite buffer sizes, the buffer of a relay becomes empty if the channel conditions are such that it is selected repeatedly for transmission (and not for reception) or full if it is selected repeatedly for reception (and not for transmission). To overcome this limitation, in [4] a hybrid relay selection (HRS) scheme, that is a combination of BRS and MMRS, was proposed.

Although MMRS and HRS improve the throughput and/or SNR gain as compared to BRS, their diversity gain is limited to N (the number of relays). This can be improved by combining adaptive link selection with MMRS, which results in the buffer-aided Max-Link [39] protocol. The main idea of Max-Link is to select in each time slot the strongest link among all the available SR and RD links (i.e., among $2N$ links) for transmission [15]. For independent and identically distributed (i.i.d.) links and no delay constraints, Max-Link achieves a diversity gain of $2N$, which is twice the diversity gain of BRS and MMRS. Thus, in Max-Link, the selected relay \hat{R} out of $2N$ available links (either for transmission or reception) is based on:

$$\hat{R} = \arg \max_{R_i, i \in \{1, \dots, N\}} (\max(|h_{S,R_i}|^2, |h_{R_i,D}|^2)). \quad (2-9)$$

Max-Link has been extended in [40] to account for direct source-destination (SD) connectivity, which provides resiliency in low transmit SNR conditions [15]. In [41–47], buffer-aided relay selection protocols were shown to improve the Max-Link performance by reducing the average packet delay, ensuring a good diversity gain, and/or achieving full diversity gain with a smaller buffer size as compared to Max-Link. In [41], the outage performance and the average packet delay of a relay system that exploits buffer-aided max-link relay selection are analyzed. In [42], a study of the average packet delay of a buffer-aided scheme that selects a relay node based on both the channel quality and the buffer state of the relay nodes was performed. In [43], the relay associ-

ated with the largest weight is selected among the qualified source-relay and relay-destination links, where each link is assigned with a weight related to the buffer status. In [44], motivated by the Max-Link and the Max-Max protocols, a hybrid buffer-aided cooperative protocol that attains the benefits of reliability and reduced packet delay is reported. In [45], a delay and diversity-aware buffer-aided relay selection policy that reduces the average delay and obtains a good diversity gain is proposed. In [46], a relay selection scheme that seeks to maintain the states of the buffers by balancing the arrival and departure rates at each relay's buffer has been reported. In [47], the best relay node is selected as the link with the highest channel gain among the links within a priority class.

Considering a single relay network, in [48] adaptive link selection for both delay-unconstrained and delay-constrained is proposed. In the first case, an optimal link selection policy is created depending on the exact CSI. In the delay-constrained case, different link activation thresholds as compared to the optimal policy are imposed to empty the relay's buffer and to reduce the maximum number of stored packets [15]. This framework is extended in [49], where adaptive link selection algorithms are proposed for a number of cases of CSI at the Transmitter (CSIT) availability which determines the use of fixed or adaptive transmission rates.

Algorithms with FD characteristics when HD relays are available by advanced SuR [15] are employed to improve the performance of BA relaying, achieving a better spectral efficiency. In [50], MMRS is extended with IRI-free SuR transmissions through isolated relays, leading to full diversity. Moreover, both adaptive and fixed-rate cases are investigated showing that the proposed Space Full-Duplex (SFD) MMRS can achieve twice the capacity of HD schemes for the adaptive rate case and a coding gain for the fixed-rate case. In a similar topology, in [51] the degrading effect of IRI in the selection algorithm is considered, thus presenting a BA Successive Opportunistic Relaying (BA-SOR) algorithm. When interference cancellation (IC) is possible, the algorithm in [51] performs close to the upper-bound provided in [50] where IRI is ignored. However, these relay selection policies depend on exact CSI. Furthermore, in [52] to reduce the communication overhead, the Distributed Switch-and-Stay Combining (DSSC) [23] process has been employed, where the previous set of relays is used again without a new round of CSI exchange when the performance is above a given threshold [15]. Moreover, a hybrid scheme which combines the Max-Link selection of [39] with the BA-SOR relaying of [51] is presented in [53, 54], where switches between BA-SOR and Max-Link are occurring, thus leading to improved throughput and resiliency at the same time.

In [45], delay and diversity issues in BA relay selection have been investigated, in which novel relay selection policies are presented that aim at reducing the average delay by considering the buffer size of the relay nodes into the relay selection process.

Relay selection policies have also been presented for FD BA relays. In [55], HD and FD BA relaying are compared in a network with a single available relay. As FD relays have multiple antennas, a part of the antennas (half, as usual) are used for reception, whereas the rest are used for transmission. In contrast, in HD operations all the antennas are either used for reception or transmission [15]. The HD BA relaying can overcome the throughput performance of FD BA relaying, as long as an extra delay can be tolerated and the number of the antennas at the source and the destination are greater than or equal to that at the relay [15]. In [56], a hybrid BA relaying algorithm integrating Max-Link and FD relaying is presented for a network with one source and multiple BA FD relays, each equipped with two antennas and one destination. The throughput performance is evaluated under the effect of loop-interference, illustrating that when FD relaying cannot support the predefined fixed-rate (usually due to high loop-interference), Max-Link is performed and reduces outages by activating the link with the best SNR [15].

Besides improving the performance of wireless networks, relaying has been employed to achieve increased spectrum reuse through cognitive spectrum access, and to provide physical-layer security when malicious nodes threaten the confidentiality of wireless transmissions [15]. Specifically, in networks where spectrum reuse is the main target, primary networks co-exist with secondary networks accessing through cognitive techniques the available frequency channels [15]. In a number of works, relay selection provides increased chances of reducing the secondary to primary interference when the relay introducing the least amount of interference is selected for reception and transmission [57–59]. Recently, BA relay selection in cognitive networks has led to further performance improvements, since the opportunities to transmit in the secondary network without incurring excessive interference increase because of the buffering capabilities [60,61]. Another important application of relay selection lies in the area of wireless physical-layer security. In networks where eavesdroppers threaten the secrecy of the transmitted signals, selecting the relay that provides the maximum secrecy rate or acting as potential jammer to the eavesdropper has been proven to enhance the reliability of information exchange [62–65]. Thus, BA relay selection increases the possibilities to avoid transmitting through links that are inclined to eavesdropping [66].

More recently, buffer-aided relay selection protocols for cooperative

multiple-antenna systems have been studied. In [67], a virtual full-duplex (FD) buffer-aided relaying to recover the loss of multiplexing gain caused by HD relaying in a multiple relay network through joint opportunistic relay selection (RS) and beamforming (BF), is presented. Moreover, in [68], a cooperative network with a buffer-aided multi-antenna source, multiple HD buffer-aided relays and a single destination is presented to recover the multiplexing loss of the network.

2.3

Advanced Relaying Concepts

In this section, we discuss the Physical-Layer Network Coding (PLNC), in particular the XOR network coding technique, and we also discuss the Two-Way and Multi-Way Relay Channels topologies, where two or more users communicate simultaneously with each other, aided by relays.

2.3.1

Physical-Layer Network Coding

Interference suppression techniques for wireless communications systems have been investigated in the last decades [69]. Unlike traditional techniques that treat interference as something to be mitigated, physical-layer network coding (PLNC) techniques take advantage of the superposition of radio signals and exploit the interference to improve throughput performance [70]. PLNC techniques have generated a number of theoretical and application-oriented studies in the last few years, and are expected to be successfully implemented in future wireless applications [71–77].

PLNC has important advantages in wireless multi-hop networks such as higher sum-rates and enhanced BER performance as compared to standard cooperative techniques [69]. In a context where multiple relay nodes are employed in a network to transmit data from sources to the destination [78], PLNC techniques allow a node to exploit signals that are received simultaneously, rather than treating them as interference [78]. Moreover, instead of decoding each incoming data stream separately, a node detects and forwards a function of the incoming data streams [79]. In this context, there are several network coding techniques, namely, XOR mapping schemes and linear network coding designs [70], [71], [72], [76], [80], [81]. In this thesis, we focus on the use of XOR schemes in Two-Way and Multi-Way relay channels, as explained in the next section.

As an example, by employing PLNC (XOR) in a Two-Way relay system with two sources S_1 and S_2 sending one packet to each other helped by

relays equipped with buffers, it is not necessary to store in the buffer of the selected relay the total of 2 packets transmitted simultaneously by the two sources in the uplink phase, but only the resulting packet (XOR outputs) with the information: "the bit transmitted by S_1 is different (or not) from the corresponding bit sent by S_2 ". The bitwise XOR requires the messages from the two sources to have the same length (i.e., symmetric relaying). Then, we employ the XOR: $v_{[i]} = \hat{x}_1[i] \oplus \hat{x}_2[i]$, for each symbol of the packet, and store the resulting packet in the buffer to be later transmitted to the sources in the downlink phase. In the case of BPSK, if a symbol $\hat{x}_1[i]$ is different from the corresponding $\hat{x}_2[i]$, the XOR output is equal to $+1$, otherwise it is equal to -1 . On the other hand, in the case of QPSK, if the real part of $\hat{x}_1[i]$ is different from the real part of the corresponding $\hat{x}_2[i]$, the output is equal to $+\sqrt{2}/2$, otherwise it is equal to $-\sqrt{2}/2$. Moreover, the same reasoning is applied to the imaginary part of $\hat{x}_1[i]$ and $\hat{x}_2[i]$, but the output is multiplied by j . Then the outputs of these two XOR operations are summed, resulting in another QPSK symbol.

Then, after the downlink transmission (from the selected relay to the sources), at S_1 we compute each symbol transmitted by S_2 by employing again the PLNC (XOR): $\hat{x}_2[i] = x_1[i] \oplus \hat{v}_1[i]$, where $\hat{v}_1[i]$ is the estimation of $v[i]$ at S_1 . The same reasoning is applied at S_2 to compute the symbol transmitted by S_1 : $\hat{x}_1[i] = x_2[i] \oplus \hat{v}_2[i]$, where $\hat{v}_2[i]$ is the estimation of $v[i]$ at S_2 .

2.3.2

Two-Way and Multi-Way Relay Channels

The two-way relay channel is a basic network topology, where two users (S_1 and S_2) exchange independent messages with the help of a common intermediate relay R . It represents ad hoc networks where various nodes share a common relay to communicate and centralized network architectures where terminals transmit their data to a centralized controller [82]. Similarly to the case of one-way relay channel, the incorporation of the two-way relay channel with multiple relay nodes can significantly improve the system performance. Besides, two-way relaying has emerged as a powerful technique to improve the spectral efficiency of wireless networks [83]. In order to adapt to 5G requirements, relaying schemes with high spectrum efficiency, such as two-way, have been recently attracted considerable attention [84]. In Multiple-Access Broadcast Channel (MABC) DF protocols, as in the two-way Max-Min scheme [82] (TW-Max-Min), transmission is organized in a prefixed schedule with two successive phases. In the MA phase, a selected relay receives and decodes the data simultaneously transmitted from two users (S_1 and S_2) and

physical layer network coding (PLNC) may be performed on the decoded data. In the BC phase, the same relay broadcasts the decoded data to the two users. Given that all the channels are reciprocal and fixed during the two phases of the MABC protocol, the TW-Max-Min relay selection protocol [82] achieves a maximum diversity gain. With non reciprocal channels, the performance of relaying schemes can be improved via a buffer-aided relaying protocol, where the relay can accumulate packets in a buffer [35], before transmitting to the destination nodes, as in the one-way Max-Link protocol. Relay selection techniques [82, 85, 89–91] for cooperative systems can improve the performance by maximizing the system sum-rate or reducing the symbol error rate.

The Multi-Way Relay Channel (mRC) [92] includes both a full data exchange model, in which each user receives data from all other users, and the pairwise data exchange model, which is composed by multiple two-way relay channels. The incorporation of the mRC with multiple relays in a system can significantly improve its performance. Considering 5G requirements [84], high spectrum efficiency relaying strategies are key due to their excellent performance. The use of a cloud as a central node can leverage the performance of relay techniques as network operations and services have recently adopted cloud-enabled solutions in communication networks [19, 93].

The mRC has multiple clusters of users in which each user aims to multicast a single message to all the other users in the same cluster [92]. Considering L users in a cluster corresponds to an L -way information exchange among the users in the same cluster. A group of N relays facilitates this exchange, by helping all the users in the system. In particular, the mRC pairwise data exchange model ($L = 2$) is formed by multiple two-way relay channels. With non reciprocal channels, the performance of relaying strategies can be enhanced by adopting buffer-aided protocols, in which the relays are able to accumulate data in their buffers [35, 39], before sending data to the destination, as in the MW-Max-Link [13] protocol for cooperative multi-input multi-output (MIMO) systems, which selects the best links among K pairs of sources (diversity gain equals $2NK$), using the extended MMD relay selection criterion [11]. Furthermore, in [14], the TW-Max-Link protocol (a special case of MW-Max-Link, for a single two-way relay channel ($K = 1$)), also using the extended MMD criterion, was presented. Some other buffer-aided relay selection protocols for cooperative single-antenna and multiple-antenna systems are presented in [67, 68, 94–100]. Moreover, sum-rate maximization is reported for relay selection using two-way protocols, with single-antenna systems [85]. However, multi-way protocols using a channel-norm based with sum-rate maximization criterion, for multiple-antenna systems, or a cloud

(in which each cluster has a particular buffer), have not been previously investigated.

2.4 MIMO Wireless Communication Systems

With the increasing number of smart terminals and their applications, Internet services such as public transport, social media, video and audio streaming, have become very important for our daily life, not only on the traditional wired networks but also on the wireless networks [10]. At this moment, designers face various challenges to develop future wireless communications systems. The demands in terms of data rates and quality of service are increasing exponentially and the radio frequency bandwidth is even more rare and energy efficient systems are needed. The growth demand on higher transmission rates by the increasing number of smart-phones as well as bandwidth-intensive applications and services makes MIMO a key technology for future wireless communication systems [10]. MIMO systems achieve high data rates, increased channel reliability and improve the spectral efficiency in wireless communications systems without the need for additional spectral resources [101]. Some of the technologies which rely on these systems are IEEE 802.11, IEEE 802.16 and IEEE 802.20 [9].

In MIMO systems multiple-antenna elements are deployed at both transmitter and receiver in order to exploit the transmission through different propagation paths. With this strategy, multiple data streams can be transmitted per time slot using the same frequency band [10]. Assuming that there is uncorrelated fading between the different transmission paths, it was shown that MIMO systems increase the channel capacity (i.e. the upper bound on the amount of information that can be reliably transmitted through the channel) by the smallest between the numbers of transmit and receiver antennas in rich scattering environments, and at sufficiently high signal-to-noise (SNR) ratios [102]. This increase in channel capacity can be referred to as multiplexing gain [103].

By using MIMO diversity, two or more versions of the same data are transmitted through independently fading channels, which leads to a smaller probability that all components fade simultaneously. Thus, it improves transmission reliability. On the other hand, the transmission of different parts of the data on different propagation paths is called spatial multiplexing [10]. In this case, the data streams are divided into different independent sub-streams before the transmission, and then they are transmitted simultaneously via sufficiently separated antennas (half of the wavelength or more, to obtain

highly uncorrelated and independent signals). This leads to a considerable increase in the transmission data rate due to the additional data streams. This thesis focuses on MIMO spatial-multiplexing systems in order to meet the high throughput and the energy efficiency requirements of the 5G wireless networks.

2.4.1 System Model

In a general MIMO system model the transmitter is equipped with M_{Tx} transmit antennas and the receiver is equipped with M_{Rx} receive antennas. The received signal vector $\mathbf{y} \in \mathbb{C}^{M_{Rx} \times 1}$ is given by

$$\mathbf{y} = \mathbf{H}\mathbf{x} + \mathbf{n}, \quad (2-10)$$

where the input signal $\mathbf{x} \in \mathbb{C}^{M_{Tx} \times 1}$ is subject to an average power constraint equal to P . The noise vector $\mathbf{n} \in \mathbb{C}^{M_{Rx} \times 1}$ is assumed to be zero-mean circular symmetric Gaussian with covariance matrix $\mathbf{K}_{nn} = \sigma_n^2 \mathbf{I}_{M_{Rx}}$.

If we consider a multiuser MIMO system with K transmitters each equipped with M_{Tx} antennas in the uplink, transmitting simultaneously to a single receiver equipped with $M_{Rx} = M_{Tx}$ receive antennas, the received signal vector $\mathbf{y} \in \mathbb{C}^{M_{Rx} \times 1}$ is given by

$$\mathbf{y} = \sum_{k=1}^K \mathbf{H}_k \mathbf{x}_k + \mathbf{n}, \quad (2-11)$$

where $\mathbf{H}_k \in \mathbb{C}^{M_{Tx} \times M_{Tx}}$ represents the matrix associated with the links between each transmitter k and the single receiver and $\mathbf{x}_k \in \mathbb{C}^{M_{Tx} \times 1}$ is the vector with the symbols sent by the transmitter $k \in \{1, 2, \dots, K\}$.

Moreover, if we consider a multiuser MIMO system with K transmitters, each equipped with M_{Tx} antennas in the uplink, transmitting simultaneously to a single receiver equipped with $M_{Rx} = KUM_{Tx}$ receive antennas, where $U \in \{1, 2, \dots\}$, the received signal vector $\mathbf{y} \in \mathbb{C}^{M_{Rx} \times 1}$ is given by

$$\mathbf{y} = \mathbf{H}\mathbf{x} + \mathbf{n}, \quad (2-12)$$

where $\mathbf{H} \in \mathbb{C}^{KUM_{Tx} \times KM_{Tx}}$ represents the matrix associated with the links between all the K transmitters and the single receiver, \mathbf{x} is the $KM_{Tx} \times 1$ vector with the symbols sent by each transmitter ($\mathbf{x} = [\mathbf{x}_1^T, \mathbf{x}_2^T, \dots, \mathbf{x}_K^T]^T$), and $\mathbf{n} \in \mathbb{C}^{KUM_{Tx} \times 1}$ is the noise vector at the receiver.

2.4.2

Advantages of MIMO Systems

MIMO technique leads to significant benefits for wireless communications. It can improve the system capacity or the link reliability. As multiple antennas are physically separated, the deployment of MIMO creates additional degrees of freedom in the spatial domain which are not present in a single-antenna system [10]. With intelligently designed transceiver and signal processing algorithms, the spatial degrees of freedom due to MIMO can be used to improve the spectral efficiency, eliminate interference, and mitigate channel fading in wireless communication. Some of the advantages of MIMO techniques are described in the following [10]:

- Improve signal quality and link reliability: The transmitter can send multiple copies of a single data stream and then, the probability that at least one of the copies is not under severe fading increases. Thus, the receiver can recover the signal with a lower error rate, improving the system performance.
- Provide higher data throughput: By spatial multiplexing, independent data streams can be simultaneously sent over the same spectrum.
- Increase the covered area or reduce the transmit power: if we consider a receiver with M_{Rx} receive antennas and a transmitter with a single antenna, then the average SNR is approximately M_{Rx} times the SNR of a single-antenna system. Thus, this can increase the coverage area for a fixed transmitted power, or it can reduce the transmitted power for a given coverage area.
- Increase the channel capacity: By transmitting multiple data streams via multiple antennas, MIMO systems can increase the channel capacity by the factor $\min(M_{Tx}, M_{Rx})$ where M_{Tx} is the number of transmit antennas and M_{Rx} is the number of receive antennas, as compared to single-antenna systems [103]. This increase in channel capacity is referred to as multiplexing gain.

The use of MIMO technique provides all these benefits by sharing the same spectrum, without needing additional bandwidth for the wireless system. However, the simultaneous transmission of the multiple data streams can interfere with each other, which makes the detection and the decoding process at the receiver more complicated [10].

2.4.3 Capacity

Capacity is a measure of the maximal transmission rate for which an arbitrarily small error probability can be achieved on a given channel (Shannon's theorem) [9, 104–106]. In this section, we review the capacity of deterministic and random MIMO channels.

2.4.3.1 Channel Capacity for MIMO Communications

The capacity of a deterministic channel is given by the maximum mutual information $I(\mathbf{y}; \mathbf{x})$ between the input \mathbf{x} and the output \mathbf{y} , over all possible distributions for \mathbf{x} that satisfies the power constraint $\text{Tr}(\mathbf{Q}_{xx}) \leq P$, as given by [9, 104, 107]

$$C = \max_{p_{\mathbf{x}}(\mathbf{x})} I(\mathbf{x}; \mathbf{y}), \quad (2-13)$$

where $p_{\mathbf{x}}(\mathbf{x})$ is the probability density function of the transmit signal vector \mathbf{x} and $\mathbf{Q}_{xx} = \mathbb{E}[\mathbf{x}\mathbf{x}^H]$. The mutual information $I(\mathbf{x}; \mathbf{y})$ is related to the average information common to the transmit signal \mathbf{x} and the received signal \mathbf{y} , and can be given by

$$I(\mathbf{x}; \mathbf{y}) = \mathcal{H}(\mathbf{y}) - \mathcal{H}(\mathbf{y}|\mathbf{x}), \quad (2-14)$$

$$= \mathcal{H}(\mathbf{y}) - \mathcal{H}(\mathbf{n}), \quad (2-15)$$

where $\mathcal{H}(\mathbf{y})$ is the differential entropy of the received signal \mathbf{y} , and $\mathcal{H}(\mathbf{y}|\mathbf{x})$ the conditional differential entropy of \mathbf{y} given \mathbf{x} [9, 104, 107]. As the information in \mathbf{y} for known \mathbf{x} can only stem from the noise \mathbf{n} , mutual information in (2-14) has the form (2-15). As the noise vector is assumed to be zero-mean circularly symmetric complex Gaussian with covariance matrix $\mathbf{K}_{nn} = \sigma_n^2 \mathbf{I}_{M_{Rx}}$, the differential entropy $\mathcal{H}(\mathbf{n})$ is given by [9, 104, 107]

$$\mathcal{H}(\mathbf{n}) = \log_2(\det(\pi e \sigma_n^2 \mathbf{I}_{M_{Rx}})). \quad (2-16)$$

The maximization of (2-15) with respect to $p_{\mathbf{x}}(\mathbf{x})$ only concerns the term $\mathcal{H}(\mathbf{y})$ as the noise \mathbf{n} is independent of the sent signal. Thus, the maximization of $I(\mathbf{x}; \mathbf{y})$ results in maximizing $\mathcal{H}(\mathbf{x})$. In [102] the next concept was presented: circularly symmetric complex Gaussian random variables are entropy maximizers. Thus, if \mathbf{x} is a zero mean complex random vector with covariance $\mathbb{E}[\mathbf{x}\mathbf{x}^H] = \mathbf{Q}_{xx}$, we have $\mathcal{H}(\mathbf{x}) \leq \log_2(\pi e \mathbf{Q}_{xx})$ with equality holding if and only if \mathbf{x} has a circularly symmetric complex Gaussian distribution.

Thus, the assumption of Gaussian input signals provides an upper bound on the capacity for discrete input alphabets. Moreover, the received signal \mathbf{y} is zero-mean with covariance $\mathbb{E}[\mathbf{y}\mathbf{y}^H] = \sigma_n^2 \mathbf{I}_{M_{Rx}} + \mathbf{H}\mathbf{Q}_{xx}\mathbf{H}^H$. So, we have

$$\mathcal{H}(\mathbf{y}) \leq \log_2(\det(\pi e(\sigma_n^2 \mathbf{I}_{M_{Rx}} + \mathbf{H}\mathbf{Q}_{xx}\mathbf{H}^H))), \quad (2-17)$$

By substituting (2-16) and (2-17) in (2-15), the expression of the mutual information is given by

$$I(\mathbf{y}; \mathbf{x}) = \log_2(\det(\pi e(\sigma_n^2 \mathbf{I}_{M_{Rx}} + \mathbf{H}\mathbf{Q}_{xx}\mathbf{H}^H))) - \log_2(\det(\pi e\sigma_n^2 \mathbf{I}_{M_{Rx}})) \quad (2-18)$$

$$= \log_2 \left[\det \left(\mathbf{I}_{M_{Rx}} + \frac{\mathbf{H}\mathbf{Q}_{xx}\mathbf{H}^H}{\sigma_n^2} \right) \right]. \quad (2-19)$$

By introducing (2-19) in (2-13) the deterministic capacity is obtained as

$$C = \max_{\text{Tr}(\mathbf{Q}_{xx})=P} \log_2 \left[\det \left(\mathbf{I}_{M_{Rx}} + \frac{\mathbf{H}\mathbf{Q}_{xx}\mathbf{H}^H}{\sigma_n^2} \right) \right]. \quad (2-20)$$

If we consider single-antenna systems (the special case where $M_{Tx} = M_{Rx} = 1$), the instantaneous capacity is given by

$$C = \log_2 \left(1 + |h|^2 \frac{\sigma_x^2}{\sigma_n^2} \right). \quad (2-21)$$

where h is the channel coefficient and $\sigma_x^2 = P$.

Moreover, if we consider a multiuser MIMO system with K transmitters, each equipped with M_{Tx} antennas, transmitting simultaneously to a single receiver equipped with $M_{Rx} = KUM_{Tx}$ receive antennas, where $U \in \{1, 2, \dots\}$, the deterministic uplink capacity is given by (2-20), but $\mathbf{H} \in \mathbb{C}^{KUM_{Tx} \times KM_{Tx}}$ represents the matrix associated with the links between all the K transmitters and the single receiver, and \mathbf{x} is the $KM_{Tx} \times 1$ vector with the symbols sent by each transmitter ($\mathbf{x} = [\mathbf{x}_1^T, \mathbf{x}_2^T, \dots, \mathbf{x}_K^T]^T$), and $\mathbf{I}_{M_{Rx}}$ is an $KUM_{Tx} \times KUM_{Tx}$ identity matrix.

2.4.3.2

Capacity of random MIMO channels

Due to the mobility of the transmitter and also the attributes of the propagation channel, the channel coefficients change randomly over the transmission time and, so, they are not deterministic. Both the fast and slow fading are modelled by the channel matrix \mathbf{H} . The fast fading coefficients are fixed during the transmission of one data packet, they change only in the transition

of a data packet to another one. On the other hand, the slow fading channel coefficients are considered fixed during the transmission of several data packets [10].

As the channel changes randomly, the channel capacity becomes a random variable which is a function of the channel. Thus, the random MIMO channel capacity is obtained by computing the average capacity across time. By assuming that the channel is an ergodic process, the ergodic capacity is defined as the statistical average of the channel capacity with respect to the channel matrix \mathbf{H} [9, 105, 108]. Therefore, the ergodic capacity is given by

$$C_{\text{ergodic}} = \mathbb{E}_{\mathbf{H}} \left\{ \max_{\text{Tr}(\mathbf{Q}_{\mathbf{xx}})=P} \log_2 \left[\det \left(\mathbf{I}_{M_{Rx}} + \frac{\mathbf{H}\mathbf{Q}_{xx}\mathbf{H}^H}{\sigma_n^2} \right) \right] \right\}. \quad (2-22)$$

We consider the special case of a system without CSI at the transmitter and the best strategy in this case is that each antenna transmits with the same average signal power σ_x^2 and the ergodic maximum sum rate is given by

$$C_{\text{ergodic}} = \mathbb{E}_{\mathbf{H}} \left\{ \log_2 \left[\det \left(\mathbf{I}_{M_{Rx}} + \frac{\sigma_x^2}{\sigma_n^2} \mathbf{H}\mathbf{H}^H \right) \right] \right\}. \quad (2-23)$$

If we consider single-antenna systems (the special case where $M_{Tx} = M_{Rx} = 1$), the ergodic maximum sum rate is given by

$$C_{\text{ergodic}} = \mathbb{E}_h \left\{ \log_2 \left(1 + |h|^2 \frac{\sigma_x^2}{\sigma_n^2} \right) \right\}. \quad (2-24)$$

Moreover, if we consider a multiuser MIMO system with K transmitters, each equipped with M_{Tx} antennas, transmitting simultaneously to a single receiver equipped with $M_{Rx} = KUM_{Tx}$ receive antennas, where $U \in \{1, 2, \dots\}$, the ergodic uplink maximum sum rate is given by (2-23), but $\mathbf{H} \in \mathbb{C}^{KUM_{Tx} \times KM_{Tx}}$ represents the matrix associated with the links between all the K transmitters and the single receiver, and \mathbf{x} is the $KM_{Tx} \times 1$ vector with the symbols sent by each transmitter ($\mathbf{x} = [\mathbf{x}_1^T, \mathbf{x}_2^T, \dots, \mathbf{x}_K^T]^T$), and $\mathbf{I}_{M_{Rx}}$ is an $KUM_{Tx} \times KUM_{Tx}$ identity matrix.

2.4.4 Modulation Schemes

Modulation schemes are techniques to carry digital data over analog waveforms to be transmitted on a radio frequency [109]. The modulation scheme maps digital information (sets of one or more bits) onto sine-wave carriers while demodulation reverses this process at the receiver. A group of n

bits of information, where $n = \log_2 m$ and m is denoted as the modulation order [118], are mapped onto symbols that are represented by a complex number in a complex plane. A set of possible symbols of a modulation scheme can be depicted on a two-dimensional graph known as constellation diagram whose axes are denoted as In-phase (real part) and Quadrature (imaginary part). The use of M-ary symbols allow the transmission of an amount of information on the channel $k = \log_2 m$ times faster, keeping the bandwidth used initially. Thus, M-ary modulation schemes are appropriate for higher data rates and results in an efficient bandwidth use [109].

In a digital communication system, information bits are represented by symbols of a constellation diagram and then they are transmitted by radio frequency through a channel that suffers from noise and interference. The goal of the receiver is to demodulate and detect the received signal to recover the transmitted information. Unfortunately, due to the noise, interference and also imperfections in the detection and decoding process, the demodulated symbols are unlikely to be identical to the constellation points. Then, the received symbols are attributed to the closest constellation point by an operator denoted as *slicer*, and the set of bits that were related to that constellation point is the received data bits. In this thesis the slicer operator is denoted as $D(\cdot)$ [10].

In this thesis, we focus on binary phase-shift keying (BPSK), quadrature phase-shift keying (QPSK) and 16 quadrature amplitude modulation (16-QAM) schemes whose constellation diagrams are illustrated in Fig 2.2. In the modulation schemes presented by Fig. 2.2 the Gray code scheme was adopted to map codewords to constellation points. The goal of this scheme is to reduce the number of data bit errors when a symbol detection error occurs. The Gray code consists of encoding each constellation point with a particular codeword, and the adjacent symbols differ in only one bit position [109]. By considering this scheme, each symbol error is most likely to result in only a single bit error.

2.4.5

Precoding and Related Techniques

Let us consider the downlink of a multiuser MIMO system, with a number of antenna elements equal to M_{Tx} at the transmitter, which communicates with K users in the system, where each user is equipped with M_{Rx} antenna elements.

Strategies for mitigating the multiuser interference at the transmitter node [110] in downlink include transmit beamforming [111] and precoding based on linear minimum mean square error (MMSE) [112] or zero-forcing (ZF) [113] approaches and nonlinear techniques such as dirty paper coding (DPC) that performs interference cancellation combined with an implicit user

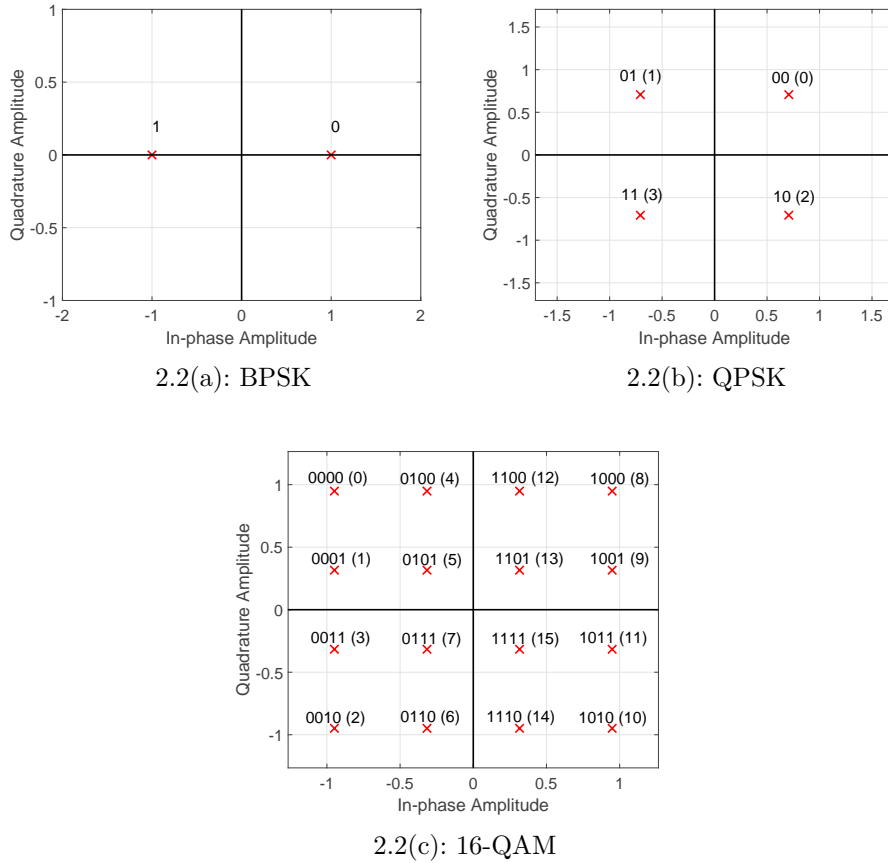


Figure 2.2: Constellation diagrams of BPSK, QPSK and 16-QAM modulation schemes with unitary average power.

scheduling and power loading algorithm [114], Tomlinson-Harashima precoding (THP) [115] and vector perturbation [116].

Transmit matched filtering (TMF) is the simplest method for processing data at the transmitter node and has been recently adopted by a number of works for large-scale MIMO systems [111, 117]. The basic idea is to apply the conjugate of the channel matrix to the data symbol vector $\mathbf{s}[i]$ prior to transmission as given by

$$\mathbf{x}[i] = \mathbf{H}^H \mathbf{s}[i], \quad (2-25)$$

where the $M_{Tx} \times K M_{Rx}$ matrix \mathbf{H}^H contains the parameters of all the links, $\mathbf{s}[i]$ is a $K M_{Rx} \times 1$ vector with the symbols and the $M_{Tx} \times 1$ vector $\mathbf{x}[i]$ represents the information processed by TMF. Linear precoding approaches as ZF and MMSE precoding are based on channel inversion operations and are interesting due to their relative simplicity for MIMO systems with a small to moderate number of antennas [110]. However, channel inversion based precoding requires

a higher average transmit power than other precoding algorithms especially for ill conditioned channel matrices, which could lead to a poor performance [110]. A linear precoder performs a linear transformation to the data symbol vector $\mathbf{s}[i]$ prior to transmission as given by

$$\mathbf{x}[i] = \mathbf{W}_k \mathbf{s}_k[i] + \sum_{l=1, l \neq k}^K \mathbf{W}_l \mathbf{s}_l[i] \quad (2-26)$$

where the $M_{Tx} \times M_{Rx}$ matrix \mathbf{W}_l contains the parameters of the channels and the $M_{Rx} \times 1$ data symbol vectors $\mathbf{s}_k[i]$ represent the data processed by the linear precoder [110]. The linear MMSE precoder is given by $\mathbf{W}_{MMSE} = \mathbf{H}^H (\mathbf{H}\mathbf{H}^H + \frac{\sigma_n^2}{\sigma_x^2} \mathbf{I})^{-1}$ and the linear ZF precoder is given by $\mathbf{W}_{ZF} = \mathbf{H}^H (\mathbf{H}\mathbf{H}^H)^{-1}$ [110].

2.4.6 Receiver Design

Spatial Multiplexing is a promising solution to achieve the higher data rates that are needed in the next generations of wireless systems [10]. In Spatial Multiplexing, different parts of data are transmitted through multiple antennas and these additional data streams result in an increase of the transmission data rate of the system. The data are transmitted through independent data streams and then are linearly combined by a channel with different propagation effects, before arriving at the receiver. The main aim at the receiver is to recover the transmitted data.

The methods used to recover the transmitted data from a received signal are named detection techniques. The main task consists of creating powerful signal processing techniques capable of separating those transmitted signals with an acceptable complexity and desired performance. The main detection methods are filtering, searches or algorithmic processes. Considering perfect CSI at the receiver, a number of strategies such as linear, successive, tree search and the maximum likelihood, can be used to mitigate the effect of the channel and recover the transmitted signals. The linear detection methods are low complex, however, they provide a low performance in comparison to the optimum performance provided by the Maximum Likelihood (ML) detector which is more complex [10]. This detector depends on an exhaustive search which has an exponential complexity in the number of transmit antennas and constellation set size. In order to solve this detection problem we have cost-effective linear detectors. Linear detection techniques estimate each of the transmitted multiplexed data streams as a linear combination of the received signals and present a computational complexity that grows linearly

in the number of antennas [10]. In this case, the basic idea is to recover the transmitted information by linear filtering of the received signal, as illustrated in Fig. 2.3. After the linear filtering, the resulting signals are approximated to the closest constellation points by a slicer. In this section we illustrate the ML, the Zero-Forcing (ZF) and the minimum mean square error (MMSE) detection schemes.

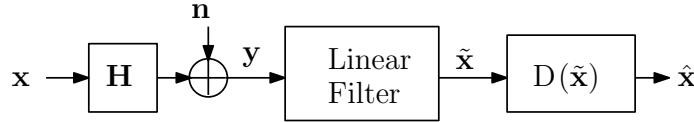


Figure 2.3: MIMO spatial multiplexing linear detection scheme.

2.4.6.1

Maximum Likelihood receiver

The ML receiver is the optimum method to recover the transmitted signal in MIMO systems when the messages are equiprobable [118]. The estimated symbols in this receiver are obtained by exhaustive search that compares all possible transmitted signal vectors to one that maximizes the likelihood function, based on the knowledge of the received vector \mathbf{y} and the channel matrix \mathbf{H} [118]. In most MIMO systems, the noise vector is considered to be white, i.e. $\mathbf{K}_{nn} = \sigma_n^2 \mathbf{I}_{M_{Rx}}$, and then, with the given channel matrix \mathbf{H} , this receiver calculates the Euclidean distance $\mathcal{J}(\mathbf{x}) = \|\mathbf{y} - \mathbf{H}\hat{\mathbf{x}}\|^2$ for each possible transmit signal vector [108]. The signal vector with the smallest Euclidean distance is chosen as the estimate of the transmitted signal vector, as given by

$$\begin{aligned}
 \hat{\mathbf{x}}_{ML} &= \arg \max_{\mathbf{x} \in \mathbb{X}^{M_{Tx}}} P(\mathbf{y}|\mathbf{x}, \mathbf{H}), \\
 &= \arg \max_{\mathbf{x} \in \mathbb{X}^{M_{Tx}}} \frac{1}{(\pi\sigma_n^2)^{M_{Tx}}} \exp\left(-\frac{\|\mathbf{y} - \mathbf{H}\hat{\mathbf{x}}\|^2}{\sigma_n^2}\right), \\
 &= \arg \min_{\mathbf{x} \in \mathbb{X}^{M_{Tx}}} \mathcal{J}(\mathbf{x}), \tag{2-27}
 \end{aligned}$$

where $\mathbb{X}^{M_{Tx}}$ is the set space which contains all possible transmit signal vectors when a total of M_{Tx} transmit antennas is adopted. Although this receiver provides the best performance, its computational complexity scales exponentially higher when the number of transmit antennas or the constellation size increases [119]. Thus, its use is impractical, except for small systems and constellations.

2.4.6.2

Zero-forcing receiver

The aim of the ZF receiver is to reduce the inter-symbol interference (ISI) to zero by pre-multiplying the received signal \mathbf{y} [106] by a conditioning matrix \mathbf{W}_{ZF} that is obtained from the cost function:

$$\begin{aligned}\varepsilon &= \|\mathbf{y} - \mathbf{H}\hat{\mathbf{x}}\|^2, \\ &= (\mathbf{y} - \mathbf{H}\hat{\mathbf{x}})^H(\mathbf{y} - \mathbf{H}\hat{\mathbf{x}}), \\ &= \mathbf{y}\mathbf{y}^H - \mathbf{y}^H\mathbf{H}\hat{\mathbf{x}} - \hat{\mathbf{x}}^H\mathbf{H}^H\mathbf{y} + \hat{\mathbf{x}}^H\mathbf{H}^H\mathbf{H}\hat{\mathbf{x}}.\end{aligned}\quad (2-28)$$

where $\hat{\mathbf{x}}$ represents the estimated transmitted symbols. To find the ZF filter coefficients we calculate the derivative of (2-28) with respect to $\hat{\mathbf{x}}^H$, equate this result to zero and solve for $\hat{\mathbf{x}}^H$, as given by

$$\frac{\partial \varepsilon}{\partial \hat{\mathbf{x}}^H} = -\mathbf{H}^H\mathbf{y} + \mathbf{H}^H\mathbf{H}\hat{\mathbf{x}} = 0, \quad (2-29)$$

whose solution is

$$\hat{\mathbf{x}} = (\mathbf{H}^H\mathbf{H})^{-1}\mathbf{H}^H\mathbf{y} = \mathbf{W}_{ZF}\mathbf{y}, \quad (2-30)$$

where $\mathbf{W}_{ZF} = (\mathbf{H}^H\mathbf{H})^{-1}\mathbf{H}^H = \mathbf{H}^\dagger$ is known as the Moore-Penrose pseudo inverse. This approach ensures that the effects of the propagation channel are forced to zero to totally remove the ISI. However, it does not consider the possibility that some of the loss is caused by noise. Thus, a noise-free environment is the ideal case for adopting the ZF algorithm, although it does not happen in real systems. Thus, in a normal noisy channel, the ZF algorithm performance is limited because of the effects of noise that will tend to be amplified by multiplying the ZF equalizer by the received signal vector \mathbf{y} . This disadvantage is indicated by the error covariance matrix given by

$$\begin{aligned}\mathcal{E}_{ZF} &= \mathbb{E}[(\hat{\mathbf{x}} - \mathbf{x})(\hat{\mathbf{x}} - \mathbf{x})^H] \\ &= \mathbb{E}[(\mathbf{W}_{ZF}\mathbf{y} - \mathbf{x})(\mathbf{W}_{ZF}\mathbf{y} - \mathbf{x})^H] \\ &= \mathbb{E}[(\mathbf{x} + \mathbf{W}_{ZF}\mathbf{n} - \mathbf{x})(\mathbf{x} + \mathbf{W}_{ZF}\mathbf{n} - \mathbf{x})^H] \\ &= \mathbf{W}_{ZF}\mathbb{E}[\mathbf{n}\mathbf{n}^H]\mathbf{W}_{ZF}^H \\ &= \sigma_n^2\mathbf{W}_{ZF}\mathbf{W}_{ZF}^H = \sigma_n^2(\mathbf{H}^H\mathbf{H})^{-1}\mathbf{H}^H\mathbf{H}(\mathbf{H}^H\mathbf{H})^{-1} \\ &= \sigma_n^2(\mathbf{H}^H\mathbf{H})^{-1}\end{aligned}\quad (2-31)$$

The mean squared error (MSE) can be computed by the trace of the error

covariance matrix, then $\text{MSE}_{ZF} = \text{Tr}[\sigma_n^2(\mathbf{H}^H\mathbf{H})^{-1}]$ [119]. Thus, although the ZF detector mitigates the interference between parallel streams, the power of the noise increases which thereby results in bad performance [119]. To mitigate the noise enhancement introduced by the ZF detector, the MMSE detector is presented. In this technique, the noise variance is considered in the designing of the filtering matrix \mathbf{W}_{MMSE} [9, 108, 119].

2.4.6.3

Minimum Mean Square Error receiver

The MMSE technique minimizes the average square error function between the desired signal \mathbf{x} and the estimated signal $\hat{\mathbf{x}} = \mathbf{W}_{MMSE}^H\mathbf{y}$ as given by

$$\mathbf{W}_{MMSE} = \arg \min_{\mathbf{W} \in \mathbb{C}^{M_{Tx} \times M_{Rx}}} \mathbb{E}[\|\mathbf{x} - \mathbf{W}^H\mathbf{y}\|^2], \quad (2-32)$$

where M_{Tx} and M_{Rx} represents the total transmit and receive antennas of the system, respectively.

A solution of this problem is also given by setting the partial derivative of the cost function with respect to \mathbf{W}^H , equating the derivatives to zero and solving for \mathbf{W} :

$$\begin{aligned} \frac{\partial \varepsilon}{\partial \mathbf{W}^H} \mathbb{E}[\text{Tr}[(\mathbf{x} - \mathbf{W}^H\mathbf{y})(\mathbf{x} - \mathbf{W}^H\mathbf{y})^H]]] &= \\ \frac{\partial \varepsilon}{\partial \mathbf{W}^H} \mathbb{E}[\text{Tr}[\mathbf{xx}^H - \mathbf{xy}^H\mathbf{W} - \mathbf{W}^H\mathbf{yx}^H + \mathbf{W}^H\mathbf{yy}^H\mathbf{W}]] &= \\ \frac{\partial \varepsilon}{\partial \mathbf{W}^H} \text{Tr}[\mathbf{R}_{xx} - \mathbf{R}_{xy}\mathbf{W} - \mathbf{W}^H\mathbf{R}_{xy}^H + \mathbf{W}^H\mathbf{R}_{yy}\mathbf{W}] &= \\ = \mathbf{R}_{yy}\mathbf{W} - \mathbf{R}_{xy}^H &= 0, \end{aligned} \quad (2-33)$$

leading to the well-known Wiener-Hopf [106, 120, 121] solution:

$$\mathbf{W}_{MMSE} = \mathbf{R}_{yy}^{-1}\mathbf{R}_{xy}^H \quad (2-34)$$

To determine the cross-correlation matrix \mathbf{R}_{xy} and the autocorrelation matrix \mathbf{R}_{yy} some considerations from the MIMO model are adopted. First, both the AWGN and the transmitted symbols are i.i.d, complex circular symmetric Gaussian random variables with zero mean and respective variances σ_n^2 and σ_x^2 . Moreover, the data symbols are considered statistically independent

of the noise samples. It results in the next equations:

$$\mathbf{K}_{nn} = \mathbb{E}[\mathbf{nn}^H] = \sigma_n^2 \mathbf{I}_{M_{Rx}}, \quad (2-35)$$

$$\mathbf{R}_{xx} = \mathbb{E}[\mathbf{xx}^H] = \sigma_x^2 \mathbf{I}_{M_{Tx}}, \quad (2-36)$$

$$\mathbf{R}_{xn} = \mathbb{E}[\mathbf{xn}^H] = \mathbf{0}. \quad (2-37)$$

With these results the autocorrelation matrix of the received signal can be calculated by

$$\mathbf{R}_{yy} = \mathbb{E}[\mathbf{yy}^H] = \sigma_x^2 \mathbf{H}\mathbf{H}^H + \sigma_n^2 \mathbf{I}_{M_{Rx}}, \quad (2-38)$$

and the crosscorrelation matrix between the transmitted signal and the received signal by

$$\mathbf{R}_{xy} = \mathbb{E}[\mathbf{xy}^H] = \sigma_x^2 \mathbf{H}^H \quad (2-39)$$

Inserting (2-38) and (2-39) in (2-34), we obtain the MMSE receive filter

$$\begin{aligned} \mathbf{W}_{MMSE} &= (\sigma_x^2 \mathbf{H}\mathbf{H}^H + \sigma_n^2 \mathbf{I}_{M_{Rx}})^{-1} \sigma_x^2 \mathbf{H} \\ &= (\mathbf{H}\mathbf{H}^H + \frac{\sigma_n^2}{\sigma_x^2} \mathbf{I}_{M_{Rx}})^{-1} \mathbf{H}. \end{aligned} \quad (2-40)$$

By analyzing the result in (2-40), we conclude that both MMSE and ZF receive filters have similarities, except for the MMSE that incorporates the variance of the noise. The addition of the noise variance improves the accuracy of the MMSE receiver at low SNR values. However, as the SNR grows large, then $\sigma_n \rightarrow 0$ and the MMSE receive filter converges to the ZF receive filter.

2.4.6.4

Successive Interference Cancellation (SIC) and Decision Feedback (DF)

SIC is a nonlinear technique in which the received symbols are detected sequentially, that provides a better performance than linear approaches. However, the SIC detection technique presents a higher computational complexity and also has a more complex hardware implementation than linear approaches [10]. This scheme consists of decoding one data stream at each step and subtracting its contribution from the received signal to improve the accuracy of detection of the remaining data streams [10]. At each iteration, one reference data stream is decoded and the other streams are considered as interference. The interference from the decoded stream is then subtracted from the vector of received symbols, leading to a modified received vector in which fewer interferences are present. At the next iteration, the selected stream is

decoded with one less interference [101, 108, 122]. With this scheme SIC can achieve a higher signal to interference plus noise ratio (SINR) of the remaining data symbols, and then improve the BER performance in MIMO systems [10]. The generation of the filtering matrix can still be based on the linear filters, such as ZF or MMSE. Table 1 and Figure 2.4 illustrate the algorithm adopted for the SIC scheme.

Algorithm 1 MMSE-SIC Detection Algorithm

- 1: $\mathbf{x} \in \mathbb{C}^{M_{Tx} \times 1}$ whose entries $\in \{\text{BPSK, QPSK, 16-QAM, } \dots\}$.
 - 2: $\mathbf{n} \in \mathbb{C}^{M_{Rx} \times 1}$ whose entries are $\left(\frac{\sigma_n}{\sqrt{2}}\right) \mathcal{CN}(0, 1)$;
 - 3: $\mathbf{y}_1 = \mathbf{H}\mathbf{x} + \mathbf{n}$;
 - 4: $\mathbf{W} = (\mathbf{H}\mathbf{H}^H + \frac{\sigma_n^2}{\sigma_x^2} \mathbf{I}_{M_{Rx}})^{-1} \mathbf{H}$;
 - 5: **for** $i = 1$ to M_{Tx} **do**
 - 6: $\hat{\mathbf{x}}_i = \mathbf{W}^H(i, :) \mathbf{y}_i$;
 - 7: $\tilde{\mathbf{x}}_i = \text{D}(\hat{\mathbf{x}}_i)$;
 - 8: $\mathbf{y}_{i+1} = \mathbf{y}_i - \tilde{\mathbf{x}}_i \mathbf{H}(:, i)$;
 - 9: $\mathbf{H}(:, i) = \mathbf{0}$;
 - 10: $\mathbf{W} = (\mathbf{H}\mathbf{H}^H + \frac{\sigma_n^2}{\sigma_x^2} \mathbf{I}_{M_{Rx}})^{-1} \mathbf{H}$;
 - 11: **end for**
-

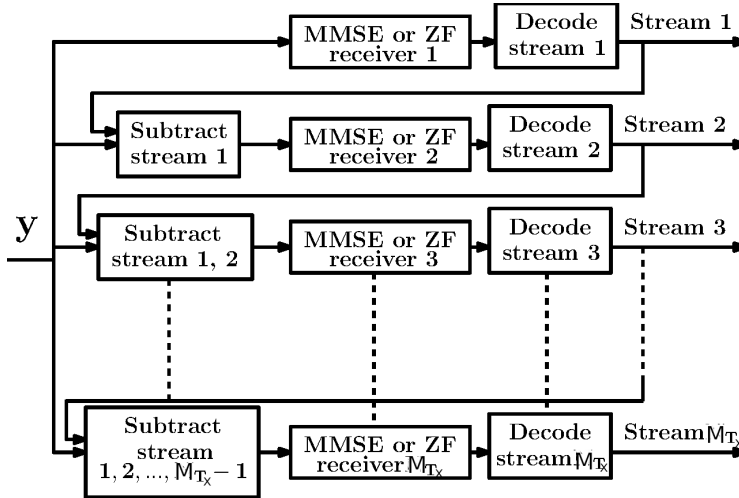


Figure 2.4: SIC algorithm.

However, all SIC techniques suffer from error propagation [10]. One error in earlier computed steps impairs the consecutive estimates. Thus, it is necessary to detect reliable signals in the previous steps to avoid error propagation. Therefore, detection nulling and cancellation order (NCO) has an important influence on the performance of SIC techniques [10]. A popular technique to improve performance of the SIC detector is ranking the data streams based on certain reliability measure. One well-known algorithm is named Vertical-Bell Laboratories Layered Space-Time (V-BLAST), whose

detection is ordered by the signal-to-noise ratio (SNR) and the estimators are based on MMSE or ZF [9]. This algorithm detects data symbols with the highest SNR, and then cancels out its effect on the remaining data streams improving the BER in MIMO systems [10].

Decision-driven detection algorithms such as SIC techniques and decision feedback (DF) [123] detectors are strategies that can offer interesting trade-offs between performance and complexity [110]. Prior work on SIC and DF schemes has been reported with DF detectors with SIC (S-DF) [123, 124] and DF receivers with parallel interference cancellation (PIC) (PDF) [125, 126], combinations of these schemes [125, 127, 128] and mechanisms to reduce error propagation [129, 130]. DF detectors [123–125] employ feedforward and feedback matrices that can be based on the receive matched filter (RMF), ZF and MMSE designs [110] as given by

$$\hat{\mathbf{s}} = Q(\mathbf{W}\mathbf{r}[i] - \mathbf{F}^H\hat{\mathbf{s}}_0), \quad (2-41)$$

where $\hat{\mathbf{s}}_0$ represents the initial decision vector that is usually performed by the linear section of the DF receiver (e.g., $\hat{\mathbf{s}}_0 = Q(\mathbf{W}^H\mathbf{r})$) prior to the application of the feedback section. The receive filters \mathbf{W} and \mathbf{F} can be computed using design criteria and optimization algorithms [110].

2.4.7

Computational Complexity

The goal of detection strategies in MIMO systems is to detect the information that was transmitted with the highest accuracy and also with the lowest possible computational cost [10]. The complexity is an evaluation to estimate the computational cost of an algorithm. This evaluation can be calculated through the total complex additions and multiplications that are required to run the algorithm. Some examples of computational complexities achieved by some matrix operations are illustrated in Table 2.1. This table will be adopted as a reference to calculate the computational complexity of the algorithms that are presented in this thesis.

2.5

Summary

In this chapter we have provided an overview of the research in cooperative MIMO systems and the principles and techniques upon which the contents of this thesis are based. Some of the main aspects of cooperative relaying and system models along with expressions for the capacity of the MIMO system

Table 2.1: Computational complexity of some matrix calculations

Task	Additions	Multiplications
$\underbrace{\mathbf{H}}_{n \times m} \underbrace{\mathbf{G}}_{m \times n}$	$n^2(m-1)$	n^2m
$\underbrace{\mathbf{H}}_{n \times m} \underbrace{\mathbf{g}}_{m \times 1}$	$n(m-1)$	nm
$\underbrace{\mathbf{H}}_{n \times n} \underbrace{\mathbf{G}}_{n \times m}$	$m(n^2 - n)$	n^2m
$\underbrace{\mathbf{H}}_{n \times m} \odot \underbrace{\mathbf{G}}_{n \times m}$	0	nm
$\underbrace{\mathbf{H}}_{n \times m} + \underbrace{\mathbf{G}}_{n \times m}$	nm	0
$\underbrace{\mathbf{H}^{-1}}_{n \times n}$	$\mathcal{O}(n^3)$	$\mathcal{O}(n^3)$

and the sum rates achieved with deterministic and random channels were presented. We also have discussed some important system parameters such as modulation schemes and MIMO detection techniques covering the topics of linear filtering, and their computational complexity.

3

Switched Max-Link Relay Selection Based on Maximum Minimum Distance for Cooperative MIMO Systems

In this chapter, we present a switched relaying framework for multiple-input multiple-output (MIMO) relay systems where a source node may transmit directly to a destination node or aided by relays. We also investigate relay selection techniques for the proposed switched relaying framework, whose relays are equipped with buffers. In particular, we develop a novel relay selection protocol based on switching and the selection of the best link, denoted as Switched Max-Link. We then propose the Maximum Minimum Distance (MMD) relay selection criterion for MIMO systems, which is based on the optimal Maximum Likelihood (ML) principle and can provide significant performance gains over other criteria, along with algorithms that are incorporated into the proposed Switched Max-Link protocol. An analysis of the proposed Switched Max-Link protocol and the MMD relay selection criterion in terms of computational cost, pairwise error probability, sum-rate and average delay is carried out. Simulations show that Switched Max-Link using the MMD criterion outperforms previous works in terms of sum-rate, pairwise error probability, average delay and bit error rate.

3.1

Introduction

In wireless networks, signal fading caused by multipath propagation is a channel propagation phenomenon that can be mitigated through the use of cooperative diversity [1–3]. In cooperative communications with multiple relays, where a number of relays help a source to transmit data packets to a destination, by receiving, decoding and forwarding these packets, relay selection schemes are key because of their high performance [4–6]. As cooperative communication can improve the throughput and extend the coverage of wireless communications systems, the task of relay selection serves as a building block to realize it. In this context, relay schemes have been included in recent/future wireless standards such as Long Term Evolution (LTE) Advanced [17, 18] and 5G standards [19].

3.1.1 Prior and Related Work

In conventional relaying, using half duplex (HD) and decode-and-forward protocols, transmission is often organized in a prefixed schedule with two successive time slots. In the first time slot, the relay receives and decodes the data transmitted from the source, and in the second time slot the relay forwards the decoded data to the destination. Single relay selection schemes use the same relay for reception and transmission, and cannot simultaneously exploit the best available source-relay (SR) and relay-destination (RD) channels. The most common schemes are bottleneck based and maximum harmonic mean based best relay selection (BRS) [4].

The performance of relaying schemes can be improved if the link with the highest power is used in each time slot. This can be achieved via a buffer-aided relaying protocol, where the relay can accumulate packets in its buffer prior to transmission. The use of buffers provides an improved performance and extra degrees of freedom for system design [17,35]. However, it suffers from additional delay that must be well managed for delay-sensitive applications. Buffer-aided relaying protocols require not only the acquisition of channel state information (CSI), but control of the buffer status. Applications of buffer-aided relaying are: vehicular, cellular, and sensor networks [17].

In Max-Max Relay Selection (MMRS) [4], in the first time slot, the relay selected for reception can store the received packets in its buffer and forward them at a later time when selected for transmission. In the second time slot, the relay selected for transmission can transmit the first packet in the queue of its buffer, which was received from the source earlier. MMRS assumes infinite buffer sizes. However, considering finite buffer sizes, the buffer of a relay becomes empty if the channel conditions are such that it is selected repeatedly for transmission (and not for reception) or full if it is selected repeatedly for reception (and not for transmission). To overcome this limitation, in [4] a hybrid relay selection (HRS) scheme, which is a combination of BRS and MMRS, was proposed.

Although MMRS and HRS improve the throughput and/or SNR gain as compared to BRS, their diversity gain is limited to the number of relays N . This can be improved by combining adaptive link selection with MMRS, which results in the Max-Link [39] protocol. The main idea of Max-Link is to select in each time slot the strongest link among all the available SR and RD links (i.e., among $2N$ links) for transmission [15]. For independent and identically distributed (i.i.d.) links and no delay constraints, Max-Link achieves a diversity gain of $2N$, which is twice the diversity gain of BRS and MMRS.

Max-Link has been extended in [40] to account for direct source-destination (SD) connectivity, which provides resiliency in low transmit SNR conditions [15]. In [41–47], buffer-aided relay selection protocols were shown to improve the Max-Link performance by reducing the average packet delay, ensuring a good diversity gain, and/or achieving full diversity gain with a smaller buffer size as compared to Max-Link. In [41], the outage performance and the average packet delay of a relay system that exploits buffer-aided max-link relay selection are analyzed. In [42], a study of the average packet delay of a buffer-aided scheme that selects a relay node based on both the channel quality and the buffer state of the relay nodes was performed. In [43], the relay associated with the largest weight is selected among the qualified source-relay and relay-destination links, where each link is assigned with a weight related to the buffer status. In [44], motivated by the Max-Link and the Max-Max protocols, a hybrid buffer-aided cooperative protocol that attains the benefits of reliability and reduced packet delay is reported. In [45], a delay and diversity-aware buffer-aided relay selection policy that reduces the average delay and obtains a good diversity gain is proposed. In [46], a relay selection scheme that seeks to maintain the states of the buffers by balancing the arrival and departure rates at each relay's buffer has been reported. In [47], the best relay node is selected as the link with the highest channel gain among the links within a priority class. In summary, the previous schemes (MMRS, HRS and Max-Link) only use buffer-aided relay selection for cooperative single-antenna systems.

More recently, buffer-aided relay selection protocols for cooperative multiple-antenna systems have been studied. In [67], a virtual full-duplex (FD) buffer-aided relaying to recover the loss of multiplexing gain caused by HD relaying in a multiple relay network through joint opportunistic relay selection (RS) and beamforming (BF), is presented. Moreover, in [68], a cooperative network with a buffer-aided multi-antenna source, multiple HD buffer-aided relays and a single destination is presented to recover the multiplexing loss of the network.

3.1.2 Contributions

In this chapter, we develop a switched relaying framework extended for MIMO relay systems that considers direct or cooperative transmissions with Maximum Likelihood (ML) detection and a Switched Max-Link protocol for cooperative MIMO systems, with non reciprocal channels, which selects the best links among N relay nodes and whose preliminary results were reported in [11]. We then consider the novel MMD relay selection criterion [11], which

is based on the optimal ML principle and the Pairwise Error Probability (PEP) [11, 13, 14], and the existing Quadratic Norm (QN) criterion and devise relay selection algorithms for Switched Max-Link. An analysis of the proposed scheme in terms of PEP, sum-rate, average delay and computational cost is also carried out. Simulations illustrate the excellent performance of the proposed framework, the proposed Switched Max-Link protocol and the MMD-based relay selection algorithm as compared to previously reported approaches. The main contributions of this work can be summarized as:

1. A switched relaying framework extended for MIMO relay systems that considers direct or cooperative transmissions with ML detection;
2. The Switched Max-Link protocol for cooperative MIMO relay systems;
3. The MMD criterion for MIMO relay systems, along with a relay selection algorithm;
4. An analysis of the proposed Switched Max-Link scheme with the MMD relay selection criterion in terms of PEP, sum-rate, average delay and computational cost.

Table 3.1 shows the description of the main symbols adopted in this work.

This chapter is structured as follows. Section 3.2 describes the system model and the main assumptions made. Section 3.3 details the proposed Switched Max-Link protocol with the MMD relay selection criterion whereas Section 3.4 analyzes it. Section 3.5 illustrates and discusses the numerical results whereas Section 3.6 gives the concluding remarks.

3.2 System Description

We consider a multiple-antenna relay network with one source node, S , one destination node, D , and N half-duplex decode-and-forward (DF) relays, R_1, \dots, R_N . The S and D nodes have M_S antennas for transmission and reception, respectively, and each relay $M_R = UM_S$ antennas, where $U \in \{1, 2, 3, \dots\}$. All the M_R antennas are used for reception ($M_{R_{rx}} = M_R$) and a set of M_S antennas is selected among M_R to be used for transmission ($M_{R_{tx}} = M_S$). Thus, this configuration forms a spatial multiplexing network, in which the channel matrices are square or formed by multiple square submatrices. Each relay is equipped with a buffer, whose size is J packets and the transmission is organized in time slots [4]. This configuration is considered for simplicity. The considered system is shown in Fig. 3.1.

Table 3.1: Description of the symbols

Symbols	Description
D	Destination node
\mathcal{D}	MMD metric
\mathcal{D}_{\min}	Minimum distance
\mathcal{D}'_{\min}	Minimum value of the PEP argument
d_c	Distances between the constellation symbols
$E[d_n]^{MMD}$	Average delay of the MMD-Max-Link protocol
$E[d_n]^{SML}$	Average delay of the Switched Max-Link protocol
$E[L_n]$	Average queue length
E_S	Energy transmitted from S
E_{R_j}	Energy transmitted from R_j
$E[T_n]$	Average throughput of a relay
$\mathbf{H}_{S,D}$	Matrix of SD links
\mathbf{H}_{S,R_k}	Matrix of SR_k links
\mathbf{H}_{S,R_k}^u	Submatrix of SR_k links
$\mathbf{H}_{R_j,D}$	Matrix of R_jD links
$\mathbf{H}_{R_j,D}^u$	Submatrix of R_jD links
J	Size of the buffer (in packets)
L	Queue length
M_S	Number of antennas at S and D
M_R	Number of antennas at the relays
N	Number of relays
N_s	Number of constellation symbols
N_0	Power spectral density of the AWGN
\mathbf{n}_D	AWGN at D
\mathbf{n}_{R_k}	AWGN at R_k
P_{ML}^S	Probability of operating in the Max-Link mode
\mathcal{Q}	QN metric
$\mathbf{Q}_{S,D}$	Covariance matrix of the transmitted symbols (for SD)
\mathbf{Q}_{S,R_k}	Covariance matrix of the transmitted symbols (for SR_k)
$\mathbf{Q}_{R_j,D}$	Covariance matrix of the transmitted symbols (for R_jD)
R_k	Relay selected for reception
R_j	Relay selected for transmission
\mathcal{R}	Sum-Rate
S	Source node
\mathcal{S}	Switch of the Switched Max-Link protocol
U	Number of sets of M_S antennas at the relays
\mathbf{x}	Vector of transmitted symbols
$\hat{\mathbf{x}}$	Estimate of the vector of transmitted symbols
\mathcal{X}	Number of calculations of the MMD metric
$\mathbf{y}_{S,D}$	Received vector of symbols (for SD links)
\mathbf{y}_{S,R_k}	Received vector of symbols (for SR_k links)
$\mathbf{y}_{R_j,D}$	Received vector of symbols (for R_jD links)
ρ	Average data rate

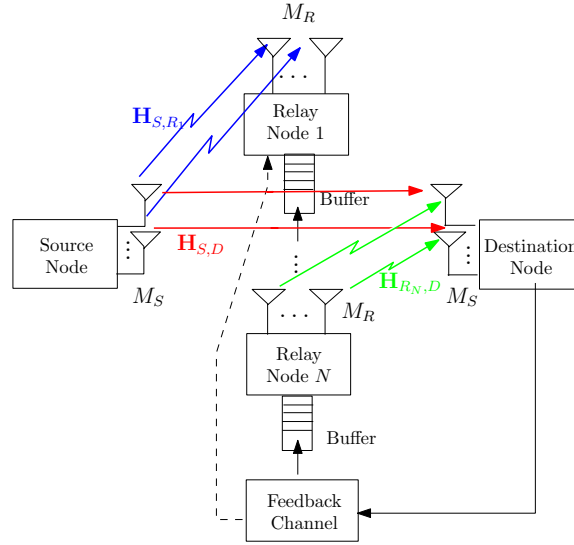


Figure 3.1: System Model of the multiple-antenna buffer-aided relay network.

3.2.1 Assumptions

In cooperative transmissions two time slots are needed to transmit data packets from S to D , so the energy transmitted in direct transmissions (from S to D) is twice the energy E_S transmitted in cooperative transmissions, from S to the relay selected for reception R_k or from the relay selected for transmission R_j to D (E_{R_j}), $E_{R_j} = E_S = E$. For this reason, the energy transmitted from each antenna in cooperative transmissions equals E/M_S and the energy transmitted from each antenna in direct transmissions equals $2E/M_S$. We consider that the channel coefficients are modeled by mutually independent zero mean complex Gaussian random variables. Moreover, we assume that the transmission is organized in data packets and the channels are constant for the duration of one time slot and vary independently from one time slot to the next. Fig. 3.2 illustrates the frame of the data packets. The information about the order of the data packets is contained in the preamble of each packet, so the original order is restored at D . Other information such as signaling for CSI estimation are also inserted in the preamble of the packet. We consider perfect and imperfect CSI. A distributed implementation can reduce signaling overheads and reduce the impact of outdated CSI. Furthermore, we assume that the relays do not communicate with each other. We also assume that D is the central node, being responsible for deciding whether S or a relay should transmit in a given time slot i . The central node has access to the channel and the buffer state information, so it may run the algorithm in each time slot and select the relay for transmission or reception through a feedback channel. This

assumption can be ensured by an appropriate signalling that provides global CSI at D [39]. Furthermore, we assume that S has no CSI and each relay has only information about its SR channels and buffer status.

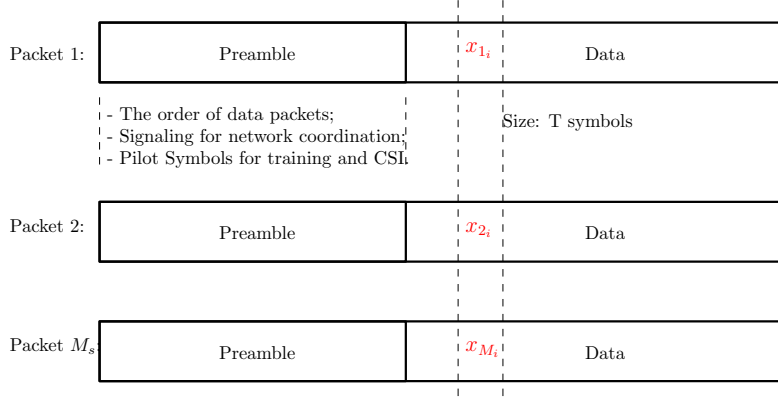


Figure 3.2: The frame of each packet.

3.2.2 System Model

The proposed system can operate in each time slot in two modes: "Direct Transmission" (DT) or "Max-Link". Thus, depending on the relay selection metrics (explained in Section 3.3), the system may operate in each time slot with three options:

- a) DT mode: S transmits M_S packets directly to D ;
- b) Max-Link- SR mode: S transmits M_S packets to R_k ;
- c) Max-Link- RD mode: R_j transmits M_S packets to D .

If the relay selection algorithm decides to operate in the DT mode, the received signal from the S to D is organized in an $M_S \times 1$ vector $\mathbf{y}_{S,D}[i]$ given by

$$\mathbf{y}_{S,D}[i] = \sqrt{\frac{2E}{M_S}} \mathbf{H}_{S,D} \mathbf{x}[i] + \mathbf{n}_D[i], \quad (3-1)$$

where $\mathbf{x}[i]$ represents the vector formed by M_S symbols sent by S , $\mathbf{H}_{S,D}$ represents the $M_S \times M_S$ matrix of SD links and \mathbf{n}_D denotes the zero mean additive white complex Gaussian noise (AWGN) at D . Assuming synchronization and perfect CSI, at D we employ the ML receiver which yields

$$\hat{\mathbf{x}}[i] = \arg \min_{\mathbf{x}'[i]} \left(\left\| \mathbf{y}_{S,D}[i] - \sqrt{\frac{2E}{M_S}} \mathbf{H}_{S,D} \mathbf{x}'[i] \right\|^2 \right), \quad (3-2)$$

where $\mathbf{x}'[i]$ represents each possible vector formed by M_S symbols. Thus, the ML receiver computes the vector of transmitted symbols which is the optimal solution. As an example, if we have BPSK (number of constellation symbols $N_s = 2$), unit power symbols and $M_S = 2$, the estimated vector of transmitted symbols $\hat{\mathbf{x}}[i]$ may be $[-1 \ -1]^T$, $[-1 \ +1]^T$, $[+1 \ -1]^T$ or $[+1 \ +1]^T$.

Otherwise, if the relay selection algorithm decides to operate in the Max-Link- SR mode, the received signal from S to R_k is organized in an $UM_S \times 1$ vector $\mathbf{y}_{S,R_k}[i]$ given by

$$\mathbf{y}_{S,R_k}[i] = \sqrt{\frac{E}{M_S}} \mathbf{H}_{S,R_k} \mathbf{x}[i] + \mathbf{n}_{R_k}[i], \quad (3-3)$$

where \mathbf{H}_{S,R_k} represents the $UM_S \times M_S$ matrix of SR_k links and \mathbf{n}_{R_k} represents the AWGN at R_k . Note that \mathbf{H}_{S,R_k} is formed by U square submatrices of dimensions $M_S \times M_S$ as given by

$$\mathbf{H}_{S,R_k} = [\mathbf{H}_{S,R_k}^1; \mathbf{H}_{S,R_k}^2; \dots; \mathbf{H}_{S,R_k}^U]. \quad (3-4)$$

Assuming synchronization and perfect CSI, at R_k we employ the ML receiver [5]:

$$\hat{\mathbf{x}}[i] = \arg \min_{\mathbf{x}'[i]} \left(\left\| \mathbf{y}_{S,R_k}[i] - \sqrt{\frac{E}{M_S}} \mathbf{H}_{S,R_k} \mathbf{x}'[i] \right\|^2 \right). \quad (3-5)$$

Moreover, if the relay selection algorithm decides to operate in the Max-Link- RD mode, the signal transmitted from R_j to D is structured in an $M_S \times 1$ vector $\mathbf{y}_{R_j,D}[i]$ given by

$$\mathbf{y}_{R_j,D}[i] = \sqrt{\frac{E}{M_S}} \mathbf{H}_{R_j,D}^u \hat{\mathbf{x}}[i] + \mathbf{n}_D[i], \quad (3-6)$$

where $\hat{\mathbf{x}}[i]$ is the vector formed by M_S previously decoded symbols in the relay selected for reception and stored in its buffer and now transmitted by R_j and $\mathbf{H}_{R_j,D}^u$ is an $M_S \times M_S$ matrix of R_jD links. Note that $\mathbf{H}_{R_j,D}^u$ is selected among U submatrices of dimension $M_S \times M_S$ contained in $\mathbf{H}_{R_j,D}$ as given by

$$\mathbf{H}_{R_j,D} = [\mathbf{H}_{R_j,D}^1; \mathbf{H}_{R_j,D}^2; \dots; \mathbf{H}_{R_j,D}^U]. \quad (3-7)$$

At D , we also resort to the ML receiver which computes

$$\hat{\mathbf{x}}[i] = \arg \min_{\mathbf{x}'[i]} \left(\left\| \mathbf{y}_{R_j,D}[i] - \sqrt{\frac{E}{M_S}} \mathbf{H}_{R_j,D}^u \mathbf{x}'[i] \right\|^2 \right). \quad (3-8)$$

Considering imperfect CSI, the estimated channel matrix $\hat{\mathbf{H}}$ is assumed, instead of \mathbf{H} in (3-2), (3-5) and (3-8): a channel error matrix \mathbf{H}_e is added to the channel matrix (\mathbf{H}_{S,R_k} , $\mathbf{H}_{R_j,D}$ or $\mathbf{H}_{S,D}$) and we focus on the case where errors decay as $O(SNR^{-\alpha})$ for some constant $\alpha \in [0, 1]$ [131]. Thus, the variance of the \mathbf{H}_e coefficients is given by $\sigma_e^2 = \beta E^{-\alpha}$ ($\beta \geq 0$), in the case of \mathbf{H}_{S,R_k} or $\mathbf{H}_{R_j,D}$, and $\sigma_e^2 = \beta(2E)^{-\alpha}$, in the case of $\mathbf{H}_{S,D}$. As an example, in the case of \mathbf{H}_{S,R_k} , the estimated channel matrix is given by $\hat{\mathbf{H}}_{S,R_k} = \mathbf{H}_{S,R_k} + \mathbf{H}_e$.

3.3 Principles of Switched Max-Link Relay Selection Based on MMD

In this section, we detail the proposed Switched Max-Link relay selection protocol.

3.3.1 Principles of Switched Max-Link Relay Selection

The system presented in Fig. 3.1 is equipped with the proposed Switched Max-Link relay selection protocol, that in each time slot may operate in two possible modes ("DT" or "Max-Link"), with three options:

- a) work in DT mode: S sends M_S packets directly to D ;
- b) work in Max-Link- SR mode: S sends M_S packets to R_k and these packets are stored in its buffer;
- c) work in Max-Link- RD mode: R_j forwards M_S packets from its buffer to D .

The proposed Switched Max-Link protocol uses the MMD relay selection criterion. As the scheme proposed in [132], the proposed MMD relay selection criterion is based on the ML principle. However, the metrics calculated by MMD are different from those of the scheme in [132], which leads to considerably better performance. MMD is also based on the worst case of the PEP and chooses the relay associated with the largest minimum Euclidian distance. So, it requires the distance between the $N_s^{M_S}$ possible vectors of transmitted symbols. The MMD-based relay selection algorithm, in the Max-Link- SR mode, chooses the relay R_k and the associated channel matrix \mathbf{H}_{S,R_k}^{MMD} with the largest minimum distance as given by

$$\mathbf{H}_{S,R_k}^{MMD} = \arg \max_{\mathbf{H}_{S,R_i}} \mathcal{D}_{\min SR_i}, \quad (3-9)$$

where $\mathcal{D}_{\min SR_i} = \min \left(\frac{E}{M_S} \left\| \mathbf{H}_{S,R_i}^u (\mathbf{x}_l - \mathbf{x}_n) \right\|^2 \right)$, $u \in \{1, \dots, U\}$, $i \in \{1, \dots, N\}$, \mathbf{x}_l and \mathbf{x}_n represent each possible vector formed by M_S symbols and $l \neq n$. The metric $\frac{E}{M_S} \left\| \mathbf{H}_{S,R_i}^u (\mathbf{x}_l - \mathbf{x}_n) \right\|^2$ is calculated for each of the $C_2^{N_s^{M_S}}$ (combination

of $N_s^{M_S}$ in 2) possibilities, for each submatrix \mathbf{H}_{S,R_i}^u , and $\mathcal{D}_{\min SR_i}$ is the smallest of these values, for each R_i . Thus, the selected matrix \mathbf{H}_{S,R_k}^{MMD} has the largest $\mathcal{D}_{\min SR_i}$ value.

Moreover, the MMD-based relay selection algorithm, in the Max-Link-RD mode, chooses the relay R_j and the associated channel matrix $\mathbf{H}_{R_j,D}^{MMD}$ with the largest minimum distance as given by

$$\mathbf{H}_{R_j,D}^{MMD} = \arg \max_{\mathbf{H}_{R_i,D}} \mathcal{D}_{\min R_i D}, \quad (3-10)$$

where $\mathcal{D}_{\min R_i D} = \max(\mathcal{D}_{\min R_i D}^u)$ and $\mathcal{D}_{\min R_i D}^u = \min\left(\frac{E}{M_S} \|\mathbf{H}_{R_i,D}^u(\mathbf{x}_l - \mathbf{x}_n)\|^2\right)$. Note that the submatrix $\mathbf{H}_{R_j,D}^u$ associated with the largest $\mathcal{D}_{\min R_i D}^u$ value is selected among U submatrices of dimension $M_S \times M_S$ contained in $\mathbf{H}_{R_j,D}^{MMD}$. Table 3.2 shows the Switched Max-Link pseudo-code and the following subsections explain how this protocol works.

3.3.2

Calculation of relay selection metric

In the first step we calculate the metrics $\mathcal{D}_{SR_i}^u$ related to the SR channels of each submatrix \mathbf{H}_{S,R_i}^u of each relay R_i , in Max-Link mode:

$$\mathcal{D}_{SR_i}^u = \left\| \sqrt{\frac{E}{M_S}} \mathbf{H}_{S,R_i}^u \mathbf{x}_l - \sqrt{\frac{E}{M_S}} \mathbf{H}_{S,R_i}^u \mathbf{x}_n \right\|^2, \quad (3-11)$$

where $u \in \{1, \dots, U\}$, $i \in \{1, \dots, N\}$, \mathbf{x}_l and \mathbf{x}_n represent each possible vector formed by M_S symbols and $l \neq n$. This metric is calculated for each of the $C_2^{N_s^{M_S}}$ (combination of $N_s^{M_S}$ in 2) possibilities. As an example, if $M_S = 2$ and $N_s = 2$, we have $C_2^4 = 6$ possibilities. Then, we store the smallest metric ($\mathcal{D}_{\min SR_i}^u$), for being critical (a bottleneck) in terms of performance, and thus each relay will have a minimum distance associated with its SR channels. In the second step we calculate the metrics $\mathcal{D}_{R_i D}^u$ related to the RD channels of each submatrix $\mathbf{H}_{R_i,D}^u$ of each relay R_i :

$$\mathcal{D}_{R_i D}^u = \left\| \sqrt{\frac{E}{M_S}} \mathbf{H}_{R_i,D}^u \mathbf{x}_l - \sqrt{\frac{E}{M_S}} \mathbf{H}_{R_i,D}^u \mathbf{x}_n \right\|^2, \quad (3-12)$$

where $l \neq n$. This metric is also calculated for each of the $C_2^{N_s^{M_S}}$ possibilities. Then, we store the minimum distance ($\mathcal{D}_{\min R_i D}^u$), and thus each submatrix $\mathbf{H}_{R_i,D}^u$ will have a minimum distance associated with its RD channels. In the third step, we find the largest minimum distance $\mathcal{D}_{\min R_i D}$, and thus each relay will have its best channel submatrix $\mathbf{H}_{R_i,D}^u$ which is associated with this

distance:

$$\mathcal{D}_{\min R_i D} = \max(\mathcal{D}_{\min R_i D}^u). \quad (3-13)$$

In the fourth step, after calculating the metrics $\mathcal{D}_{\min SR_i}^u$ and $\mathcal{D}_{\min R_i D}$ for each of the relays, as described previously, we empirically compute the expected values of $\mathcal{D}_{\min SR_i}^u$ and $\mathcal{D}_{\min R_i D}$ and adjust the $\mathcal{D}_{\min SR_i}^u$ values to balance the number of time slots selected for Max-Link- SR and Max-Link- RD modes:

$$\mathcal{D}_{\min SR_i} = \frac{\mathbb{E}[\mathcal{D}_{\min R_i D}]}{\mathbb{E}[\mathcal{D}_{\min SR_i}^u]} \mathcal{D}_{\min SR_i}^u, \quad (3-14)$$

Then, we perform ordering and select the largest value of these distances:

$$\mathcal{D}_{\max \min SR-RD} = \max(\mathcal{D}_{\min SR_i}, \mathcal{D}_{\min R_i D}). \quad (3-15)$$

Therefore, we select the relay that is associated with $\mathcal{D}_{\max \min SR-RD}$, considering its buffer status. This relay will be selected for reception (if its buffer is not full) or transmission (if its buffer is not empty), depending on this metric is associated with the SR or RD channels, respectively. Otherwise, the algorithm checks if the next maximum minimum distance and the associated relay meet the necessary requirements related to the buffer status.

3.3.3 Calculation of the metric for direct transmission

In this step we calculate the metric \mathcal{D}_{SD} related to the SD channels for the DT mode:

$$\mathcal{D}_{SD} = \left\| \sqrt{\frac{2E}{M_S}} \mathbf{H}_{S,D} \mathbf{x}_l - \sqrt{\frac{2E}{M_S}} \mathbf{H}_{S,D} \mathbf{x}_n \right\|^2, \quad (3-16)$$

where $l \neq n$. This metric is calculated for each of the $C_2^{N_s^{M_S}}$ possibilities. Then, we store the minimum distance ($\mathcal{D}_{\min SD}$). Considering imperfect CSI, the estimated channel matrix $\hat{\mathbf{H}}$ is assumed, instead of \mathbf{H} in (3-11), (3-12) and (3-16). After finding $\mathcal{D}_{\max \min SR-RD}$ and $\mathcal{D}_{\min SD}$, we compare these parameters and select the transmission mode that is equal to

$$\begin{cases} \text{Max-Link-}SR, & \text{if } (\mathcal{D}_{\max \min} = \max(\mathcal{D}_{\min SR_i})) \& (G > \mathcal{S}), \\ \text{Max-Link-}RD, & \text{if } (\mathcal{D}_{\max \min} = \max(\mathcal{D}_{\min R_i D})) \& (G > 1), \\ \text{DT}, & \text{otherwise.} \end{cases}$$

where $\mathcal{D}_{\max \min} = \mathcal{D}_{\max \min SR-RD}$, $G = \frac{\mathcal{D}_{\max \min}}{\mathcal{D}_{\min SD}}$, and $\mathcal{S} \in \{0, 1, 2, \dots\}$ is a parameter that works as a switch. In [11], assuming symmetric channels and applications without critical delay constraints, the switch \mathcal{S} is equal to one. If we consider asymmetric channels and the need for a short average delay, we select an \mathcal{S} that takes for granted that the protocol achieves a good BER and average delay performance. If \mathcal{S} is equal to zero, the protocol is selected to operate only in the Max-Link mode and we do not have the possibility of a direct SD connectivity and, consequently, we have another scheme called "MMD-Max-Link". Otherwise, when we increase \mathcal{S} , the number of time slots in which the protocol is selected to operate in the DT mode increases.

3.4

Analysis of MMD: Impact on Relay Selection, PEP, Complexity, Sum-rate and Average Delay

In this section, we first analyze the proposed MMD and the existing QN relay selection criteria. We compare the PEP and the computational complexity of the MMD criterion versus the QN criterion. We then derive expressions to compute the sum-rate and the average delay of the Switched Max-Link protocol.

3.4.1

Impact of the MMD and QN criteria on relay selection

The metrics \mathcal{D} ($\mathcal{D}_{SR_i}^u$, $\mathcal{D}_{R_i D}^u$ and \mathcal{D}_{SD}) are calculated in (3-11), (3-12) and (3-16), for each of the $C_2^{N_s^{M_S}}$ possibilities. However, in the following, we will show that it is not necessary to calculate all these possibilities. The total number of calculations of the metric \mathcal{D} , needed by the MMD criterion, depends on the number M_S of antennas at S and D and the number M_R of antennas at each relay. Furthermore, it depends on the constellation (BPSK, QPSK, 16-QAM...), specifically on the number of different distances between the constellation symbols. For the MMD criterion to compute the metric \mathcal{D} , it is necessary to consider the absolute value of the distances between the constellation symbols (d_c). If we have BPSK and unit power symbols, $d_c = 2$. Otherwise, if we have QPSK, there are $W = 3$ different values for d_c : $d_{c_1} = \sqrt{2}$, $d_{c_2} = \sqrt{2}j$ and $d_{c_3} = \sqrt{2} + \sqrt{2}j$.

We may consider that the $M_S \times M_S$ channel matrix \mathbf{H}^u represents \mathbf{H}_{S,R_i}^u , $\mathbf{H}_{R_i,D}^u$ or $\mathbf{H}_{S,D}$. In the case of $\mathcal{D}_{SR_i}^u$ and $\mathcal{D}_{R_i D}^u$, if \mathbf{x}_n and \mathbf{x}_l are different from

each other in just one symbol in position j , we have:

$$\begin{aligned}
 \mathcal{D}_j &= \left\| \sqrt{\frac{E}{M_S}} \mathbf{H}^u \mathbf{x}_l - \sqrt{\frac{E}{M_S}} \mathbf{H}^u \mathbf{x}_n \right\|^2 \\
 &= \frac{E}{M_S} \|\mathbf{H}^u (\mathbf{x}_l - \mathbf{x}_n)\|^2 \\
 &= \frac{E}{M_S} \left\| \mathbf{H}^u [0 \dots \pm d_{c_w} \dots 0]^T \right\|^2 \\
 &= \frac{|d_{c_w}|^2 E}{M_S} \sum_{i=1}^{M_S} |H_{i,j}^u|^2
 \end{aligned} \tag{3-17}$$

$$w = 1, \dots, W.$$

If \mathbf{x}_n and \mathbf{x}_l are different from each other in two symbols in positions j and k , we have:

$$\begin{aligned}
 \mathcal{D}_{j,k} &= \frac{E}{M_S} \left\| \mathbf{H}^u [0 \dots \pm d_{c_w} \dots \pm d_{c_h} \dots 0]^T \right\|^2 \\
 &= \frac{E}{M_S} \sum_{i=1}^{M_S} |\pm d_{c_w} H_{i,j}^u \pm d_{c_h} H_{i,k}^u|^2
 \end{aligned} \tag{3-18}$$

$$w, h = 1, \dots, W,$$

where the indices w and h may be different from each other.

If \mathbf{x}_n and \mathbf{x}_l are different from each other in M_S symbols, we have:

$$\begin{aligned}
 \mathcal{D}_{1,\dots,M_S} &= \frac{E}{M_S} \left\| \mathbf{H}^u [\pm d_{c_w} \dots \pm d_{c_v}]^T \right\|^2 \\
 &= \frac{E}{M_S} \sum_{i=1}^{M_S} |\pm d_{c_w} H_{i,1}^u \dots \pm d_{c_v} H_{i,M_S}^u|^2
 \end{aligned} \tag{3-19}$$

$$w, v = 1, \dots, W,$$

where the indices w and v may be different from each other.

We can simplify the equations, making $\mathcal{D} = E/M_S \times \mathcal{D}'$, where $\mathcal{D}' = \|\mathbf{H}^u (\mathbf{x}_n - \mathbf{x}_l)\|^2$, for $\mathcal{D}_{S_{R_i}}^u$ and $\mathcal{D}_{R_i D}^u$, or $\mathcal{D}' = 2\|\mathbf{H}^u (\mathbf{x}_n - \mathbf{x}_l)\|^2$, for \mathcal{D}_{SD} . We know that the PEP considers the error event when \mathbf{x}_n is transmitted and the detector computes an incorrect \mathbf{x}_l (where $l \neq n$), based on the received symbol [133, 134]. If we consider $M_R = M_S$, then $U = 1$ and, consequently, $\mathbf{H} = \mathbf{H}^u$ and the PEP is given by

$$\mathbf{P}(\mathbf{x}_n \rightarrow \mathbf{x}_l | \mathbf{H}) = Q \left(\sqrt{\frac{E_s}{2N_0 M_S} \mathcal{D}'} \right), \tag{3-20}$$

where N_0 is the power spectrum density of the AWGN. The MMD criterion, by maximizing the value of the minimum distance \mathcal{D}_{\min} , also maximizes the minimum value of the PEP argument \mathcal{D}'_{\min} (PEP worst case). The PEP argument \mathcal{D}' is related to the sum of the powers of the coefficients of each column (or the combination of two or more columns by addition or subtraction) of the matrix \mathbf{H} . Moreover, when $U > 1$, \mathbf{H} is formed by multiple square submatrices \mathbf{H}^u , and the maximization of the minimum distances related to \mathbf{H}^u also implies the maximization of the minimum value of the PEP argument.

As an example, if we have BPSK and unit power symbols ($d_c = 2$) and $M_S = M_R = 2$ ($U = 1$), for each matrix \mathbf{H}^u (\mathbf{H}_{S,R_i}^u or $\mathbf{H}_{R_i,D}^u$), we have to calculate 4 different values for \mathcal{D}' :

$$\begin{aligned} \mathcal{D}'_1 &= 4 \sum_{i=1}^2 |H_{i,1}^u|^2, \quad \mathcal{D}'_2 = 4 \sum_{i=1}^2 |H_{i,2}^u|^2, \\ \mathcal{D}'_{1,2(+)} &= 4 \sum_{i=1}^2 |H_{i,1}^u + H_{i,2}^u|^2, \\ \mathcal{D}'_{1,2(-)} &= 4 \sum_{i=1}^2 |H_{i,1}^u - H_{i,2}^u|^2. \end{aligned} \quad (3-21)$$

If we have the direct transmission option, by considering the matrix $\mathbf{H}_{S,D}$, we also have to calculate the same expressions described in (3-21), multiplied by 2. Note that these examples were considered by adopting BPSK, but other constellations (QPSK, 16-QAM...) can be adopted.

The MMD metric \mathcal{D} is based on the minimum Euclidian distances between the possible vectors of transmitted symbols. In contrast, in the QN criterion, that is based only on the total power of these links (as the traditional Max-Link), the metric \mathcal{Q} is related to the quadratic norm (the sum of the powers of all the coefficients) of each matrix \mathbf{H} :

$$\begin{aligned} \mathcal{Q} &= \|\mathbf{H}\|^2 \\ &= \sum_{j=1}^{M_S} \sum_{i=1}^{M_R} |H_{i,j}|^2. \end{aligned} \quad (3-22)$$

Thus, the QN criterion selects the channel matrix \mathbf{H}^{QN} , as given by

$$\mathbf{H}^{QN} = \arg \max_{\mathbf{H}} \|\mathbf{H}\|^2 \quad (3-23)$$

where $\mathbf{H} \in \{\mathbf{H}_{S,R_1}, \dots, \mathbf{H}_{S,R_N}, \mathbf{H}_{R_1,D}, \dots, \mathbf{H}_{R_N,D}\}$ and $H_{i,j} \in \mathbb{C}(0, \sigma^2)$.

The MMD criterion, differently from the QN criterion, takes into account the minimum distances related to \mathcal{D}_j in (3-17), $\mathcal{D}_{j,k}$ in (3-18) and $\mathcal{D}_{1,\dots,M_S}$ in

(3-19), to select \mathbf{H}^{MMD} :

$$\mathbf{H}^{MMD} = \arg \max_{\mathbf{H}} \min (\mathcal{D}_j, \mathcal{D}_{j,k}, \dots, \mathcal{D}_{1,\dots,M_S}) \quad (3-24)$$

$$j, k = 1, \dots, M_S, j \neq k,$$

where $\mathbf{H} \in \{\mathbf{H}_{S,R_1}, \dots, \mathbf{H}_{S,R_N}, \mathbf{H}_{R_1,D}, \dots, \mathbf{H}_{R_N,D}, \mathbf{H}_{S,D}\}$ and $H_{i,j} \in \mathbb{C}(0, \sigma^2)$.

The advantage of the MMD algorithm as compared to QN is that MMD, by maximizing \mathcal{D}_{\min} , also maximizes the minimum value of the PEP argument \mathcal{D}'_{\min} , whereas QN does not take it into account. So, the minimum value of the PEP argument \mathcal{D}'_{\min}^{QN} associated with \mathbf{H}^{QN} , selected by the QN criterion, may be not as high as the minimum value of the PEP argument $\mathcal{D}'_{\min}^{MMD}$ associated with \mathbf{H}^{MMD} , selected by the MMD criterion.

Example 1: consider BPSK, unit power symbols and a network formed by S , D , one relay R (without direct transmission), and two antennas in each node ($M_S = M_R = 2$), where $\mathbf{H}_{S,R}$ and $\mathbf{H}_{R,D}$ are given by:

$$\begin{bmatrix} b & 2b \\ g & 2g \end{bmatrix} \text{ and } \begin{bmatrix} 2b + \epsilon & 2b \\ 2g + \epsilon & 2g \end{bmatrix}, \text{ respectively, where } \epsilon \rightarrow 0.$$

By applying the QN criterion and calculating the quadratic norm of $\mathbf{H}_{S,R}$, we have: $\mathcal{Q} = 5|b|^2 + 5|g|^2$. And the quadratic norm of $\mathbf{H}_{R,D}$ is equal to: $\mathcal{Q} = |2b + \epsilon|^2 + |2g + \epsilon|^2 + 4|b|^2 + 4|g|^2$. $\mathcal{Q} \rightarrow 8|b|^2 + 8|g|^2$. Thus, by considering (3-23), we have: $\mathbf{H}^{QN} = \mathbf{H}_{R,D}$. In contrast, by applying the MMD criterion and calculating the minimum distance of $\mathbf{H}_{S,R}$, we have: $\mathcal{D}_{\min} = \frac{4E}{M_S}(|2b - b|^2 + |2g - g|^2) = \frac{4E}{M_S}(|b|^2 + |g|^2)$. And the minimum distance of $\mathbf{H}_{R,D}$ is equal to: $\mathcal{D}_{\min} = \frac{4E}{M_S}(|2b - 2b - \epsilon|^2 + |2g - 2g - \epsilon|^2) = \frac{8E}{M_S}|\epsilon|^2$. $\mathcal{D}_{\min} \rightarrow 0$. Thus, by considering (3-24), we have: $\mathbf{H}^{MMD} = \mathbf{H}_{S,R}$. Moreover, by calculating the minimum values of the PEP argument, we have: $\mathcal{D}'_{\min}^{MMD} = 4(|b|^2 + |g|^2)$ and $\mathcal{D}'_{\min}^{QN} = 8|\epsilon|^2$. $\mathcal{D}'_{\min}^{QN} \rightarrow 0$.

Example 2: consider BPSK, unit power symbols and a network formed by S , D , one relay R (without direct transmission), and $M_S = M_R = 2$, where $\mathbf{H}_{S,R}$ and $\mathbf{H}_{R,D}$ are given by:

$$\begin{bmatrix} \epsilon_1 & 5b \\ \epsilon_2 & 4g \end{bmatrix} \text{ and } \begin{bmatrix} b & 3b \\ g & 3g \end{bmatrix}, \text{ respectively, where } \epsilon_1 \rightarrow 0 \text{ and}$$

$\epsilon_2 \rightarrow 0$.

By applying the QN criterion and calculating the quadratic norm of $\mathbf{H}_{S,R}$, we have: $\mathcal{Q} = 25|b|^2 + 16|g|^2 + |\epsilon_1|^2 + |\epsilon_2|^2$. $\mathcal{Q} \rightarrow 25|b|^2 + 16|g|^2$. And the quadratic norm of $\mathbf{H}_{R,D}$ is equal to: $\mathcal{Q} = 10|b|^2 + 10|g|^2$. Thus, by considering (3-23), we have: $\mathbf{H}^{QN} = \mathbf{H}_{S,R}$. In contrast, by applying the MMD criterion and calculating the minimum distance of $\mathbf{H}_{S,R}$, we have: $\mathcal{D}_{\min} = \frac{4E}{M_S}(|\epsilon_1|^2 + |\epsilon_2|^2)$. $\mathcal{D}_{\min} \rightarrow 0$. And the minimum distance of $\mathbf{H}_{R,D}$ is equal to: $\mathcal{D}_{\min} = \frac{4E}{M_S}(|b|^2 + |g|^2)$. Thus, by considering (3-24), we have: $\mathbf{H}^{MMD} = \mathbf{H}_{R,D}$. Moreover, by calculating the minimum values of the PEP argument, we have: $\mathcal{D}'_{\min}{}^{MMD} = 4(|b|^2 + |g|^2)$ and $\mathcal{D}'_{\min}{}^{QN} = 4(|\epsilon_1|^2 + |\epsilon_2|^2)$. $\mathcal{D}'_{\min}{}^{QN} \rightarrow 0$.

We have seen in these examples that: $\mathbf{H}^{MMD} \neq \mathbf{H}^{QN}$ and $\mathcal{D}'_{\min}{}^{MMD} > \mathcal{D}'_{\min}{}^{QN}$. In the Appendix A, we develop a proof that shows that:

$$\mathcal{D}'_{\min}{}^{MMD} \geq \mathcal{D}'_{\min}{}^{QN}. \quad (3-25)$$

Note that these examples were considered by using BPSK, but other constellations (QPSK, 16-QAM...) can be adopted.

3.4.2 Pairwise Error Probability

As we have seen in (3-20), the PEP considers the error event when \mathbf{x}_n is transmitted and the detector computes an incorrect \mathbf{x}_l (where $l \neq n$), based on the received symbol. If we consider $M_R = M_S$, then $U = 1$ and, consequently, $\mathbf{H} = \mathbf{H}^u$ and the PEP will have its maximum value for the minimum value of \mathcal{D}' (worst case of the PEP). So, for the worst case of the PEP (\mathcal{D}'_{\min}), in direct SD transmissions, in each time slot, we have

$$\mathbf{P}(\mathbf{x}_n \rightarrow \mathbf{x}_l | \mathbf{H}) = Q \left(\sqrt{\frac{E}{2N_0M_S} \mathcal{D}'_{\min}} \right). \quad (3-26)$$

Assuming that the probability of having no error in the two phases of the system is approximately given by the square of $(1 - \mathbf{P}(\mathbf{x}_n \rightarrow \mathbf{x}_l | \mathbf{H}))$, an expression for calculating the worst case of the PEP for cooperative transmissions (CT), in each time slot (regardless of whether it is an SR or RD link), is given by

$$\begin{aligned} \mathbf{P}^{CT}(\mathbf{x}_n \rightarrow \mathbf{x}_l | \mathbf{H}) &= 1 - (1 - \mathbf{P}(\mathbf{x}_n \rightarrow \mathbf{x}_l | \mathbf{H}))^2 \\ &= 1 - \left(1 - Q \left(\sqrt{\frac{E}{2N_0M_S} \mathcal{D}'_{\min}} \right) \right)^2. \end{aligned} \quad (3-27)$$

Note that this expression may be used for calculating the worst case of the PEP, for both symmetric and asymmetric channels. The metric \mathcal{D}'_{min} is maximized by the MMD criterion and the same does not happen to the QN criterion. The PEP is given by a Q function and its argument is given by the root square of a constant $\left(\frac{E}{2N_0M_S}\right)$ multiplied by \mathcal{D}'_{min} . We know that by the characteristic of the Q function when its argument grows its value decreases. Therefore, if we consider (3-25), (3-26) and (3-27), we have

$$\mathbf{P}^{MMD}(\mathbf{x}_n \rightarrow \mathbf{x}_l | \mathbf{H}^{MMD}) \leq \mathbf{P}^{QN}(\mathbf{x}_n \rightarrow \mathbf{x}_l | \mathbf{H}^{QN}), \quad (3-28)$$

where $\mathbf{P}^{MMD}(\mathbf{x}_n \rightarrow \mathbf{x}_l | \mathbf{H}^{MMD})$ is the PEP for the worst case in the MMD criterion and $\mathbf{P}^{QN}(\mathbf{x}_n \rightarrow \mathbf{x}_l | \mathbf{H}^{QN})$ is the PEP for the worst case in the QN criterion. Note that when $U > 1$, \mathbf{H} is formed by multiple square submatrices \mathbf{H}^u , and the maximization of the minimum distances related to \mathbf{H}^u done by the MMD criterion also implies the maximization of the minimum value of the PEP argument.

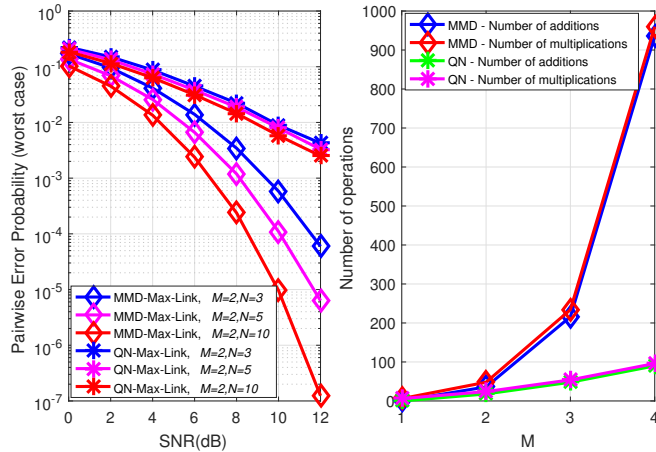


Figure 3.3: MMD-Max-Link and QN-Max-Link a) PEP performance and b) Computational Complexity.

Fig. 3.3 a) shows the theoretical PEP worst case performance (computed by the algorithm based on the selected channel matrix \mathbf{H} , in each time slot) of the MMD-Max-Link and QN-Max-Link protocols, for $M_S = M_R = M = 2$, $N = 3, 5$ and 10 , $J = 4$, BPSK and perfect CSI. Note that for multiple antennas the PEP worst case performance of the MMD-Max-Link scheme is much better than that of QN-Max-Link for the total range of SNR values tested. When we increase N , the MMD-Max-Link has its performance improved and the gap between the curves is increased. The same does not happen to QN-Max-Link, as the QN criterion does not take the metric \mathcal{D}'_{min} into account. Note that this

example was considered by adopting BPSK, but other constellations (QPSK, 16-QAM...) can be considered.

3.4.3 Computational Complexity

We may generalize the total number \mathcal{X} of calculations of the metric \mathcal{D} , needed by the MMD criterion, for each matrix $\mathbf{H}_{S,R}^u$, $\mathbf{H}_{R,D}^u$ or $\mathbf{H}_{S,D}$:

$$\mathcal{X} = \sum_{i=1}^{M_S} 2^{i-1} W^i C_i^{M_S}, \quad (3-29)$$

where W is the total number of different distances between the constellation symbols (d_c). If we have BPSK, $W = 1$, and QPSK, $W = 3$. In QPSK, the calculation of some of these metrics is redundant, so the number of calculations \mathcal{X} may be less than the indicated in (3-29), but it was considered in this way, by the greater ease of implementation of the algorithm.

Table 3.3 shows the complexity of the MMD and QN criteria for a number of N relays, M_S antennas at S and D , and $M_R = UM_S$ antennas at the relays, considering only the cooperative transmission and the constellation type (BPSK, QPSK, 16-QAM...). Fig. 3.3 b) also shows the complexity of the MMD and QN criteria, for $N = 3$ (S , D and 3 relays), $M_S = M_R = M$ antennas at each node and BPSK. This result shows that the complexity of the MMD criterion with $M_S = 2$ is not much higher than the complexity of the QN criterion. If we increase the number of antennas to $M_S = 3$ (or more) in each node, the complexity of MMD becomes considerably higher than the complexity of QN.

3.4.4 Sum-Rate

The sum-rate of a given system is upper bounded by the system capacity. In this context, the capacity of the cooperative system in a given time slot, using a single relay selection scheme is given by [1, 102]:

$$C_{DF} = \frac{1}{2} \min\{I_{DF}^{SR}, I_{DF}^{RD}\}, \quad (3-30)$$

where the first term in (3-30) represents the maximum rate at which the relay can reliably decode the message from S , while the second term in (3-30) is the maximum rate at which D can reliably decode the estimated message from S transmitted by the relay [1].

Note that in the Switched Max-Link and MMD-Max-Link schemes, differently from a single relay scheme, the selected relay for reception R_k may be different from the selected relay for transmission R_j . Therefore, the capacity of the MMD-Max-Link and the Switched Max-Link (operating in the Max-Link mode) is given by

$$C_{DF} = \frac{1}{2} \min\{I_{DF}^{SR_k}, I_{DF}^{R_jD}\}, \quad (3-31)$$

where the first term in (3-31) is the maximum rate at which R_k can reliably decode the message from S , while the second term in (3-31) is the maximum rate at which D can reliably decode the estimated message from S transmitted by R_j . The capacity of direct transmission is given by

$$C_{DT} = I_{DT}^{SD}. \quad (3-32)$$

As Switched Max-Link may operate in both transmission modes (Max-Link or DT), the expected sum-rate \mathcal{R} in bits/Hz of this scheme, considering symmetric channels, may be expressed as: $C_{DF} \leq \mathcal{R} \leq C_{DT}$. The relationship between mutual information and entropy can be expanded as follows for a given \mathbf{H}_{S,R_k} (channel matrix from S to R_k):

$$\begin{aligned} I_{DF}^{SR_k} &= I_{DF}(\mathbf{x}; \mathbf{y}_{S,R_k} | \mathbf{H}_{S,R_k}) \\ &= \mathcal{H}(\mathbf{y}_{S,R_k}) - \mathcal{H}(\mathbf{y}_{S,R_k} | \mathbf{x}) \\ &= \mathcal{H}(\mathbf{y}_{S,R_k}) - \mathcal{H}(\mathbf{H}_{S,R_k} \mathbf{x} + \mathbf{n}_{R_k} | \mathbf{x}) \\ &= \mathcal{H}(\mathbf{y}_{S,R_k}) - \mathcal{H}(\mathbf{n}_{R_k}), \end{aligned} \quad (3-33)$$

where $\mathcal{H}(\cdot)$ denotes the differential entropy of a continuous random variable. It is assumed that the transmit vector \mathbf{x} and the noise vector \mathbf{n}_{R_k} are independent.

Eq. (3-33) is maximized when \mathbf{y}_{S,R_k} is Gaussian, since the normal distribution maximizes the entropy for a given variance. For a complex Gaussian vector \mathbf{y}_{S,R_k} , the differential entropy is less than or equal to $\log_2 \det(\pi e \mathbf{K})$, with equality if and only if \mathbf{y}_{S,R_k} is a circularly symmetric complex Gaussian vector with $E[\mathbf{y}_{S,R_k} \mathbf{y}_{S,R_k}^H] = \mathbf{K}$ [102, 135]. By assuming the optimal Gaussian distribution for the transmit vector \mathbf{x} , the covariance matrix of \mathbf{y}_{S,R_k} is given

by

$$\begin{aligned}
 E[\mathbf{y}_{S,R_k} \mathbf{y}_{S,R_k}^H] &= E[(\mathbf{H}_{S,R_k} \mathbf{x} + \mathbf{n}_{R_k})(\mathbf{H}_{S,R_k} \mathbf{x} + \mathbf{n}_{R_k})^H] \\
 &= E[\mathbf{H}_{S,R_k} \mathbf{x} (\mathbf{x})^H \mathbf{H}_{S,R_k}^H + \mathbf{n}_{R_k} (\mathbf{n}_{R_k})^H] \\
 &= \mathbf{H}_{S,R_k} \mathbf{Q}_{S,R_k} \mathbf{H}_{S,R_k}^H + E[\mathbf{n}_{R_k} (\mathbf{n}_{R_k})^H] \\
 &= \mathbf{H}_{S,R_k} \mathbf{Q}_{S,R_k} \mathbf{H}_{S,R_k}^H + \mathbf{K}^n \\
 &= \mathbf{K}^d + \mathbf{K}^n,
 \end{aligned} \tag{3-34}$$

where d and n denotes respectively the signal part and the noise part of (3-34) [135]. The maximum mutual information is then given by

$$\begin{aligned}
 I_{DF}^{SR_k} &= \mathcal{H}(\mathbf{y}_{S,R_k}) - \mathcal{H}(\mathbf{n}_{R_k}) \\
 &= \log_2 \det(\pi e (\mathbf{K}^d + \mathbf{K}^n)) - \log_2 \det(\pi e \mathbf{K}^n) \\
 &= \log_2 \det(\mathbf{K}^d + \mathbf{K}^n) - \log_2 \det(\mathbf{K}^n) \\
 &= \log_2 \det(\mathbf{K}^d (\mathbf{K}^n)^{-1} + \mathbf{I}_{M_R}) \\
 &= \log_2 \det(\mathbf{H}_{S,R_k} \mathbf{Q}_{S,R_k} \mathbf{H}_{S,R_k}^H (\mathbf{K}^n)^{-1} + \mathbf{I}_{M_R}) \\
 &= \log_2 \det \left(\mathbf{H}_{S,R_k} (\mathbf{Q}_{S,R_k}/N_0) \mathbf{H}_{S,R_k}^H + \mathbf{I}_{M_R} \right).
 \end{aligned} \tag{3-35}$$

where $\mathbf{Q}_{S,R_k} = E[\mathbf{x}(\mathbf{x})^H] = \frac{E}{M_S} \mathbf{I}_{M_S}$ is the covariance matrix of the transmitted symbols, \mathbf{I}_{M_S} is an $M_S \times M_S$ identity matrix and \mathbf{I}_{M_R} is an $M_R \times M_R$ identity matrix. Note that the vectors \mathbf{x} are formed by independent and identically distributed (i.i.d.) symbols. The same reasoning can be applied to $I_{DF}^{R_j D}$ and I_{DT}^{SD} .

$$I_{DF}^{R_j D} = \log_2 \det(\mathbf{H}_{R_j,D}^u (\mathbf{Q}_{R_j,D}/N_0) (\mathbf{H}_{R_j,D}^u)^H + \mathbf{I}_{M_S}), \tag{3-36}$$

where $\mathbf{Q}_{R_j,D} = \frac{E}{M_S} \mathbf{I}_{M_S}$ and $\mathbf{H}_{R_j,D}^u$ is the selected channel submatrix from R_j to D .

$$I_{DT}^{SD} = \log_2 \det \left(\mathbf{H}_{S,D} (\mathbf{Q}_{S,D}/N_0) \mathbf{H}_{S,D}^H + \mathbf{I}_{M_S} \right), \tag{3-37}$$

where $\mathbf{Q}_{S,D} = \frac{2E}{M_S} \mathbf{I}_{M_S}$. For simplicity, to compute the sum-rate of the Switched Max-Link scheme, instead of considering (3-31), we considered an approximated expression for the sum-rate in each time slot, depending on the kind of transmission. Therefore, in the case of a time slot i selected for SR

transmission, the approximated sum-rate is given by

$$\mathcal{R}_i^{SR_k} \approx \frac{1}{2} \log_2 \det \left(\mathbf{H}_{S,R_k} (\mathbf{Q}_{S,R_k}/N_0) \mathbf{H}_{S,R_k}^H + \mathbf{I}_{M_R} \right). \quad (3-38)$$

Furthermore, in the case of a time slot i selected for RD transmission, the approximated sum-rate is given by

$$\mathcal{R}_i^{R_j D} \approx \frac{1}{2} \log_2 \det (\mathbf{H}_{R_j,D}^u (\mathbf{Q}_{R_j,D}/N_0) (\mathbf{H}_{R_j,D}^u)^H + \mathbf{I}_{M_S}). \quad (3-39)$$

In the case of a time slot i selected for SD transmission, the approximated sum-rate is given by

$$\mathcal{R}_i^{SD} \approx \log_2 \det \left(\mathbf{H}_{S,D} (\mathbf{Q}_{S,D}/N_0) \mathbf{H}_{S,D}^H + \mathbf{I}_{M_S} \right). \quad (3-40)$$

Therefore, by summing the sum-rate values found in each time slot and dividing this result by the total number of time slots, we have that the average sum-rate (\mathcal{R}) of the Switched Max-Link scheme can be approximated by

$$\mathcal{R} \approx \frac{\sum_{i=1}^{n_{SR}} \mathcal{R}_i^{SR_k} + \sum_{i=1}^{n_{RD}} \mathcal{R}_i^{R_j D} + 2 \sum_{i=1}^{n_{SD}} \mathcal{R}_i^{SD}}{n_{SR} + n_{RD} + 2n_{SD}}, \quad (3-41)$$

where n_{SR} and n_{RD} represent the total number of time slots selected for transmission from S to R_k and from R_j to D , respectively, in the Max-Link operation mode ($n_{SR} \cong n_{RD}$), and n_{SD} is the total number of time slots selected for transmission from S to D , in DT mode.

Considering only the Max-Link operation mode in (3-41), without the possibility of direct SD transmissions, we note that the expression takes into account the average of the sum rates $\left(\frac{\mathcal{R}_i^{SR_k} + \mathcal{R}_i^{R_j D}}{2} \right)$, for each pair of corresponding time slots (a time slot used for R_k receiving M_S packets and a time slot used for R_j transmitting the same packets), instead of the minimum operator used in (3-31). On the other hand, by considering both the transmission modes (Max-Link and DT), the terms \mathcal{R}_i^{SD} and n_{SD} are then multiplied by two to balance the expression, as the terms used for the sum-rates in the Max-Link mode are counted two times (cooperative transmissions need two time slots and direct transmissions only one time slot).

3.4.5

States of buffers, outage probability and throughput

In [39], a framework based on Discrete Time Markov Chains (DTMC) is proposed to analyze the traditional Max-Link algorithm, considering single-antenna systems. This framework has been used in many subsequent works to

analyze other buffer-aided relay selection protocols whose buffer is finite [45]. In the following, we use this framework to analyze the MMD-Max-Link and the Switched Max-Link protocols for multiple-antenna systems.

The states of the DTMC represent all the possible states of the buffers, for both MMD-Max-Link and Switched Max-Link protocols, and also the state of direct link SD , for Switched Max-Link. So, in the Switched Max-Link protocol, the transitions between the states are given by the probabilities of successful transmissions of packets and a state of the DTMC is represented not only by the number of sets of M_S packets stored in each buffer (as in the MMD-Max-Link), but it also includes a state which depicts the reception of M_S packets directly from S at D , denoted by \mathcal{E}_d [40]. This state $\mathcal{E}_d \in \{0, 1\}$ changes every time a set of M_S packets is received directly from S . If \mathcal{E}_d is in state 1 and D receives a set of M_S packets directly from S then it moves to state 0, and if \mathcal{E}_d is in state 0 and D receives a set of M_S packets directly from S then it moves to state 1. Note that the state \mathcal{E}_d does not change if a set of M_S packets is received by a relay, or by D from a relay node.

In the Switched Max-Link protocol, the state \mathcal{E}_r of the DTMC can be represented by

$$\mathcal{E}_r = (\mathcal{E}_d B_1^r B_2^r \dots B_N^r), \quad r \in \mathbb{N}_+, 1 \leq r \leq (L+1)^N, \quad (3-42)$$

where $L = \frac{J}{M_S}$, B_n^r is the state of the buffer of each relay R_n and represents the number of sets of M_S packets stored in the buffer. The states are predefined in a random way as all the possible $(L+1)^N$ combinations of the buffer sizes combined with the \mathcal{E}_d state [40]. We consider that $\mathbf{A} \in \mathbb{R}^{2(L+1)^N \times 2(L+1)^N}$ denotes the state transition matrix of the DTMC [40], in which the entry $A_{i,j} = P(\mathcal{E}_i \rightarrow \mathcal{E}_j) = P(\mathcal{E}_{t+1} = \mathcal{E}_j | \mathcal{E}_t = \mathcal{E}_i)$ is the transition probability to move from state \mathcal{E}_i at time t to state \mathcal{E}_j at time $(t+1)$. In order to construct the state transition matrix \mathbf{A} , we have to identify the connectivity between the different states of the buffers [39, 40]. For each time slot, the buffer and the \mathcal{E}_d status can be modified as follows: (a) the number of packets stored in a relay buffer can be decreased by M_S , if a relay node is selected for transmission in Max-Link mode (and the system is not in outage), changing the buffer status, (b) the number of packets stored in a relay buffer can be increased by M_S , if S is selected for transmission in Max-Link mode (and the system is not in outage), changing the buffer status, (c) if S is selected for transmission in DT mode (and the system is not in outage), changing the \mathcal{E}_d status, (d) the buffer and the \mathcal{E}_d status remain unchanged when there is an outage event (all the SR , RD and SD links in outage).

As the buffer of each relay is finite, the DTMC can be shown to be stationary, irreducible and aperiodic (SIA) [45,136]. In the following, analytical expressions are derived for the outage probability, average throughput and average packet delay.

An outage event occurs only when there is no change in the buffer and \mathcal{E}_d status. Hence, the outage probability of the system is given by the sum of the product of the probabilities of being at a stage r and having an outage event [39, 40], as given by

$$P_{outage} = \sum_{r=1}^{Z(L+1)^N} \pi_r \bar{p}_r = \text{diag}(\mathbf{A})\pi, \quad (3-43)$$

where $Z = 1$ and $Z = 2$ in the MMD-Max-Link and Switched Max-Link protocols, respectively. By considering the MMD-Max-Link and the Switched Max-Link (operating in Max-Link mode), if there is only one transmission per time-slot, the average data rate ρ is 0.5 since two hops are required to reach D . Otherwise, in schemes with successive transmissions, ρ is approaching 1 [45]. The proportion of the packets that make it through is $(1 - P_{outage})$. Thus, the average throughput is given by $E[T] = \rho(1 - P_{outage})$ [45], where $\rho \in (0.5, 1)$. Note that if the links are i.i.d., then the average throughput of a relay R_n [45] in the MMD-Max-Link protocol is given by

$$E[T_n] = \frac{\rho(1 - P_{outage})}{N}. \quad (3-44)$$

And the average throughput of R_n in the Switched Max-Link protocol is given by

$$E[T_n] = \frac{\rho_{SML}(1 - P_{outage})}{N}, \quad (3-45)$$

where $\rho_{SML} = \frac{2\rho P_{ML}^{S'}}{P_{ML}^{S'} + 1}$, and $P_{ML}^{S'}$ is the probability of a packet being transmitted in the Max-Link mode (passing by the relays) for a given \mathcal{S}' , considering $\mathcal{S}' = 1$, if $\mathcal{S} \geq 1$, and $\mathcal{S}' = \mathcal{S}$, if $\mathcal{S} < 1$.

3.4.6 Average Delay

Similarly to the traditional Max-Link [39], Switched Max-Link and MMD-Max-Link were originally considered for applications without critical delay constraints. In this work, by considering the importance of a short average delay in most modern applications, an expression for the average delay of the proposed Switched Max-Link protocol is presented. The average delay is

calculated by considering the time a packet needs to reach the destination once it has left the source (no delay is measured when the packet resides at S [40]). In the Switched Max-Link protocol, the direct transmission is considered to have no delays and for packets that are processed by the relays, the delay is the number of time slots the packet stays in the buffer of the relay [40].

For i.i.d. channels, the average delay is the same on all relays. Hence, it is enough to analyze the average delay on a single relay [45]. By Little's law, the average packet delay at R_n , denoted by $E[d_n]$ is given by

$$E[d_n] = \frac{E[L_n]}{E[T_n]}, \quad (3-46)$$

where $E[L_n]$ and $E[T_n]$ are the average queue length and average throughput, respectively [45]. So, the average queue length at R_n , in the MMD-Max-Link and Switched Max-Link protocols, is given by

$$E[L_n] = \sum_{r=1}^{(L+1)^N} \pi_r B_n^r. \quad (3-47)$$

And the average throughput is given in (3-44). Thus, by substituting (3-43), (3-44) and (3-47) into (3-46), we have that the average delay in the MMD-Max-Link protocol is given by

$$E[d_n]^{MMD} = \frac{N \sum_{r=1}^{(L+1)^N} \pi_r B_n^r}{\rho \left(1 - \sum_{r=1}^{(L+1)^N} \pi_r \bar{p}_r\right)}, \quad (3-48)$$

where $\rho = 0.5$, considering one transmission per time slot. The derivation for the average delay at the high SNR regime is given in [136]. First the throughput of each relay is found. As the selection of a relay is equiprobable, the average throughput at any relay R_n is ρ/N , where ρ is the average data rate. Since we have half-duplex links, $\rho = 1/2$ and therefore $E[T_n] = \frac{1}{2N}$. Also, it can be shown that the average queue length at any relay is $E[L_n] = \frac{L}{2}$. Thus, by Little's law, $E[d_n]^{MMD} = E[d] = NL = N \frac{J}{M_S}$. So, as either the number of relays or the buffer size increases, the average delay of the MMD-Max-Link algorithm increases.

As the MMD-Max-Link protocol operates only in the Max-Link mode (similarly to the traditional Max-Link, but with multiple antennas), we consider that the average delay of MMD-Max-Link is similar to the average delay of Max-Link. In contrast, the average delay of Switched Max-Link is lower than that of Max-Link, because of its advantage (the possibility of operating

in DT mode). The average delay of the Switched Max-Link protocol is given by

$$\begin{aligned}
 E[d_n]^{SML} &= \frac{N \sum_{r=1}^{(L+1)^N} \pi_r B_n^r}{\rho_{SML} \left(1 - \sum_{r=1}^{2(L+1)^N} \pi_r \bar{p}_r\right)} \times P_{ML}^S \\
 &\approx \frac{E[d_n]^{MMD} (P_{ML}^{S'} + 1)}{2P_{ML}^{S'}} \times P_{ML}^S,
 \end{aligned} \tag{3-49}$$

where P_{ML}^S is the probability of a packet being transmitted in the Max-Link mode, for a given \mathcal{S} . When the switch \mathcal{S} tends to zero, P_{ML}^S tends to one (Switched Max-Link operates only in the Max-Link mode and its average delay equals the average delay of MMD-Max-Link). Otherwise, when \mathcal{S} tends to ∞ , P_{ML}^S tends to zero (Switched Max-Link operates only in DT mode, and its average delay tends to zero).

3.5 Numerical Results

This section illustrates and discusses the simulation results of the proposed Switched Max-Link, the MMD-Max-Link, the Max-Link with direct transmission capability [40], the conventional MIMO (direct transmission, without relaying) and the Max-Link with the QN criterion (QN-Max-Link). QN-Max-Link with a single antenna refers to the traditional Max-Link [39]. The proposed Switched Max-Link scheme is considered in a network with N relays and M_S antennas at S and D and M_R antennas at the relays. We considered different values for the buffer size J and adopted $J = 4$ packets as it is sufficient to ensure a good performance. We have also adopted $M_S = 1$ and 2 antennas. Since different packets may be stored at different relays for different amounts of time, the packets transmitted by S may arrive at D in an order different from the order at S [4]. To restore the original order at D , it was necessary to insert in the preamble of each packet the order information (its position in the binary format, ranging from 1 to the total number of packets). We assume that the transmitted signals belong to BPSK or QPSK constellations. The 16-QAM constellation was not included in this work because of its higher complexity. We also assume $N_0 = 1$ and $E_S = E_{R_j} = E$ (total energy transmitted). Scenarios with asymmetric channels were also tested in order to depict the performance of the proposed Switched Max-Link and MMD-Max-Link algorithms. The transmit signal-to-noise ratio SNR (E/N_0) ranges from 0 to 12 dB and the performances of the transmission schemes were tested for $10000M_S$ packets, each containing 100 symbols.

3.5.1 Analysis accuracy validation: PEP and BER performance

In the following we present the theoretical PEP worst case and the simulated BER performance to validate the accuracy of our analysis related to the MMD relay selection criterion, adopted in the Switched Max-Link and the MMD-Max-Link protocols. Then, the BER, average throughput and average delay performances of the Switched Max-Link and Max-Link with direct transmission capability [40] protocols are compared. We also present the BER performance considering BPSK, QPSK and outdated CSI of the Switched Max-Link, MMD-Max-Link and conventional MIMO protocols, considering unit power links ($\sigma_{S,R}^2 = \sigma_{R,D}^2 = \sigma_{S,D}^2 = 1$).

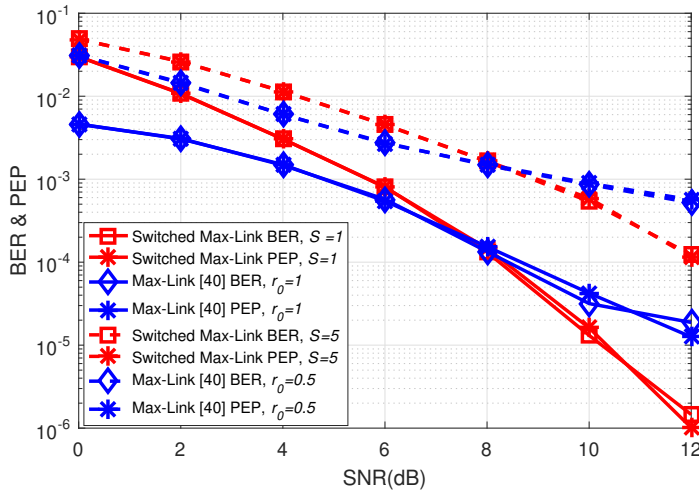


Figure 3.4: Switched Max-Link and Max-Link [40] PEP and BER performances.

Fig. 3.4 shows the theoretical PEP performance that yields from our theoretical framework that has been presented in Section 3.4 and the BER performance of the Switched Max-Link and Max-Link [40] protocols, for BPSK, $M_S = M_R = 1$, $N = 3$ and $J = 4$. In Switched Max-Link, we have $\mathcal{S} = 1$ (solid curve) and 5 (dashed curve), and in Max-Link, we have $r_0 = 1$ (solid curve) and 0.5 BPCU (bits per channel use) (dashed curve). By comparing the solid curves, the result shows that for low SNR values (less than 8dB), the Max-Link protocol has a better BER performance than that of Switched Max-Link. This is because if an outage event occurs in Max-Link, the packet is not transmitted (improving the BER, but reducing the average throughput). In contrast, Switched Max-Link has a better BER performance than that of Max-Link for SNR values greater than 8dB, resulting also in a higher diversity gain. And the results are the same when we compare the dashed curves. These results show that the theoretical PEP performance matches the BER performance and

validate the accuracy of our analysis. Note that in this case we have just a pair of possible transmitted symbols, so the BER performance is comparable to the PEP performance.

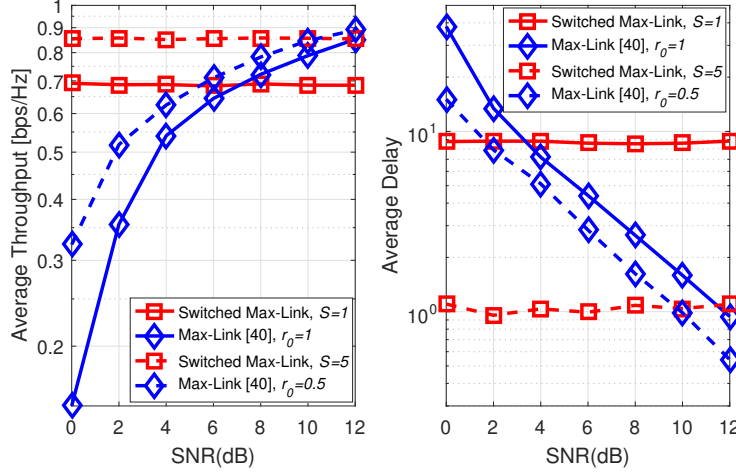


Figure 3.5: Switched Max-Link and Max-Link [40] a) average throughput and b) average delay.

Fig. 3.5 shows the average throughput and average delay performances of the Switched Max-Link and Max-Link [40] protocols, for the same configuration described in Fig. 3.4. The Switched Max-Link protocol has a high average throughput even for low SNR values. This does not happen to Max-Link, as in this protocol, if an outage event occurs, the packet is not transmitted (reducing the average throughput). Moreover, Switched Max-Link has a low average delay (when $\mathcal{S} = 5$) even for low SNR values as opposed to Max-Link.

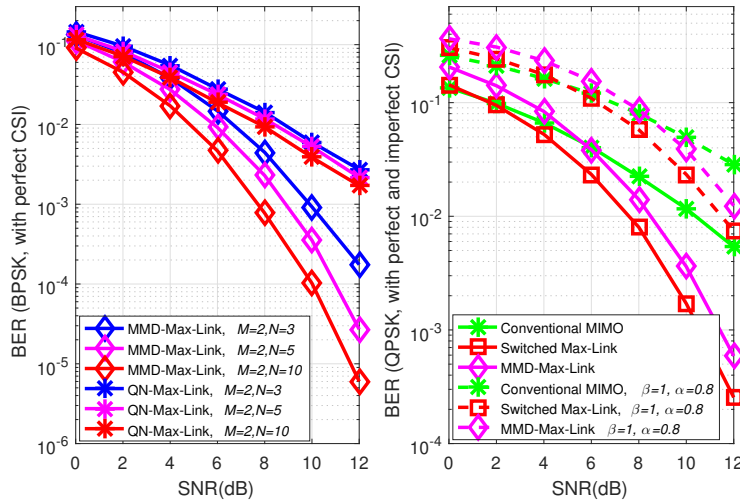


Figure 3.6: a) BER performance for BPSK and b) BER performance for QPSK, with perfect and imperfect channel knowledge.

Fig. 3.6 a) shows the BER performance of the MMD-Max-Link and QN-Max-Link protocols, for $M_S = M_R = M = 2$, $N = 3, 5$ and 10 , $J = 4$, BPSK and perfect CSI. Note that for multiple antennas the BER performance of the MMD-Max-Link scheme is much better than that of QN-Max-Link for the total range of SNR values tested. When we increase N , the MMD-Max-Link has its performance improved. The same does not happen to QN-Max-Link, as the QN criterion does not take the metric \mathcal{D}'_{\min} into account. This result validates the accuracy of our analysis in Section 3.4, illustrating that a better theoretical PEP worst case performance achieved by the MMD relay selection criterion implies also a better BER performance for the MMD-Max-Link protocol. Fig. 3.6 b) shows the Switched Max-Link, the MMD-Max-Link and the conventional MIMO BER performance comparison for $M_S = M_R = 2$, $N = 10$, $J = 4$, $\mathcal{S} = 1$, QPSK, perfect and imperfect CSI ($\beta = 1$ and $\alpha = 0.8$). The QN-Max-Link was not considered as its performance is worse than the performance of the proposed protocol. Both for perfect and imperfect CSI, the performance of Switched Max-Link is considerably better than that of the conventional MIMO for a wide range of SNR values. Switched Max-Link also outperforms MMD-Max-Link, and has resiliency in low transmit SNR conditions. Moreover, we note that outdated CSI results in diversity loss.

3.5.2 Performance under asymmetric channels

In the following we consider the BER, sum-rate and average delay performances of the proposed and existing schemes under asymmetric channels.

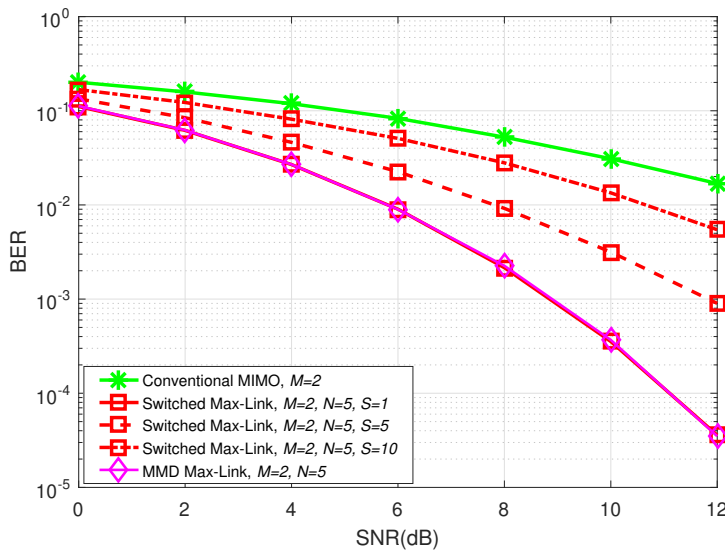


Figure 3.7: BER performance, with low power SD links.

Fig. 3.7 shows the BER performance of the Switched Max-Link, MMD-Max-Link and the conventional MIMO protocols, for $M_S = M_R = M = 2$, $N = 5$, $J = 4$, $\mathcal{S} = 1, 5$ and 10 , BPSK, perfect CSI and low power SD links ($\sigma_{S,R}^2 = \sigma_{R,D}^2 = 1$ and $\sigma_{S,D}^2 = 0.2$). The performance of the proposed Switched Max-Link scheme, for $\mathcal{S} = 1$, is very close to that of the MMD-Max-Link, illustrating the importance of switching to the Max-Link mode, when we have low power SD links.

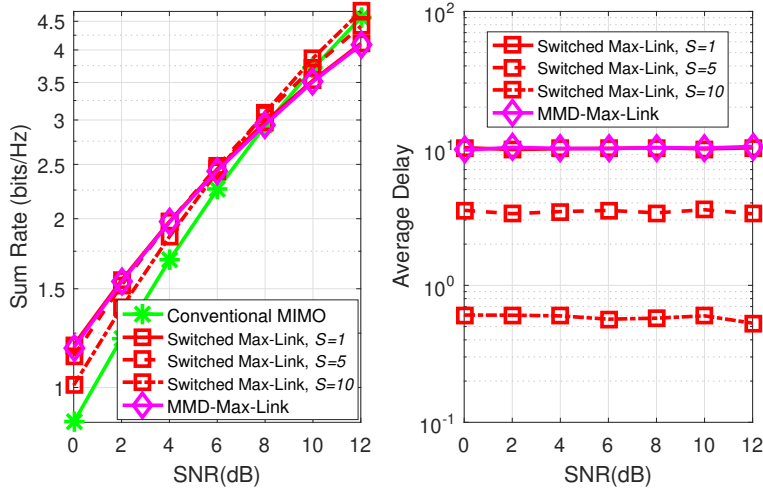


Figure 3.8: a) Sum-rate and b) average delay performances, with low power SD links.

Fig. 3.8 shows the sum-rate (assuming Gaussian signaling) and the average delay performances of the Switched Max-Link, MMD-Max-Link and the conventional MIMO protocols, for the same configuration described in Fig. 3.7. We notice that the simulated average delay of the MMD-Max-Link is equal to its theoretical value ($\frac{NJ}{M_S} = 10$). This result validates the accuracy of our analysis in Section 3.4. When we increase \mathcal{S} in the proposed Switched Max-Link, the average delay reduces and is less than 1 time slot, when \mathcal{S} is equal to 10. This result also validates the accuracy of our analysis. Moreover, the sum-rate of the proposed Switched Max-Link, for SNR values less than 6dB, is increased when we reduce \mathcal{S} , and, for SNR values greater than 6dB, it is increased when we increase \mathcal{S} .

Fig. 3.9 shows the BER performance of the Switched Max-Link, MMD-Max-Link and the conventional MIMO protocols, for $M_S = M_R = M = 2$, $N = 5$, $J = 4$, $\mathcal{S} = 1, 3$ and 5 , BPSK, perfect CSI and high power SD links ($\sigma_{S,R}^2 = \sigma_{R,D}^2 = 1$ and $\sigma_{S,D}^2 = 5$). The performance of the proposed Switched Max-Link scheme, for the \mathcal{S} values tested, is better than that of the conventional MIMO and considerably better than that of the MMD-Max-Link scheme, illustrating the importance of switching to DT mode, when we have high power SD links.

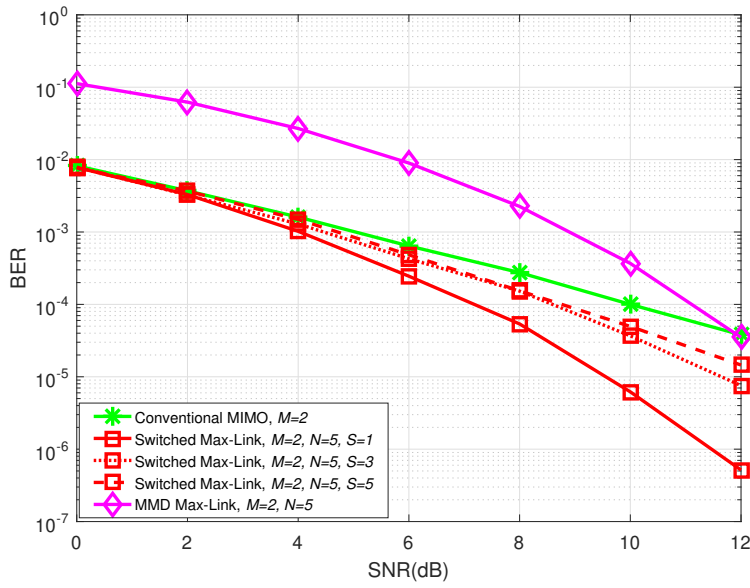


Figure 3.9: BER performance, with high power SD links.

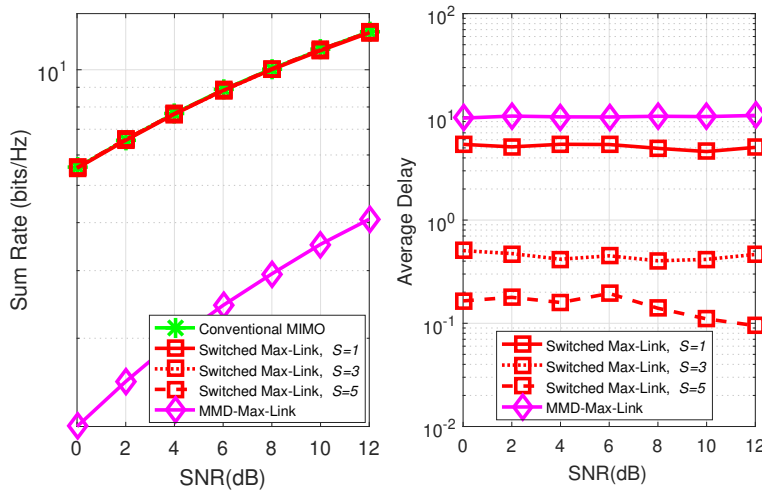


Figure 3.10: a) Sum-rate and b) average delay performances, with high power SD links.

Fig. 3.10 shows the sum-rate and the average delay performances of the Switched Max-Link, MMD-Max-Link and the conventional MIMO protocols, for the same configuration described in Fig. 3.9. When we increase \mathcal{S} in the proposed Switched Max-Link, the average delay reduces and is less than 1 time slot, when \mathcal{S} is greater than 3. Moreover, the sum-rate performance of the proposed Switched Max-Link (for all the \mathcal{S} values tested) is very close to that of conventional MIMO, for all the range of SNR values tested, and considerably higher than that of the MMD-Max-Link scheme.

Fig. 3.11 shows the BER performance of the Switched Max-Link, MMD-Max-Link and the conventional MIMO protocols, for $M_S = M_R = M = 2$,

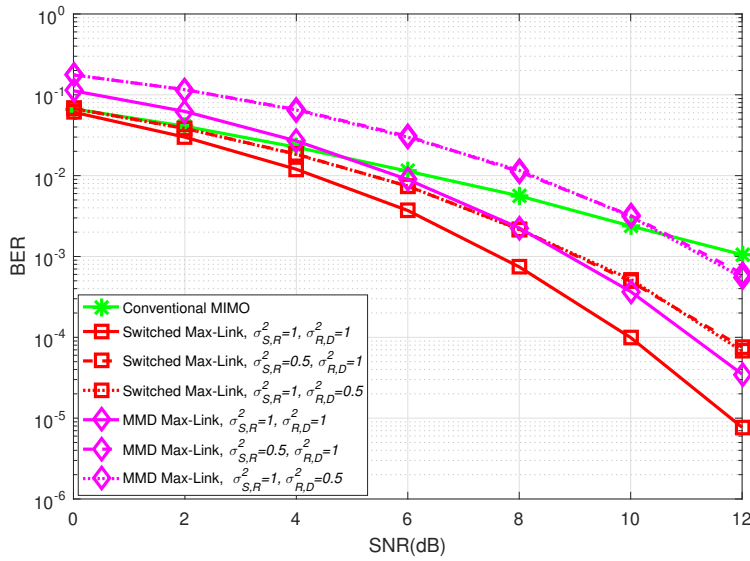


Figure 3.11: BER performance, with low power SR or RD links.

$N = 5$, $J = 4$, $\mathcal{S} = 1$, BPSK, perfect CSI and low power SR or RD links ($\sigma_{S,R}^2 = 0.5$ and 1 , $\sigma_{R,D}^2 = 0.5$ and 1 , $\sigma_{S,D}^2 = 1$). Switched Max-Link outperforms conventional MIMO and MMD-Max-Link schemes, illustrating that even with low power SR or RD links, Switched Max-Link has a better performance than that of conventional MIMO.

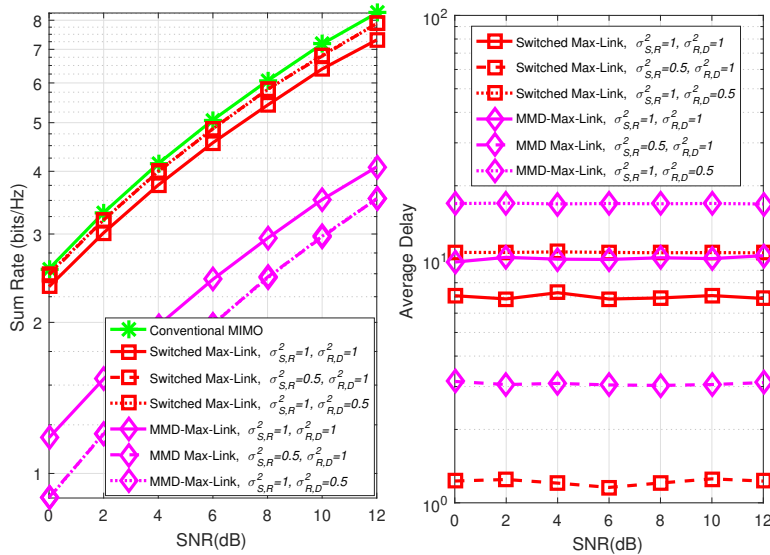


Figure 3.12: a) Sum-rate and b) average delay performances, with low power SR or RD links.

Fig. 3.12 shows the sum-rate and the average delay performances of the Switched Max-Link, MMD-Max-Link and the conventional MIMO protocols, for the same configuration described in Fig. 3.11. When we have low power SR

links ($\sigma_{S,R}^2 = 0.5$ and $\sigma_{R,D}^2 = 1$), the probability of selecting an SR link is less than the probability of selecting an RD link, so the average delay is less than the average delay with equal unit power channels ($\sigma_{S,R}^2 = 1$ and $\sigma_{R,D}^2 = 1$). Otherwise, when we have low power RD links ($\sigma_{S,R}^2 = 1$ and $\sigma_{R,D}^2 = 0.5$), the probability of selecting an RD link is less than the probability of selecting an SR link, so the average delay is greater than the average delay with equal unit power channels. Moreover, the sum-rate performance of the proposed Switched Max-Link is very close to that of conventional MIMO, even for low power SR or RD links, and considerably higher than that of the MMD-Max-Link scheme. The slightly worse sum-rate performance of Switched Max-Link compared to conventional MIMO is justified, as the proposed scheme is able to transmit with higher order modulation due to the improved BER performance.

3.5.3 Performance for Massive MIMO

In the following we consider the performance of the proposed scheme for massive MIMO (with a small number of antennas at S and D and a large number of antennas at the relays).

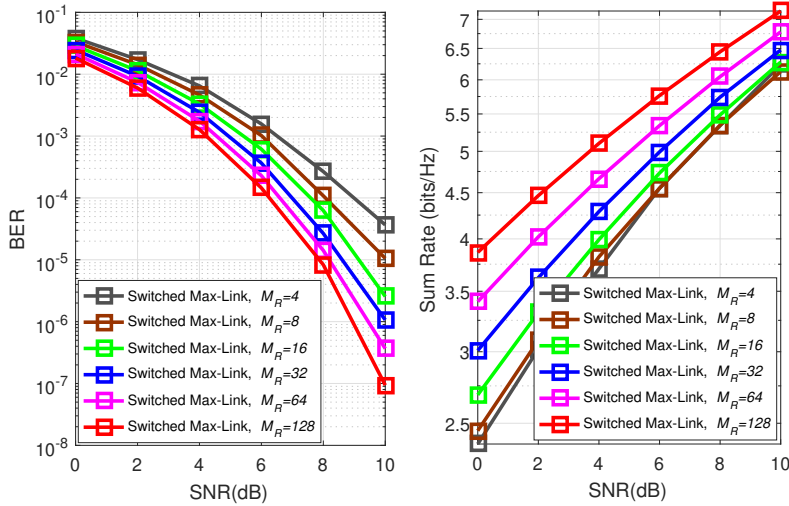


Figure 3.13: a) BER and b) sum-rate performances, for massive MIMO.

Fig. 3.13 shows the BER and sum-rate performances of the Switched Max-Link protocol, for $M_S = 2$, $M_R = 4, 8, 16, 32, 64$ and 128 , $N = 5$, $J = 4$, $\mathcal{S} = 1$, BPSK, perfect CSI and unit power links ($\sigma_{S,R}^2 = \sigma_{R,D}^2 = \sigma_{S,D}^2 = 1$). Both the BER and sum-rate performances are considerably improved when we increase M_R , illustrating that the proposed protocol can be used for massive MIMO (with a small number of antennas at S and D and a large number of antennas at the relays). This result validates the accuracy of our analysis, as

when $U > 1$, the maximization of the minimum distances related to \mathbf{H}^u also implies the maximization of the minimum value of the PEP argument. Note that the achieved BER values were considerably reduced, thus the transmit signal-to-noise ratio SNR (E/N_0) ranges from 0 to 10 dB.

3.6

Summary

In this chapter, we have presented the benefits of using a novel relay selection protocol based on switching and the selection of the best link, denoted as Switched Max-Link. We then consider the MMD relay selection criterion for MIMO systems, along with algorithms that are incorporated into the proposed Switched Max-Link protocol. Switched Max-Link was evaluated experimentally and outperformed the conventional direct transmission and the existing QN Max-Link scheme. Despite the higher complexity of the proposed Switched Max-Link with the MMD relay selection criterion, it is an attractive solution for relaying systems with source and destination nodes equipped with a small number of antennas ($M_S \leq 2$) and relay nodes equipped with a small or large number of antennas due to its high performance and reduced delay.

Table 3.2: Switched Max-Link Pseudo-Code

-
- 1: Calculate the metrics $\mathcal{D}_{SR_i}^u$, of each submatrix \mathbf{H}_{S,R_i}^u of R_i

$$\mathcal{D}_{SR_i}^u = \left\| \sqrt{E/M_S} \mathbf{H}_{S,R_i}^u \mathbf{x}_l - \sqrt{E/M_S} \mathbf{H}_{S,R_i}^u \mathbf{x}_n \right\|^2 ;$$

$$i = 1, \dots, N$$

$$u = 1, \dots, U$$

$$l = 1, \dots, N_s^{M_S} - 1$$

$$n = l + 1, \dots, N_s^{M_S}$$
 - 2: Find the minimum distance - $\mathcal{D}_{\min SR_i}^u$

$$\mathcal{D}_{\min SR_i}^u = \min (\mathcal{D}_{SR_i}^u);$$
 - 3: Calculate the metrics $\mathcal{D}_{R_i D}^u$, of each submatrix $\mathbf{H}_{R_i,D}^u$ of R_i

$$\mathcal{D}_{R_i D}^u = \left\| \sqrt{E/M_S} \mathbf{H}_{R_i,D}^u \mathbf{x}_l - \sqrt{E/M_S} \mathbf{H}_{R_i,D}^u \mathbf{x}_n \right\|^2 ;$$
 - 4: Find the minimum distance - $\mathcal{D}_{\min R_i D}^u$

$$\mathcal{D}_{\min R_i D}^u = \min (\mathcal{D}_{R_i D}^u);$$
 - 5: Find the largest minimum distance - $\mathcal{D}_{\min R_i D}$

$$\mathcal{D}_{\min R_i D} = \max (\mathcal{D}_{\min R_i D}^u);$$
 - 6: Compute the expected values and $\mathcal{D}_{\min SR_i}$

$$\mathcal{D}_{\min SR_i} = \frac{\mathbb{E}[\mathcal{D}_{\min R_i D}]}{\mathbb{E}[\mathcal{D}_{\min SR_i}^u]} \mathcal{D}_{\min SR_i}^u ;$$
 - 7: Perform ordering on $\mathcal{D}_{\min SR_i}$ and $\mathcal{D}_{\min R_i D}$
 - 8: Find the maximum minimum distance
$$\mathcal{D}_{\max \min SR-RD} = \max (\mathcal{D}_{\min SR_i}, \mathcal{D}_{\min R_i D});$$
 - 9: Calculate the metrics \mathcal{D}_{SD}

$$\mathcal{D}_{SD} = \left\| \sqrt{2E/M_S} \mathbf{H}_{S,D} \mathbf{x}_l - \sqrt{2E/M_S} \mathbf{H}_{S,D} \mathbf{x}_n \right\|^2 ;$$
 - 10: Find the minimum distance - $\mathcal{D}_{\min SD}$

$$\mathcal{D}_{\min SD} = \min (\mathcal{D}_{SD});$$
 - 11: Select the transmission mode
$$\mathcal{D}_{\max \min} = \mathcal{D}_{\max \min SR-RD};$$

$$G = \frac{\mathcal{D}_{\max \min}}{\mathcal{D}_{\min SD}};$$

$$\text{Mode} = \begin{cases} \text{Max-Link-SR}, & \text{if } (\mathcal{D}_{\max \min} = \max (\mathcal{D}_{\min SR_i})) \& (G > \mathcal{S}),^\dagger \\ \text{Max-Link-RD}, & \text{if } (\mathcal{D}_{\max \min} = \max (\mathcal{D}_{\min R_i D})) \& (G > 1), \\ \text{DT}, & \text{otherwise.} \end{cases}$$

[†] Note that $\mathcal{S} \in \{0, 1, 2, \dots\}$ is a parameter that works as a switch. When $\mathcal{S} = 0$ the scheme operates only in the Max-Link-(SR or RD) mode (MMD-Max-Link protocol). Moreover, when $\mathcal{S} > 0$ the scheme operates in the Max-Link-(SR or RD) or DT mode (Switched-Max-Link protocol).

Table 3.3: Computational Complexity of Criteria

Operations/Criterion	Maximum Minimum Distance	Quadratic Norm
additions	$2NUM_S(\mathcal{X} - 1)$	$2NU(M_S^2 - 1)$
multiplications	$2NUM_S\mathcal{X}$	$2NUM_S^2$

4

Buffer-Aided Max-Link Relay Selection for Multi-Way Cooperative Multi-Antenna Systems

In this chapter, we present a relay-selection strategy for multi-way cooperative multi-antenna systems that are aided by a central processor node, where a cluster formed by two users is selected to simultaneously transmit to each other with the help of relays. In particular, we present a novel multi-way relay selection strategy based on the selection of the best link, exploiting the use of buffers and physical-layer network coding, that is called Multi-Way Buffer-Aided Max-Link (MW-Max-Link). We compare the proposed MW-Max-Link to existing techniques in terms of bit error rate, pairwise error probability, sum rate and computational complexity. Simulations are then employed to evaluate the performance of the proposed and existing techniques.

4.1

Introduction

The Multi-Way Relay Channel [92] includes a full data exchange model, in which each user receives messages of all other users, and the pairwise data exchange model, which consists of multiple two-way relay channels over which two users (U_1 and U_2) exchange messages with the help of a common intermediate relay R . In order to adapt to modern requirements, relaying schemes with high spectrum efficiency have recently attracted considerable attention [84].

An important two-way protocol category is called Multiple-Access Broadcast-Channel (MABC). In MABC DF protocols, as in TW-Max-Min [82], transmission is organized in a prefixed schedule with two consecutive time slots. In the first time slot (MA phase), a selected relay receives and decodes the data simultaneously transmitted from two source nodes and physical layer network coding (PLNC) may be employed on the decoded data. In the second time slot (BC phase), the same relay forwards the decoded data to the two source nodes, which become destinations. Since all the channels are reciprocal (restricted to Time Division Multiplexing - TDM) and fixed during the two phases of the MABC protocol, the TW-Max-Min protocol [82] achieves a maximum diversity

gain. On the other hand, by considering non reciprocal channels, the performance of relaying schemes may be improved by using a buffer-aided relaying protocol, where the relay may accumulate packets in a buffer [35], before transmitting to the destination nodes, as in the one-way Max-Link protocol, which selects in each time slot the more powerful channel among all the available SR and RD channels (i.e., among $2N$ channels) [39]. For independent and identically distributed (i.i.d.) channels, Max-Link achieves a diversity gain of $2N$, where N is the number of relays. Prior work has not considered multi-way protocols for multi-antenna systems or the use of a multi-way Max-Link (in which each pair of users has a particular buffer in the relays) or a central processor node.

In this chapter, we propose a multi-way Max-Link protocol for buffer-aided cooperative multi-antenna systems (MW-Max-Link) in non reciprocal channels. The proposed MW-Max-Link protocol selects the best channels among Z pairs of users and achieves a diversity gain of $2NZ$. The TW-Max-Link [14] protocol (a special case of MW-Max-Link, for a single two-way relay channel ($Z = 1$)), is also presented. We also extend the MMD criterion [11] to multi-way systems for selection of relays in the proposed scheme and the existing TW-Max-Min (here adapted for multi-antenna systems) and carry out pairwise error probability (PEP), sum rate and computational complexity analyses.

4.2 System Description

We consider a multi-antenna multi-way MABC relay scheme with $Z \in \{1, 2, 3, \dots\}$ pairs of users and N half-duplex DF relays, R_1, \dots, R_N . The users are equipped with M antennas and each relay with $2M$ antennas. In [14], the performance of TW-Max-Link with $2M$ antennas at each relay was shown to be considerably better than that with only M antennas. In MW-Max-Link, a total of Z buffers are employed by the selected relays for storing or extracting (each pair of users has a particular buffer established on demand in the relays), as shown in Fig. 4.1. In the MA phase, a relay R_g will be selected to receive simultaneously M packets from a selected cluster (pair of users U_1 and U_2) and decode the data. Then, PLNC is employed on the decoded data and the resulting packets are stored in their particular buffers. In the BC phase, a relay R_f will be selected to transmit M packets from the particular buffer to the selected cluster.

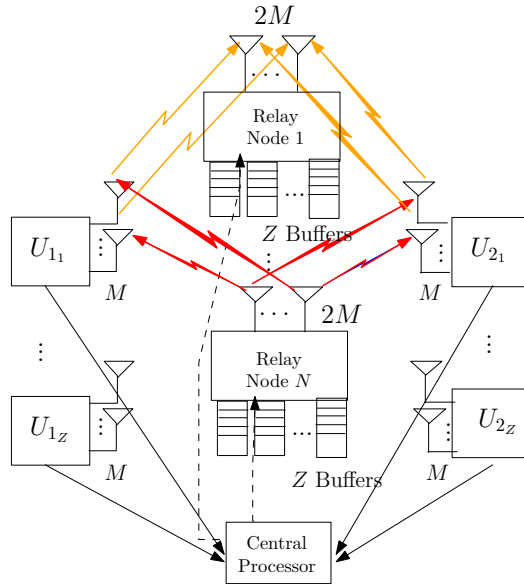


Figure 4.1: System model of a buffer-aided multi-way relay system.

4.2.1 Assumptions

In each time slot, the total energy transmitted from each user to the relay selected for reception or from the relay selected for transmission to the selected cluster is the same and equal to E . The channel coefficients are drawn from mutually independent zero mean complex Gaussian random variables. The transmission is performed in data packets and the channels are assumed constant for the duration of one packet and vary independently from one packet to the following. Fig. 4.2 illustrates the frame of the data packets. The order of the data packets is inserted in the preamble of each packet, so the original order is restored at the destination nodes. Pilot symbols for training and estimation of channel state information (CSI), and signaling for network coordination are also inserted in the preamble of the packet. A central processor node is responsible for deciding whether a cluster or the relay should transmit in a given time slot i , through a feedback channel. This can be ensured by an appropriate signalling that provides global CSI at the central processor node [39]. Furthermore, we assume that each relay only has information about its U_1R and U_2R channels. The use of a unique central processor node reduces its complexity, since a single central node is responsible for deciding which node will transmit (rather than all destination nodes being responsible together).

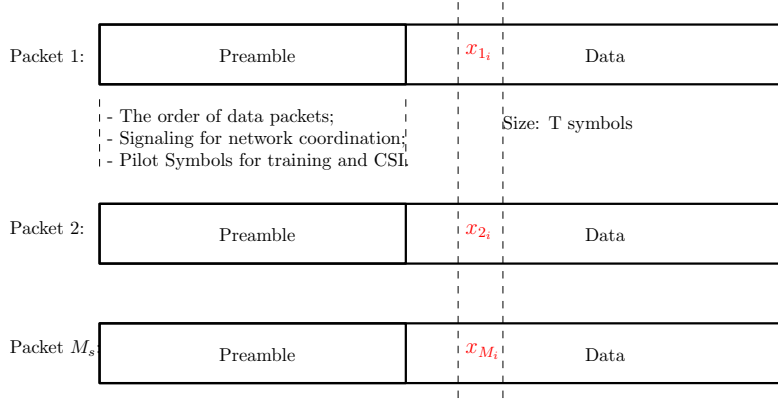


Figure 4.2: The frame of each packet.

4.2.2 System Model

At the MA phase of multi-way MABC DF systems, the received signal from the selected cluster U (formed by U_1 and U_2) to the selected relay R_g is formed by an $2M \times 1$ vector $\mathbf{y}_{U,R_g}[i]$ given by

$$\mathbf{y}_{U,R_g}[i] = \sqrt{\frac{E}{M}} \mathbf{H}_{U,R_g} \mathbf{x}[i] + \mathbf{n}_{R_g}[i], \quad (4-1)$$

where $\mathbf{x}[i]$ represents the vector formed by M symbols transmitted by U_1 and U_2 ($\mathbf{x}_1[i]$ and $\mathbf{x}_2[i]$), \mathbf{H}_{U,R_g} is the $2M \times 2M$ matrix of $U_1 R_g$ and $U_2 R_g$ channels and \mathbf{n}_{R_g} represents the zero mean additive white complex Gaussian noise (AWGN) at the relay selected for reception.

Assuming synchronization, we employ the Maximum Likelihood (ML) receiver at the selected relay for reception:

$$\hat{\mathbf{x}}[i] = \arg \min_{\mathbf{x}'[i]} \left(\left\| \mathbf{y}_{U,R_g}[i] - \sqrt{\frac{E}{M}} \mathbf{H}_{U,R_g} \mathbf{x}'[i] \right\|^2 \right), \quad (4-2)$$

where $\mathbf{x}'[i]$ represents each of the N_s^{2M} possible transmitted symbols vector $\mathbf{x}[i]$ (N_s is the number of constellation symbols). The ML receiver computes an estimate of the vector of symbols transmitted by the users $\hat{\mathbf{x}}[i]$. Considering Binary Phase Shift Keying (BPSK) ($N_s = 2$), unit power symbols and $M = 1$, the estimated symbol vector $\hat{\mathbf{x}}[i]$ may be $[-1 \ -1]^T$, $[-1 \ +1]^T$, $[+1 \ -1]^T$ or $[+1 \ +1]^T$.

By employing PLNC (XOR), it is not necessary to store the $2M$ packets transmitted by the selected cluster, but only the resulting M packets (XOR outputs) with the information: "the bit transmitted by U_1 is different (or not) from the corresponding bit transmitted by U_2 ". Then, we employ the XOR:

$\mathbf{v}[i] = \hat{\mathbf{x}}_1[i] \oplus \hat{\mathbf{x}}_2[i]$ and store the resulting packets in the buffer.

In the case of BPSK, if a symbol $\hat{x}_1[i] \in \hat{\mathbf{x}}_1[i]$ is different from the corresponding $\hat{x}_2[i] \in \hat{\mathbf{x}}_2[i]$, the XOR output is equal to +1, otherwise it is equal to -1, resulting in another vector of M BPSK symbols. On the other hand, in the case of QPSK, if the real part of $\hat{x}_1[i]$ is different from the real part of the corresponding $\hat{x}_2[i]$, the output is equal to $+\sqrt{2}/2$, otherwise it is equal to $-\sqrt{2}/2$. Moreover, the same reasoning is applied to the imaginary part of $\hat{x}_1[i]$ and $\hat{x}_2[i]$, but the output is multiplied by j . Then the outputs of these two XOR operations are summed, resulting in another vector of M QPSK symbols.

At the BC phase, the signal transmitted from the selected relay R_f and received at the selected cluster (U_1 and U_2) is formed by an $M \times 1$ vector $\mathbf{y}_{R_f, U_{1(2)}}[i]$ given by

$$\mathbf{y}_{R_f, U_{1(2)}}[i] = \sqrt{\frac{E}{M}} \mathbf{H}_{R_f, U_{1(2)}} \mathbf{v}[i] + \mathbf{n}_{U_{1(2)}}[i], \quad (4-3)$$

where $\mathbf{H}_{R_f, U_{1(2)}}$ is the $M \times M$ matrix of $R_f U_{1(2)}$ channels and $\mathbf{n}_{U_{1(2)}}[i]$ represents the AWGN at U_1 or U_2 . At the selected cluster, we also employ the ML receiver which yields

$$\hat{\mathbf{v}}_{1(2)}[i] = \arg \min_{\mathbf{v}'[i]} \left(\left\| \mathbf{y}_{R_f, U_{1(2)}}[i] - \sqrt{\frac{E}{M}} \mathbf{H}_{R_f, U_{1(2)}} \mathbf{v}'[i] \right\|^2 \right) \quad (4-4)$$

where $\mathbf{v}'[i]$ represents each possible vector formed by M symbols. Then, at U_1 we compute the vector of symbols transmitted by U_2 by employing PLNC (XOR): $\hat{\mathbf{x}}_2[i] = \mathbf{x}_1[i] \oplus \hat{\mathbf{v}}_1[i]$. The same reasoning is applied at U_2 to compute the vector of symbols transmitted by U_1 : $\hat{\mathbf{x}}_1[i] = \mathbf{x}_2[i] \oplus \hat{\mathbf{v}}_2[i]$. In scenarios with imperfect CSI when applying the ML receiver, the estimated channel matrix $\hat{\mathbf{H}}$ is assumed instead of \mathbf{H} in (4-2) and (4-4).

4.3

Proposed MW-Max-Link Relay Selection Scheme

The proposed MW-Max-Link scheme is aimed for use with the system shown in Fig. 4.1. This proposed scheme operates in two possible modes in each time slot: MA or BC. It is not necessary that a number of buffer elements be filled with packets before the system starts its normal operation for this scheme to work properly and may be empty. Despite that, in this work, we consider that half of the buffer elements are filled in an initialization phase [11], by allowing the users to transmit a number of packets to the relays, before the

scheme is used. During this initialization phase the relays do not transmit and the users transmit to the relay with the best set of M U_1R and U_2R links among the available relays. Table 4.1 shows the MW-Max-Link pseudo-code and the following subsections explain how this protocol works.

Table 4.1: MW-Max-Link Pseudo-Code

-
- 1: Calculate the metrics \mathcal{B}_{UR_n} , for the MA mode

$$\mathcal{B}_{UR_n} = \left\| \sqrt{\frac{E}{M}} \mathbf{H}_{U,R_n} \mathbf{x}_i - \sqrt{\frac{E}{M}} \mathbf{H}_{U,R_n} \mathbf{x}_j \right\|^2;$$

$$\begin{aligned} n &= 1, \dots, N \\ i &= 1, \dots, N_s^{2M} - 1 \\ j &= i + 1, \dots, N_s^{2M} \end{aligned}$$
 - 2: Find the minimum distance - $\mathcal{B}_{\min UR_n}$

$$\mathcal{B}_{\min UR_n} = \min(\mathcal{B}_{UR_n});$$
 - 3: Perform ordering on $\mathcal{B}_{\min UR_n}$ and find the largest distance, for each cluster

$$\mathcal{B}_{z_{\max \min UR}} = \max(\mathcal{B}_{\min UR_n});$$
 - 4: Calculate the metrics $\mathcal{B}_{R_n U_1}$, for each cluster, for the BC mode

$$\mathcal{B}_{R_n U_1} = \left\| \sqrt{\frac{E}{M}} \mathbf{H}_{R_n, U_1} \mathbf{x}_i - \sqrt{\frac{E}{M}} \mathbf{H}_{R_n, U_1} \mathbf{x}_j \right\|^2;$$

$$\begin{aligned} n &= 1, \dots, N \\ i &= 1, \dots, N_s^M - 1 \\ j &= i + 1, \dots, N_s^M \end{aligned}$$
 - 5: Find the minimum distance - $\mathcal{B}_{\min R_n U_1}$

$$\mathcal{B}_{\min R_n U_1} = \min(\mathcal{B}_{R_n U_1});$$
 - 6: Calculate the metrics $\mathcal{B}_{R_n U_2}$ and find $\mathcal{B}_{\min R_n U_2}$
 - 7: Compare and store the smallest distance - $\mathcal{B}_{\min R_n U}$

$$\mathcal{B}_{\min R_n U} = \min(\mathcal{B}_{\min R_n U_1}, \mathcal{B}_{\min R_n U_2});$$
 - 8: Perform ordering on $\mathcal{B}_{\min R_n U}$ and find the largest distance, for each cluster

$$\mathcal{B}_{z_{\max \min RU}} = \max(\mathcal{B}_{\min R_n U});$$
 - 9: Perform ordering and find the largest distance

$$\mathcal{B}_{\max \min RU} = \max(\mathcal{B}_{z_{\max \min RU}});$$
 - 10: Select the transmission mode

If $\frac{\mathcal{B}_{\max \min UR}}{\mathcal{B}_{\max \min RU}} \geq C$
 Operate in "MA mode";
else
 Operate in "BC mode";
end
-

4.3.1 Relay selection metric

In the first step, for each cluster formed by U_1 and U_2 , we compute the metric \mathcal{B}_{UR_n} associated with the user-relay (UR) channels of each relay R_n , for the MA mode:

$$\mathcal{B}_{UR_n} = \left\| \sqrt{\frac{E}{M}} \mathbf{H}_{U,R_n} \mathbf{x}_i - \sqrt{\frac{E}{M}} \mathbf{H}_{U,R_n} \mathbf{x}_j \right\|^2, \quad (4-5)$$

where $n \in \{1, \dots, N\}$, \mathbf{x}_i and \mathbf{x}_j represent each possible vector formed by $2M$ symbols and " i " is different from " j ". This metric is computed for each of the $C_2^{N_s 2M}$ (combination of N_s^{2M} in 2) possibilities.

In the second step, we store the smallest metric ($\mathcal{B}_{\min UR_n}$), for being critical, and thus each relay will have a minimum distance associated with its UR channels:

$$\mathcal{B}_{\min UR_n} = \min(\mathcal{B}_{UR_n}) \quad (4-6)$$

Then, in the third step, we perform ordering on $\mathcal{B}_{\min UR_n}$ and store the largest of these distances:

$$\mathcal{B}_{z_{\max \min UR}} = \max(\mathcal{B}_{\min UR_n}) \quad (4-7)$$

where $z \in \{1, \dots, Z\}$. After finding $\mathcal{B}_{z_{\max \min UR}}$ for each cluster, we perform ordering and store the largest of these distances:

$$\mathcal{B}_{\max \min UR} = \max(\mathcal{B}_{z_{\max \min UR}}) \quad (4-8)$$

Then, we select the cluster and the relay that is associated with this distance to receive simultaneously M packets from the selected cluster.

In the fourth step, for each cluster, we compute the metric $\mathcal{B}_{R_n U_1}$ associated with the RU_1 channels of each relay R_n , for the BC mode:

$$\mathcal{B}_{R_n U_1} = \left\| \sqrt{\frac{E}{M}} \mathbf{H}_{R_n, U_1} \mathbf{x}_i - \sqrt{\frac{E}{M}} \mathbf{H}_{R_n, U_1} \mathbf{x}_j \right\|^2, \quad (4-9)$$

where $n \in \{1, \dots, N\}$, \mathbf{x}_i and \mathbf{x}_j represent each possible vector formed by M symbols and " i " is different from " j ". This metric is computed for each of the $C_2^{N_s M}$ possibilities. In the fifth step, we find the minimum distance for each

relay R_n :

$$\mathcal{B}_{\min R_n U_1} = \min(\mathcal{B}_{R_n U_1}), \quad (4-10)$$

In the sixth step, we apply the same reasoning of (4-9) and (4-10), to compute the metrics $\mathcal{B}_{R_n U_2}$ and $\mathcal{B}_{\min R_n U_2}$. In the seventh step, we compare the distances $\mathcal{B}_{\min R_n U_1}$ and $\mathcal{B}_{\min R_n U_2}$ and store the smallest one:

$$\mathcal{B}_{\min R_n U} = \min(\mathcal{B}_{\min R_n U_1}, \mathcal{B}_{\min R_n U_2}) \quad (4-11)$$

In the eighth step, after finding $\mathcal{B}_{\min R_n U}$ for each relay R_n , we perform ordering and store the largest of these distances:

$$\mathcal{B}_{z_{\max \min RU}} = \max(\mathcal{B}_{\min R_n U}) \quad (4-12)$$

where $z \in \{1, \dots, Z\}$. After finding $\mathcal{B}_{z_{\max \min RU}}$ for each cluster, we perform ordering and store the largest of these distances:

$$\mathcal{B}_{\max \min RU} = \max(\mathcal{B}_{z_{\max \min RU}}) \quad (4-13)$$

Then, we select the cluster and the relay that are associated with this distance to transmit simultaneously M packets from the particular buffer to the selected cluster. Considering imperfect CSI, the estimated channel matrix $\hat{\mathbf{H}}$ is assumed, instead of \mathbf{H} in (4-5) and (4-9).

4.3.2 Comparison of metrics and choice of transmission mode

After computing all the metrics associated with the UR and RU channels and finding $\mathcal{B}_{\max \min UR}$ and $\mathcal{B}_{\max \min RU}$, we compare these parameters and choose the transmission mode:

$$\begin{cases} \text{if } \frac{\mathcal{B}_{\max \min UR}}{\mathcal{B}_{\max \min RU}} \geq C, \text{ then} & \text{"MA mode",} \\ \text{otherwise,} & \text{"BC mode",} \end{cases}$$

where $C = \frac{\mathbb{E}[\mathcal{B}_{\max \min UR}]}{\mathbb{E}[\mathcal{B}_{\max \min RU}]}$. Thus, the probability of a relay being selected for transmission is close to the probability of a relay being selected for reception, and, consequently, the protocol works in a balanced way, even for asymmetric channels.

4.4 Analysis

In this section, we first analyze the proposed MW-Max-Link in terms of PEP. Then, an approximated expression for the sum-rate of the proposed MW-Max-Link protocol is derived and the complexity of the proposed and existing schemes are also presented.

4.4.1 Pairwise Error Probability

The equations for \mathcal{B}_{UR_n} , $\mathcal{B}_{R_nU_1}$ and $\mathcal{B}_{R_nU_2}$ may be simplified by making $\mathcal{B} = E/M \times \mathcal{B}'$, where $\mathcal{B}' = \|\mathbf{H}(\mathbf{x}_i - \mathbf{x}_j)\|^2$ in (4-5) and (4-9). The PEP considers the error event when \mathbf{x}_i is transmitted and the detector computes an incorrect \mathbf{x}_j (where "i" is different from "j"), based on the received symbol [11]. The PEP is given by

$$\mathbf{P}(\mathbf{x}_i \rightarrow \mathbf{x}_j|\mathbf{H}) = Q\left(\sqrt{\frac{E}{2N_0M}\mathcal{B}'}\right), \quad (4-14)$$

where N_0 is the power spectrum density of the AWGN. The PEP will have its maximum value for the minimum value of \mathcal{B}' (PEP worst case). Thus, assuming that the probability of having no error in the two phases of the system is approximately given by the square of $(1 - \mathbf{P}(\mathbf{x}_i \rightarrow \mathbf{x}_j|\mathbf{H}))$, an expression for calculating the worst case of the PEP for cooperative transmissions (CT), in each time slot (regardless of whether it is an *UR* or *RU* channel), is given by

$$\begin{aligned} \mathbf{P}^{CT}(\mathbf{x}_i \rightarrow \mathbf{x}_j|\mathbf{H}) &= 1 - (1 - \mathbf{P}(\mathbf{x}_i \rightarrow \mathbf{x}_j|\mathbf{H}))^2 \\ &= 1 - \left(1 - Q\left(\sqrt{\frac{E}{2N_0M}\mathcal{B}'_{\min}}\right)\right)^2. \end{aligned} \quad (4-15)$$

Note that this expression may be used for calculating the worst case of the PEP, for both symmetric and asymmetric channels. The extended MMD relay selection algorithm maximizes the metric \mathcal{B}'_{\min} and, consequently, minimizes the PEP worst case in the proposed MW-Max-Link scheme.

4.4.2 Sum-Rate

The sum rate of a given system is upper bounded by the system capacity. In the MW-Max-Link scheme, as R_g may be different from R_f , its capacity is

given by [1, 102]:

$$C_{DF} = \frac{1}{2} \min\{I_{DF}^{URg}, I_{DF}^{RfU}\}, \quad (4-16)$$

where the first and second terms in (4-16) represent the maximum rate at which R_g can reliably decode the messages transmitted by the selected cluster (U_1 and U_2) and at which the selected cluster can reliably decode the estimated messages transmitted by R_f , respectively. For the mutual information between the users U_1 and U_2 and R_g , considering perfect CSI, we have

$$\begin{aligned} I_{DF}^{UR} &= I_{DF}(\mathbf{x}; \mathbf{y}_{U,R} | \mathbf{H}_{U,R}), \\ &= \log_2 \det \left(\frac{\mathbf{H}_{U,R} \mathbf{Q}_{U,R} (\mathbf{H}_{U,R})^H}{N_0} + \mathbf{I}_{2M} \right), \end{aligned} \quad (4-17)$$

where $\mathbf{H}_{U,R}$ represents a $2M \times 2M$ channel matrix and $\mathbf{Q}_{U,R} = E[\mathbf{x}(\mathbf{x})^H] = \frac{E}{M} \mathbf{I}_{2M}$ is the covariance matrix of the transmitted symbols. Note that the vectors \mathbf{x} are formed by independent and identically distributed (i.i.d.) symbols. The same reasoning can be applied to I_{DF}^{RU} :

$$I_{DF}^{RU} = \log_2 \det \left(\frac{\mathbf{H}_{R,U} \mathbf{Q}_{R,U} (\mathbf{H}_{R,U})^H}{N_0} + \mathbf{I}_M \right), \quad (4-18)$$

where $\mathbf{Q}_{R,U} = \frac{E}{M} \mathbf{I}_M$ and $\mathbf{H}_{R,U}$ represents an $M \times M$ channel matrix.

To compute the sum rate of the MW-Max-Link scheme, instead of (4-16), we consider an approximated expression for the sum rate in each time slot, depending on the kind of transmission. Then, in the case of a time slot i selected for UR transmission, the approximated sum-rate is given by

$$\mathcal{R}_i^{UR} \approx \frac{1}{2} \log_2 \det \left(\frac{\mathbf{H}_{U,R} \mathbf{Q}_{U,R} (\mathbf{H}_{U,R})^H}{N_0} + \mathbf{I}_{2M} \right). \quad (4-19)$$

Moreover, in the case of a time slot i selected for RU transmission, the approximated sum-rate is given by

$$\mathcal{R}_i^{RU_{1(2)}} \approx \frac{1}{2} \log_2 \det \left(\frac{\mathbf{H}_{R,U_{1(2)}} \mathbf{Q}_{R,U} (\mathbf{H}_{R,U_{1(2)}})^H}{N_0} + \mathbf{I}_M \right). \quad (4-20)$$

Therefore, by summing the sum-rate values found in each time slot and dividing this result by the total number of time slots, the average sum rate (\mathcal{R}) of the MW-Max-Link scheme may be approximated by

$$\mathcal{R} \approx \frac{\sum_{i=1}^{n_{UR}} \mathcal{R}_i^{UR} + \sum_{i=1}^{n_{RU}} (\mathcal{R}_i^{RU_1} + \mathcal{R}_i^{RU_2})}{n_{UR} + n_{RU}}, \quad (4-21)$$

where n_{UR} and n_{RU} represent the number of time slots selected for UR and RU transmissions, respectively.

4.4.3 Computational Complexity

The complexity of the proposed MW-Max-Link, TW-Max-Link and the existing TW-Max-Min scheme (here adapted for multiple-antenna systems) are associated with the complexity of the MMD protocol [11]. The number \mathcal{X} of calculations of the metric \mathcal{B} for each channel matrix \mathbf{H} is given by

$$\mathcal{X} = \sum_{i=1}^{M'} 2^{i-1} W^i C_i^{M'}, \quad (4-22)$$

where $M' = 2M$ in the case of \mathcal{B}_{UR_n} , for the MA mode (\mathcal{X}^{MA}), and $M' = M$ in the case of $\mathcal{B}_{R_n U_1}$ and $\mathcal{B}_{R_n U_2}$, for the BC mode (\mathcal{X}^{BC}), W is the number of different distances between the constellation symbols. If we have BPSK, $W = 1$, and QPSK, $W = 3$.

Table 4.2: MW-Max-Link - Computational Complexity

Operations	MW-Max-Link	TW-Max-Min [82]
additions	$ZNM(2\mathcal{X}^{BC} + \mathcal{X}^{MA} - 3)$	$\frac{NM}{2}(2\mathcal{X}^{BC} + \mathcal{X}^{MA} - 3)$
multiplications	$ZNM(2\mathcal{X}^{BC} + \mathcal{X}^{MA})$	$\frac{NM}{2}(2\mathcal{X}^{BC} + \mathcal{X}^{MA})$

Table 4.2 shows the complexity of the proposed MW-Max-Link and the existing TW-Max-Min, for Z clusters, N relays, M antennas at the user nodes and $2M$ antennas at the relays. Note that TW-Max-Link is a special case of MW-Max-Link, for a single two-way relay channel ($Z = 1$). The complexity of MW-Max-Link is equal to the complexity of the adapted TW-Max-Min, multiplied by $2Z$.

4.5 Simulation Results

This section illustrates and discusses the simulation results of the proposed MW-Max-Link, the TW-Max-Link [14] (a special case of MW-Max-Link, for a single two-way relay channel ($Z = 1$)) and the adapted TW-Max-Min [82], using the extended MMD relay selection criterion. The transmitted signals belong to BPSK and QPSK constellations. The use of high-order constellations as 16-QAM was not included in this work but can be considered elsewhere. We tested the performance for different J , but found that $J = 6$ packets is sufficient to ensure a good performance in TW-Max-Link and MW-Max-Link. We also assume unit power channels ($\sigma_{U,R}^2 = \sigma_{R,U}^2 = 1$) and $N_0 = 1$. The

transmit signal-to-noise ratio SNR (E/N_0) ranges from 0 to 10 dB, where E is the total energy transmitted by each user or the relay. The performances of the schemes were tested for 10000M packets, each containing 100 symbols. For imperfect CSI, the estimated channel matrix $\hat{\mathbf{H}}$ is assumed instead of \mathbf{H} : $\hat{\mathbf{H}}=\mathbf{H}+\mathbf{H}_e$, where the variance of the \mathbf{H}_e coefficients is given by $\sigma_e^2 = \beta E^{-\alpha}$ ($\beta \geq 0$ and $0 \leq \alpha \leq 1$) [131].

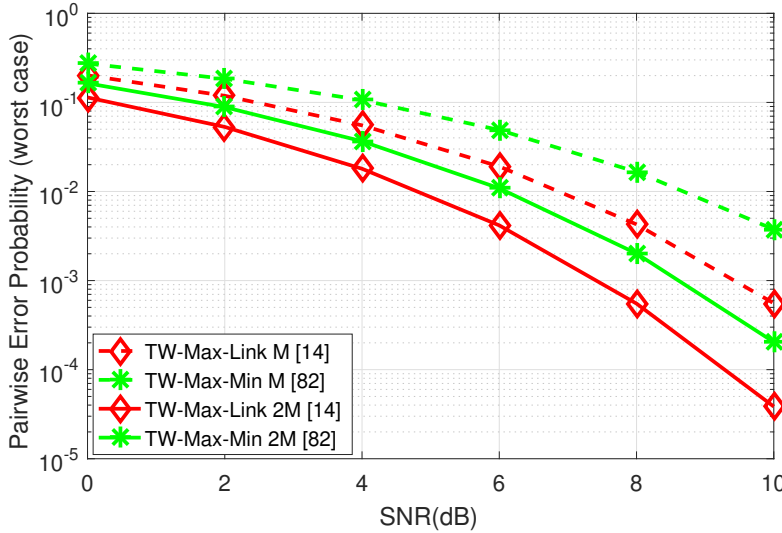


Figure 4.3: TW-Max-Link [14] and TW-Max-Min [82] PEP performance versus SNR, for BPSK and perfect CSI.

Fig. 4.3 shows the PEP (worst case) performance of the TW- Max-Link and TW-Max-Min protocols, for $M = 2$, $N = 10$, BPSK and perfect CSI, both for M or $2M$ antennas at each relay. The results show that the performance of the TW-Max-Link, for M antennas at each relay, is considerably better than the performance of TW-Max-Min for the total range of SNR values tested. When we increase the number of antennas at each relay to $2M$, both the protocols have the performance considerably improved.

Fig. 4.4 shows the BER performance of the TW-Max-Link and TW-Max-Min protocols, for $M = 1$, $N = 10$ and $N = 20$, QPSK and perfect CSI, for $2M$ antennas at each relay. The results show that the performance of the TW-Max-Link scheme is considerably better than the performance of TW-Max-Min for the total range of SNR values tested.

Fig. 4.5 shows the BER performance of the TW-Max-Link and TW-Max-Min protocols, for $M = 1$, $N = 10$, BPSK, perfect and imperfect CSI ($\alpha = 1$, $\beta = 0.5$ and $\beta = 1$), for $2M$ antennas at each relay. The performance of the TW-Max-Link scheme is considerably better than the performance of TW-Max-Min for the total range of SNR values tested, for both perfect and imperfect channel estimation.

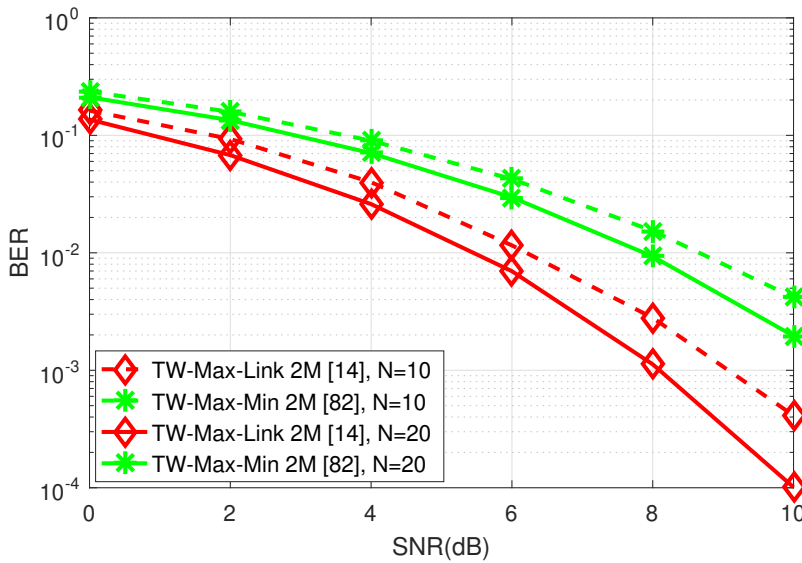


Figure 4.4: TW-Max-Link [14] and TW-Max-Min [82] BER performance versus SNR, for QPSK and perfect CSI.

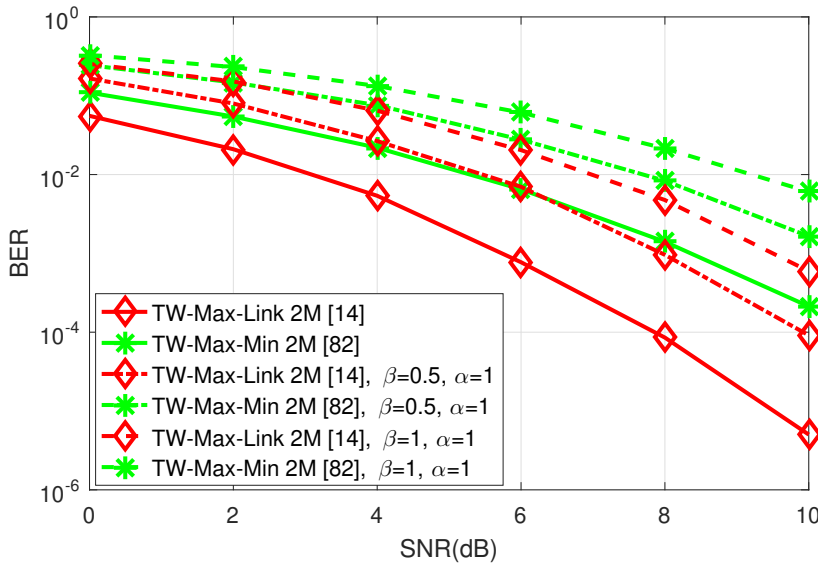


Figure 4.5: TW-Max-Link [14] and TW-Max-Min [82] BER performance versus SNR, for BPSK, perfect and imperfect CSI.

Fig. 4.6 shows the BER performance of the MW-Max-Link for $Z = 5$, TW-Max-Link [14] and TW-Max-Min protocols, for $M = 2$, $N = 10$, BPSK, perfect and imperfect CSI ($\beta = 0.5$ and $\alpha = 1$). The performances of the MW-Max-Link are considerably better than the performance of TW-Max-Link and TW-Max-Min for the total range of SNR values tested.

Fig. 4.7 shows the PEP and the Sum Rate performances, for BPSK and Gaussian distributed signals, respectively, of the MW-Max-Link (for $Z = 5$ and $Z = 10$), TW-Max-Link and TW-Max-Min protocols, for $M = 2$, $N = 10$

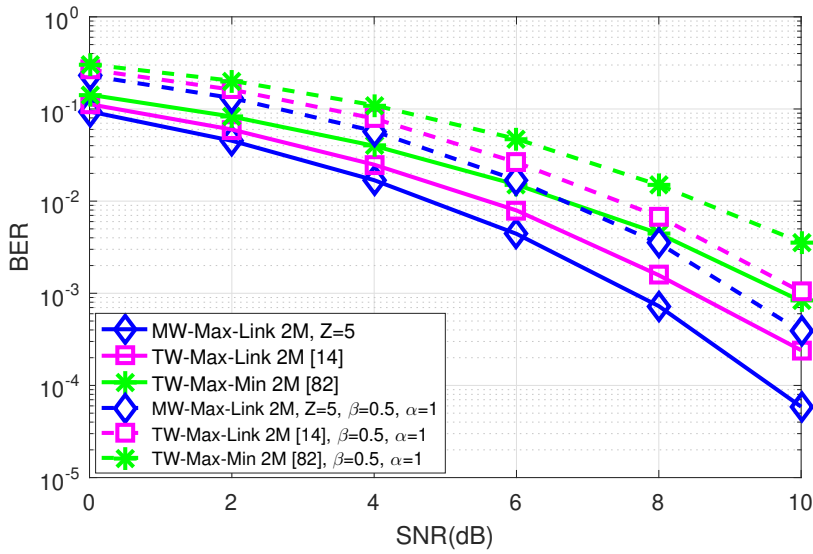


Figure 4.6: MW-Max-Link, TW-Max-Link [14] and TW-Max-Min [82] BER performance versus SNR, for BPSK, perfect and imperfect CSI.

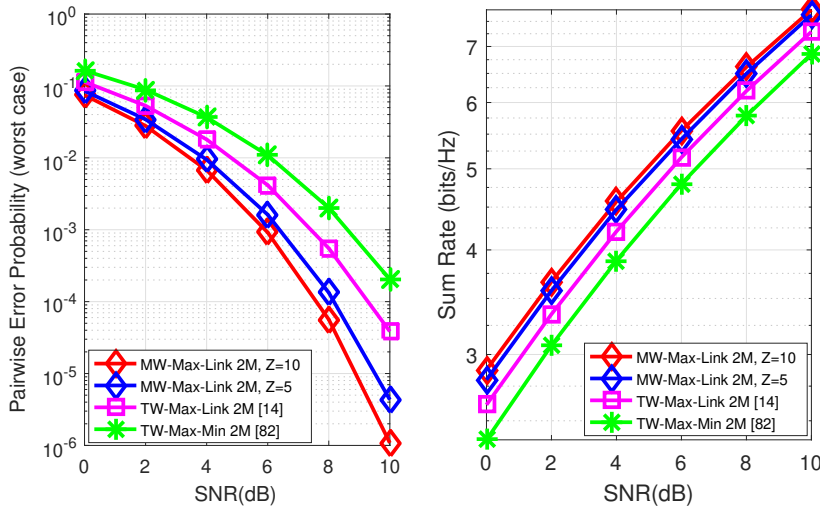


Figure 4.7: MW-Max-Link, TW-Max-Link [14] and TW-Max-Min [82] PEP and Sum-Rate performances versus SNR.

and perfect CSI. The performances of the MW-Max-Link are very close, and considerably better than the performance of TW-Max-Link and TW-Max-Min for the total range of SNR values tested.

4.6 Summary

In this chapter, we have presented a relay-selection strategy for multi-way cooperative multi-antenna systems that is aided by a central processor node, where a cluster formed by two users is selected to simultaneously

transmit to each other with the help of relays. In particular, the proposed multi-way relay selection strategy selects the best link, exploiting the use of buffers and PLNC, that is called MW-Max-Link. The proposed MW-Max-Link was evaluated experimentally and outperformed the TW-Max-Link and the existing TW-Max-Min scheme, with the cost of higher computational complexity (proportional to Z). The use of a central processor node and buffers in the relays is presented as a promising relay selection technique and a framework for multi-way protocols.

Cloud-Driven Multi-Way Multiple-Antenna Relay Systems: Joint Detection, Best-User-Link Selection and Analysis

In this chapter, we present a cloud-driven uplink framework for multi-way multiple-antenna relay systems which aids joint symbol detection in the cloud and where users are selected to simultaneously transmit to each other aided by relays. We also investigate relay selection techniques for the proposed cloud-driven uplink framework that uses cloud-based buffers and XOR network coding. In particular, we develop a novel multi-way relay selection protocol based on the selection of the best link, denoted as Multi-Way Cloud-Driven Best-User-Link (MWC-Best-User-Link). We then devise maximum-minimum-distance and channel-norm based relay selection criteria along with algorithms that are incorporated into the proposed MWC-Best-User-Link protocol. An analysis of the proposed MWC-Best-User-Link protocol in terms of computational cost, pairwise error probability, sum-rate and average delay is carried out. Simulations show that MWC-Best-User-Link outperforms previous works in terms of sum-rate, pairwise error probability, average delay and bit error rate.

5.1

Introduction

In wireless networks, the use of cooperative diversity [1, 3] can mitigate the signal fading caused by multipath propagation. The Multi-Way Relay Channel (mRC) [92] includes both a full data exchange model, in which each user receives data from all other users, and the pairwise data exchange model, which is composed by multiple two-way relay channels. The incorporation of the mRC with multiple relays in a system can significantly improve its performance [4–6]. Considering 5G requirements [84], high spectrum efficiency relaying strategies are key due to their excellent performance. The use of a cloud as a central node can leverage the performance of relay techniques as network operations and services have recently adopted cloud-enabled solutions in communication networks [19, 93]. The ability to manage interference is one of the main advantages of adopting the cloud network framework [93]. In the Cloud Radio Access Network (C-RAN) architecture, the baseband

processing, usually performed locally at each base-station (BS), is aggregated and performed centrally at a cloud processor. This is enabled by high-speed connections, denoted as fronthaul links, between the BSs and the cloud [93]. This centralized signal processing enables the interference mitigation across all the users in the uplink and downlink. The BSs in the C-RAN are also referred to as remote radio heads (RRHs) as their functionality is often limited to transmission and reception of radio signals [93]. These RRHs are driven by the cloud-processor that communicates with RRHs via fronthaul links, that can be dedicated fiber optic cables or wireless links [93]. From an information theoretical point of view, the C-RAN model is best understood as a relay network [93], in which the RRHs can be considered as relays that cooperate in the communication between the cloud and the mobile users. In the uplink, different users in the same cluster communicate their messages to the cloud through RRHs (relays). The relays, instead of decoding the messages locally, can retransmit information about their received signals to the cloud for centralized processing [93]. The uplink in the C-RAN can thus be modeled as a multiple-access relay channel [93]. Moreover, in the downlink, the cloud also communicates with multiple users through RRH and the downlink in the C-RAN can thus be modeled as a broadcast relay channel [93].

5.1.1

Prior and Related Work

The mRC has multiple clusters of users in which each user aims to multicast a single message to all the other users in the same cluster [92]. Considering \mathcal{L} users in a cluster corresponds to an \mathcal{L} -way information exchange among the users in the same cluster. A group of N relays facilitates this exchange, by helping all the users in the system. In particular, the mRC pairwise data exchange model ($\mathcal{L} = 2$) is formed by multiple two-way relay channels. In Two-Way Multiple-Access Broadcast Channel (MABC) schemes, based on the decode-and-forward (DF) protocol [82], the transmission is organized in two successive phases: 1) MA phase - a relay is selected for receiving and decoding the messages simultaneously transmitted from two users (sources S_1 and S_2) and physical-layer network coding (PLNC) is performed on the decoded messages; 2) BC phase - the same selected relay broadcasts the decoded messages to the two sources. The Two-Way Max-Min (TW-Max-Min) relay selection protocol [82] has a high performance, when all the channels are reciprocal and fixed during two consecutive time slots (MA and BC phases). Otherwise, with non reciprocal channels, the performance of relaying strategies can be enhanced by adopting buffer-aided

protocols, in which the relays are able to accumulate data in their buffers [35, 39], before sending data to the destination, as in the MW-Max-Link [13] protocol for cooperative multi-input multi-output (MIMO) systems, which selects the best links among K pairs of sources (diversity gain equals $2NK$), using the extended Maximum Minimum Distance (MMD) relay selection criterion [11, 12]. Furthermore, in [14], the TW-Max-Link protocol (a special case of MW-Max-Link, for a single two-way relay channel ($K = 1$)), also using the extended MMD criterion, was presented. Some other buffer-aided relay selection protocols for cooperative single-antenna and multiple-antenna systems are presented in [67, 68, 94–100]. Moreover, sum-rate maximization is reported for relay selection using two-way protocols, with single-antenna systems in [85]. However, multi-way protocols using a channel-norm based criterion for sum-rate maximization, with multiple-antenna systems, or a cloud (in which each cluster has a particular buffer), have not been previously investigated.

5.1.2 Contributions

In this chapter, we develop a cloud-driven framework and a Multi-Way Best-User-Link (MWC-Best-User-Link) protocol for cooperative MIMO systems, with non reciprocal channels, which selects the best links among K pairs of sources (clusters) and N relay nodes and whose preliminary results were reported in [137]. In order to perform signal detection at the cloud and the nodes, we present maximum likelihood (ML) and linear minimum mean-square error (MMSE) detectors. We then consider the extended Maximum Minimum Distance (MMD) [11, 12] criterion and a channel-norm based (CNB) criterion and devise relay selection algorithms for MWC-Best-User-Link. An analysis of the proposed scheme in terms of pairwise error probability (PEP), sum-rate, average delay and computational cost is also carried out. Simulations illustrate the excellent performance of the proposed framework, the proposed MWC-Best-User-Link protocol and the relay selection algorithms as compared to previously reported approaches. Therefore, the main contributions of this chapter are:

1. A cloud-driven framework with joint detection at the cloud and the nodes;
2. The MWC-Best-User-Link multi-way protocol for cooperative MIMO systems;

3. The MMD and CNB relay selection criteria along with relay selection algorithms;
4. An analysis of the proposed MWC-Best-User-Link scheme in terms of PEP, sum-rate, average delay and computational cost.

This chapter is structured as follows. Section 5.2 describes the system model and the main assumptions. Section 5.3 presents the proposed MWC-Best-User-Link protocol, relay selection criteria and algorithms. Section 5.4 analyzes MWC-Best-User-Link, with the extended MMD and the novel low-complexity CNB criteria for relay selection. Section 5.5 illustrates and discusses the simulation results whereas Section 5.6 gives the concluding remarks.

5.2 System Description

We assume a MIMO multi-way MABC relay network formed by K clusters (pair of sources S_1 and S_2) and N half duplex (HD) DF relays, R_1, \dots, R_N . In a C-RAN, the sources would represent mobile users and the relays would represent RRHs. The sources have M_S antennas for transmission or reception and each relay $M_R = 2UM_s$ antennas, where $U \in \{1, 2, 3 \dots\}$, all of them used by the selected relay for reception ($M_{R_{rx}} = M_R$) and M_S out of VM_S antennas are selected of each relay used for transmission ($M_{R_{tx}} = M_S$), where $V \in \{1, 2, 3 \dots\}$ and $VM_s \leq M_R$, forming a spatial multiplexing network, in which the channel matrices are square or formed by multiple square sub-matrices in the MA mode. Note that the reason for using multiples of $2M_S$ antennas at the relays is because the relay selection algorithms explained in Section 5.3 use criteria that depend on these matrices to be square or to be formed by multiple square sub-matrices. Thus, the higher V the better the system performance, as it increases the degrees of freedom. Moreover, the higher U the better the system performance as it increases the number of receive antennas at the relays. However if we increase U and V , we have a higher computational complexity, as shown in Section 5.4. There is a trade-off between system performance and computational complexity, when we increase U and V . The selected relays access a number of K cloud buffers for extracting or storing M_S packets in each time slot. Each cluster has a particular cloud buffer that is established on demand, whose size is J packets, as depicted in Fig. 5.1. In the multiple-access phase (uplink), a cluster is selected to send M_S packets simultaneously to a selected relay R_g for reception. Then, the data is decoded by the cloud processor and XOR type PLNC [13, 14, 86] is applied to combine the decoded vectors (inputs of the XOR) and generate a codeword

(output of the XOR) that is stored in their particular cloud buffers. In the broadcast-channel phase (downlink), two relays R_{f1} and R_{f2} are selected to broadcast M_S packets from the particular cloud buffer to the selected cluster. Note that R_{f2} may be different from R_{f1} . In most situations the selection of only one relay in the downlink is enough for a good performance. However, by selecting two relays, the possibility of combining the channels related to the selected relays increases the degrees of freedom of the system and, consequently, its performance is improved. The system could select more than two relays to further improve its performance, but the computational complexity would be considerably increased for a high number of relays. For simplicity, we adopt the mRC pairwise data exchange model, but the full data exchange model can be considered in future works. Moreover, other kinds of network coding, as linear PLNC [35] and analog network coding [87], can be considered in future works.

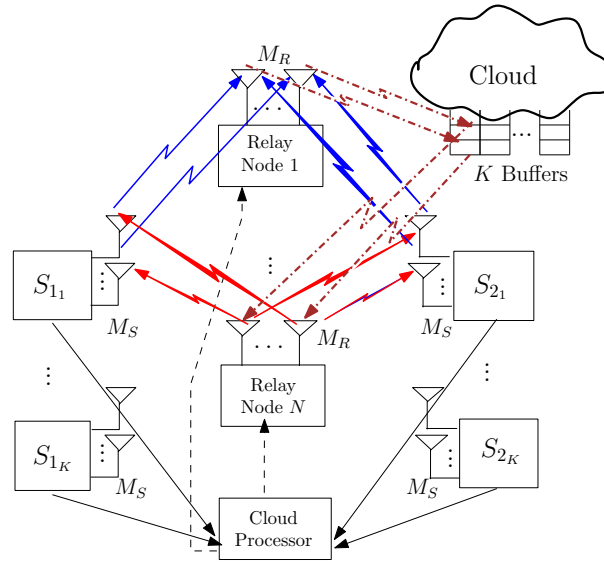


Figure 5.1: System model of the proposed cloud-driven multi-way relay scheme.

5.2.1 Assumptions

We assume a non prefixed schedule protocol, in which each time slot may be selected for uplink or downlink transmission, depending on the quality of the available links and the buffer status. Thus, the energy transmitted from each source node to the selected relay for reception (E_S) or from the selected relay(s) for transmission to the sources (E_{R_f}), in each time slot, is the same, i. e., $E_{R_f} = E_S$. The use of power allocation ($E_{R_f} \neq E_S$) would imply in a more complex relay selection algorithm, but can be considered elsewhere in future

works with prefixed schedule protocols, using precoders that rely on CSI (in practice imperfect CSI) at the transmitters. We consider mutually independent zero mean complex Gaussian random channel coefficients, which are fixed for the duration of one time slot and vary independently from one time slot to the following, and the transmission is organized in data packets. Fig. 5.2 illustrates the frame of the data packets. The order of the packets is contained in the preamble and the original order is recovered at the destination. Signaling for network coordination and pilot symbols for estimation of the channel state information (CSI) are also contained in the preamble. The cloud is the central node and decides whether a cluster or the relay(s) must transmit in a given time slot i , through a feedback channel. An appropriate signalling provides global CSI at the cloud [39]. Moreover, we assume that each relay only has information about its S_1R and S_2R links. The use of a cloud as a single central node and its buffers implies a higher control overhead. However, it reduces the system complexity and the delay, since a unique central node decides which nodes transmit (rather than all destination nodes) and the packets associated with a cluster are stored in only its particular cloud buffer instead of being spread in the buffers of all relays. In this work, we focus on the ideal case where the fronthaul links have unconstrained capacities, and the relays can convey their exact received signals to the cloud processor. This could happen only if the relays were near to the cloud and experiencing high signal-to-noise and low interference conditions. Practical systems, however, have capacity-constrained fronthaul links [93] and this limits the amount of information that the relays can retransmit. Although these unconstrained capacities in the fronthaul links simplify our analysis, they do not limit the advantages of the proposed protocol and relay selection algorithms, explained in the next section. In this context, it is worth noting that 5G systems are designed to achieve very high fronthaul links capacity, and thus, the considered unconstrained capacity assumption is reasonable for the purpose of the relay and cloud communication. Moreover, capacity-constrained fronthaul links can be considered elsewhere in future works and the performance achieved by the proposed protocol may be considered as an upper bound.

5.2.2 System Model

The wireless channel matrix \mathbf{H}_{S_k, R_i} incorporates the effects of large-scale fading, related to the propagation characteristics of the signal over long distances, and the Rayleigh-distributed small-scale fading [88]. Hence, the

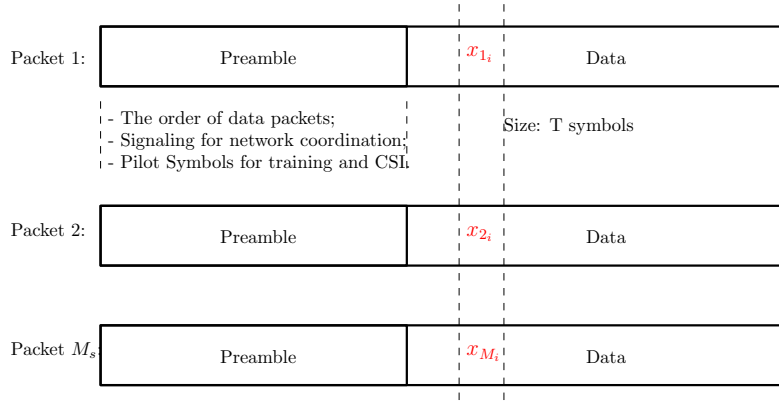


Figure 5.2: The frame of each packet.

quadratic norm of \mathbf{H}_{S_k, R_i} is given by

$$\|\mathbf{H}_{S_k, R_i}\|^2 = \gamma d_{S_k, R_i}^{-2\xi} \|\mathbf{G}_{S_k, R_i}\|^2 \quad (5-1)$$

where S_k represents each source S_{1_k} or S_{2_k} ($k \in \{1 \dots K\}$), R_i represents each relay ($i \in \{1 \dots N\}$), γ represents a constant defined by the antenna gain, carrier frequency and other system parameters, ξ is the path-loss component, \mathbf{G}_{S_k, R_i} represents a channel matrix related to the $S_k R_i$ links formed by mutually independent zero mean complex Gaussian random coefficients and d_{S_k, R_i} the respective distance between S_k and R_i . The same reasoning applies to \mathbf{H}_{R_i, S_k} and its quadratic norm is given by

$$\|\mathbf{H}_{R_i, S_k}\|^2 = \gamma d_{R_i, S_k}^{-2\xi} \|\mathbf{G}_{R_i, S_k}\|^2. \quad (5-2)$$

The proposed system can operate in each time slot in two modes: "Multiple-Access" (MA) or "Broadcast- Channel" (BC). Thus, depending on the relay selection metrics (explained in Section 5.3), the system may operate in each time slot with two options:

a) MA mode: The selected cluster transmits M_S packets directly to the selected relay R_g ;

b) BC mode: R_{f1} and R_{f2} transmits M_S packets from the cloud buffers to the selected cluster.

If the relay selection algorithm decides to operate in the MA mode, the signal sent by the selected cluster S (S_1 and S_2) and received at R_g (the relay selected for reception) is organized in an $2UM_S \times 1$ vector given by

$$\mathbf{y}_{S, R_g}[i] = \sqrt{\frac{E_S}{M_S}} \mathbf{H}_{S, R_g} \mathbf{x}[i] + \mathbf{n}_{R_g}[i], \quad (5-3)$$

where $\mathbf{x}[i]$ is an $2M_S \times 1$ vector with M_S symbols sent by S_1 ($\mathbf{x}_1[i]$) and S_2

($\mathbf{x}_2[i]$), \mathbf{H}_{S,R_g} is a $2UM_S \times 2M_S$ matrix of S_1R_g and S_2R_g links and \mathbf{n}_{R_g} is the zero mean additive white complex Gaussian noise (AWGN) at R_g . Note that \mathbf{H}_{S,R_g} is formed by U square sub-matrices of dimensions $2M_S \times 2M_S$ as given by

$$\mathbf{H}_{S,R_g} = [\mathbf{H}_{S,R_g}^1; \mathbf{H}_{S,R_g}^2; \dots; \mathbf{H}_{S,R_g}^U]. \quad (5-4)$$

Assuming perfect synchronization, we may adopt the ML receiver at the cloud processor:

$$\hat{\mathbf{x}}[i] = \arg \min_{\mathbf{x}'[i]} \left(\left\| \mathbf{y}_{S,R_g}[i] - \sqrt{\frac{E_S}{M_S}} \mathbf{H}_{S,R_g} \mathbf{x}'[i] \right\|^2 \right), \quad (5-5)$$

where $\mathbf{x}'[i]$ is each of the $N_s^{2M_S}$ possible vectors of sent symbols (N_s is the quantity of symbols in the constellation adopted). The ML receiver calculates an estimate of the vector of symbols sent by the sources $\hat{\mathbf{x}}[i]$.

In contrast, by considering linear MMSE detection [143], the estimate of the transmitted vectors \mathbf{x} is obtained by processing the received vector $\mathbf{y}_{S,R_g}[i]$ with the equalization matrix \mathbf{W}_{MMSE} , which is given by

$$\begin{aligned} \tilde{\mathbf{x}}[i] &= \mathbf{W}_{MMSE} \mathbf{y}_{S,R_g}[i] \\ &= \left(\mathbf{H}_{S,R_g}^H \mathbf{H}_{S,R_g} + \frac{\sigma_n^2}{\sigma_x^2} \mathbf{I} \right)^{-1} \mathbf{H}_{S,R_g}^H \mathbf{y}_{S,R_g}[i]. \end{aligned} \quad (5-6)$$

where $\sigma_n^2 = N_0$ is the power spectrum density of the AWGN and $\sigma_x^2 = E_S$ is the power of the signal. By performing XOR network coding, only the XOR outputs (resulting M_S packets) are stored with the information: "the bit sent by S_1 is equal (or not) to the corresponding bit sent by S_2 ". Therefore, we apply the bitwise XOR:

$$\mathbf{z}[i] = \hat{\mathbf{x}}_1[i] \oplus \hat{\mathbf{x}}_2[i] \quad (5-7)$$

and store the resulting data in the cloud buffer. Therefore, an advantage of applying XOR network coding is that we have to store only M_S packets in the cloud buffer, instead of $2M_S$.

Moreover, if the relay selection algorithm decides to operate in the BC mode, the signal sent by the relays selected for transmission R_f (R_{f_1} and R_{f_2}) and received at S_1 and S_2 is structured in an $M_S \times 1$ vector given by

$$\mathbf{y}_{R_f,S_{1(2)}}[i] = \sqrt{\frac{E_{R_f}}{2M_S}} \mathbf{H}_{R_f,S_{1(2)}}^{v,v'} \mathbf{z}[i] + \mathbf{n}_{S_{1(2)}}[i], \quad (5-8)$$

where $\mathbf{z}[i]$ is a $M_S \times 1$ vector with M_S symbols, $v \in \{1, 2, \dots, V\}$, $v' \in \{1, 2, \dots, V\}$, $\mathbf{H}_{R_f, S_{1(2)}}^{v, v'} = \mathbf{H}_{R_{f_1}, S_{1(2)}}^v + \mathbf{H}_{R_{f_2}, S_{1(2)}}^{v'}$ represents the $M_S \times M_S$ matrix of $R_{f_1} S_{1(2)}$ and $R_{f_2} S_{1(2)}$ links, and $\mathbf{n}_{S_{1(2)}}[i]$ is the AWGN at S_1 or S_2 . Note that $\mathbf{H}_{R_f, S_{1(2)}}^{v, v'}$ is selected among V^2 submatrices of dimension $M_S \times M_S$ contained in $\mathbf{H}_{R_f, S_{1(2)}}$ as given by

$$\mathbf{H}_{R_f, S_{1(2)}} = [\mathbf{H}_{R_f, S_{1(2)}}^{1,1}; \dots; \mathbf{H}_{R_f, S_{1(2)}}^{1,V}; \dots; \mathbf{H}_{R_f, S_{1(2)}}^{V,1}; \dots; \mathbf{H}_{R_f, S_{1(2)}}^{V,V}]. \quad (5-9)$$

We may also adopt the ML receiver at the selected cluster, which yields

$$\tilde{\mathbf{z}}_{1(2)}[i] = \arg \min_{\mathbf{z}'[i]} \left(\left\| \mathbf{y}_{R_f, S_{1(2)}}[i] - \sqrt{\frac{E_{R_f}}{2M_S}} \mathbf{H}_{R_f, S_{1(2)}}^{v, v'} \mathbf{z}'[i] \right\|^2 \right), \quad (5-10)$$

where $\mathbf{z}'[i]$ is each of the possible vectors with M_S symbols. In contrast, we may adopt the MMSE receiver and the solution is given by

$$\begin{aligned} \tilde{\mathbf{z}}_{1(2)}[i] &= \mathbf{W}_{MMSE} \mathbf{y}_{R_f, S_{1(2)}}[i] \\ &= \left(\mathbf{H}_{R_f, S_{1(2)}}^{v, v'H} \mathbf{H}_{R_f, S_{1(2)}}^{v, v'} + \frac{\sigma_n^2}{\sigma_x^2} \mathbf{I} \right)^{-1} \mathbf{H}_{R_f, S_{1(2)}}^{v, v'H} \mathbf{y}_{R_f, S_{1(2)}}[i]. \end{aligned} \quad (5-11)$$

Therefore, at S_1 we calculate the vector of symbols sent by S_2 by performing XOR type PLNC:

$$\hat{\mathbf{x}}_2[i] = \mathbf{x}_1[i] \oplus \hat{\mathbf{z}}_1[i]. \quad (5-12)$$

This is also applied at S_2 to calculate the vector of symbols sent by S_1 :

$$\hat{\mathbf{x}}_1[i] = \mathbf{x}_2[i] \oplus \hat{\mathbf{z}}_2[i]. \quad (5-13)$$

The estimated channel matrix $\hat{\mathbf{H}}$ is considered instead of \mathbf{H} in (5-5) and (5-10), when performing the ML receiver, and in (5-6) and (5-11), when performing the MMSE receiver, by assuming imperfect CSI. Note that $\hat{\mathbf{H}}$ is computed as $\hat{\mathbf{H}} = \mathbf{H} + \mathbf{H}_e$, where the variance of the mutually independent zero mean complex Gaussian \mathbf{H}_e coefficients is given by $\sigma_e^2 = \beta E^{-\alpha}$ ($0 \leq \alpha \leq 1$ and $\beta \geq 0$) [131], in which $E = E_S$, in the MA phase, and $E = \frac{E_S}{2}$, in the BC phase.

5.3

Proposed MWC-Best-User-Link Protocol and Relay Selection Algorithms

The system presented in Fig. 5.1 is equipped with the novel MWC-Best-User-Link protocol, which in each time slot may operate in two possible modes:

MA or BC. The relay selection algorithm needs to compute the metrics related to KNU different $2M_S \times 2M_S$ submatrices related to the uplink channels and $2KN'V^2$ different $M_S \times M_S$ submatrices related to the downlink channels, where $N' = N + C_2^N$, to select the best cluster, the best relay(s) and the mode of operation (MA or BC), in each time slot. Note that when a selected cluster formed by two source nodes is communicating with each other, the other clusters remain silent. Moreover, the relay selection algorithm may operate with two criteria: 1) using the extended MMD [11, 12] criterion; or 2) using the CNB criterion. In the first approach, if the MMD-based relay selection algorithm decides to operate in the MA mode, it chooses the relay R_g and the associated channel matrix \mathbf{H}_{S,R_g}^{MMD} with the largest minimum distance as given by

$$\mathbf{H}_{S,R_g}^{MMD} = \arg \max_{\mathbf{H}_{S,R_i}} \mathcal{B}_{min}^{MA}, \quad (5-14)$$

where \mathcal{B}_{min}^{MA} is the smallest value of the distances $\mathcal{B}^{MA} = \frac{E_S}{M_S} \left\| \mathbf{H}_{S,R_i}^u (\mathbf{x}_l - \mathbf{x}_n) \right\|^2$, $u \in \{1, \dots, U\}$, $i \in \{1, \dots, N\}$, \mathbf{x}_l and \mathbf{x}_n represent each possible vector formed by $2M_S$ symbols and $l \neq n$. The metric \mathcal{B}^{MA} is calculated for each of the $C_2^{N \cdot 2M_S}$ (combination of $N_s^{2M_S}$ in 2) possibilities, for each sub-matrix \mathbf{H}_{S,R_i}^u . Moreover, if the MMD-based relay selection algorithm decides to operate in the BC mode, it chooses the relays R_f (R_{f1} and R_{f2}) and the associated channel sub-matrix $\mathbf{H}_{R_f,S}^{v,v',MMD}$ with the largest minimum distance as given by

$$\mathbf{H}_{R_f,S}^{v,v',MMD} = \arg \max_{\mathbf{H}_{R_{ij},S}^{v,v'}} \mathcal{B}_{min}^{BC}, \quad (5-15)$$

where \mathcal{B}_{min}^{BC} is the smallest value of the distances $\mathcal{B}^{BC} = \frac{E_S}{2M_S} \left\| \mathbf{H}_{R_{ij},S}^{v,v'} (\mathbf{x}_l - \mathbf{x}_n) \right\|^2$, i and $j \in \{1, \dots, N\}$, v and $v' \in \{1, \dots, V\}$, \mathbf{x}_l and \mathbf{x}_n represent each possible vector formed by M_S symbols and $l \neq n$. The metric \mathcal{B}^{BC} is calculated for each of the $C_2^{N \cdot M_S}$ possibilities, for each sub-matrix $\mathbf{H}_{R_{ij},S}^{v,v'}$. In Appendix B, we develop a proof that shows that the MMD-based relay selection algorithm minimizes the PEP and also the error in the ML receiver, in the proposed MWC-Best-User-Link protocol.

In the second approach, if the CNB-based relay selection algorithm decides to operate in the MA mode, it chooses the relay R_g and the associated channel matrix \mathbf{H}_{S,R_g}^{CNB} as given by

$$\mathbf{H}_{S,R_g}^{CNB} = \arg \max_{\mathbf{H}_{S,R_i}} \mathcal{C}_{min}^{MA}, \quad (5-16)$$

where $\mathcal{C}_{min}^{MA} = \min \left| \det(\mathbf{H}_{S,R_i}^u) \right|$, $u \in \{1, \dots, U\}$ and $i \in \{1, \dots, N\}$. Therefore, in

the MA mode, the metric $|\det(\mathbf{H}_{S,R_i}^u)|$ is calculated for each sub-matrix \mathbf{H}_{S,R_i}^u and \mathcal{C}_{min}^{MA} is the smallest of these values. Thus, the selected matrix \mathbf{H}_{S,R_g}^{CNB} has the largest \mathcal{C}_{min}^{MA} value. Moreover, if the CNB-based relay selection algorithm decides to operate in the BC mode, it chooses the relays R_f and the associated channel sub-matrix $\mathbf{H}_{R_f,S}^{v,v'}^{CNB}$ as given by

$$\mathbf{H}_{R_f,S}^{v,v'}^{CNB} = \arg \max_{\mathbf{H}_{R_{ij},S}^{v,v'}} \mathcal{C}^{BC}, \quad (5-17)$$

where $\mathcal{C}^{BC} = |\det(\mathbf{H}_{R_{ij},S}^{v,v'})|$. Therefore, in the BC mode, the metric \mathcal{C}^{BC} is calculated for each sub-matrix $\mathbf{H}_{R_{ij},S}^{v,v'}$. Thus, the selected sub-matrix $\mathbf{H}_{R_f,S}^{v,v'}^{CNB}$ has the largest \mathcal{C}^{BC} value. Note that the reason for using multiples of $2M_S$ antennas at the relays is because this relay selection criterion depends on the channel matrices \mathbf{H}_{S,R_i} and $\mathbf{H}_{R_{ij},S}$ to be square or to be formed by multiple square sub-matrices. In Appendix C, we develop a proof that shows that the CNB-based relay selection algorithm maximizes the sum-rate in the MWC-Best-User-Link protocol and in Appendix D we show that this algorithm minimizes the effects of the effective noise in the MMSE receiver. Table 5.1 shows the pseudo-code of the relay selection algorithms of MWC-Best-User-Link and the following subsections explain how this protocol works.

5.3.1 Relay selection metric for MA and BC modes

For each cluster S (formed by S_1 and S_2), in the first step, we calculate the metric $\mathcal{A}_{SR_i}^u$ related to the SR links of each square sub-matrix \mathbf{H}_{S,R_i}^u associated with R_i , in the MA mode:

$$\mathcal{A}_{SR_i}^u = \begin{cases} \mathcal{C}^{MA} = |\det(\mathbf{H}_{S,R_i}^u)|, & \text{for CNB,} \\ \mathcal{B}_{min}^{MA}, & \text{for MMD,} \end{cases}$$

where $u \in \{1, \dots, U\}$ and $i \in \{1, \dots, N\}$. In the second step, we compute the ordering on $\mathcal{A}_{SR_i}^u$ and find the smallest metric:

$$\mathcal{A}_{SR_i} = \min(\mathcal{A}_{SR_i}^u), \quad (5-18)$$

In the third step, we compute the ordering on \mathcal{A}_{SR_i} and find the largest metric:

$$\mathcal{A}_{k_{\max SR}} = \max(\mathcal{A}_{SR_i}), \quad (5-19)$$

Table 5.1: Multi-Way Cloud-Driven Best-User-Link: pseudo-code of the relay selection algorithms

-
- 1: Calculate $\mathcal{A}_{SR_i}^u$ of each sub-matrix \mathbf{H}_{S,R_i}^u of R_i , for MA mode:

$$\mathcal{A}_{SR_i}^u = \begin{cases} \mathcal{C}^{MA} = |\det(\mathbf{H}_{S,R_i}^u)|, & \text{for CNB,} \\ \mathcal{B}_{min}^{MA}, & \text{for MMD,} \end{cases}$$
 - 2: Compute the ordering on $\mathcal{A}_{SR_i}^u$ and find the smallest metric:

$$\mathcal{A}_{SR_i} = \min(\mathcal{A}_{SR_i}^u).$$
 - 3: Compute the ordering on \mathcal{A}_{SR_i} and find the largest metric for each cluster:

$$\mathcal{A}_{k_{\max} SR} = \max(\mathcal{A}_{SR_i}).$$
 - 4: Compute the ordering and find the largest metric:

$$\mathcal{A}_{\max SR} = \max(\mathcal{A}_{k_{\max} SR}).$$
 - 5: Calculate $\mathcal{A}_{R_{ij}S_1}^{v,v'}$ of each sub-matrix $\mathbf{H}_{R_{ij},S_1}^{v,v'}$ of R_i and R_j , for BC mode:

$$\mathcal{A}_{R_{ij}S_1}^{v,v'} = \begin{cases} \mathcal{C}^{BC} = |\det(\mathbf{H}_{R_{ij},s_1}^{v,v'})|, & \text{for CNB,} \\ \mathcal{B}_{min}^{BC}, & \text{for MMD,} \end{cases}$$
 - 6: Calculate the metric $\mathcal{A}_{R_{ij}S_2}^{v,v'}$ of each sub-matrix $\mathbf{H}_{R_{ij},s_2}^{v,v'}$, for each pair of relays.
 - 7: Compare the metrics $\mathcal{A}_{R_{ij}S_1}^{v,v'}$ and $\mathcal{A}_{R_{ij}S_2}^{v,v'}$ and store the smallest one:

$$\mathcal{A}_{R_{ij}S}^{v,v'} = \min(\mathcal{A}_{R_{ij}S_1}^{v,v'}, \mathcal{A}_{R_{ij}S_2}^{v,v'}).$$
 - 8: Compute the ordering and find the largest metric:

$$\mathcal{A}_{R_{ij}S} = \max(\mathcal{A}_{R_{ij}S}^{v,v'}).$$
 - 9: Compute the ordering and find the largest metric, for each cluster:

$$\mathcal{A}_{k_{\max} RS} = \max(\mathcal{A}_{R_{ij}S}).$$
 - 10: Compute the ordering and find the largest metric:

$$\mathcal{A}_{\max RS} = \max(\mathcal{A}_{k_{\max} RS}).$$
 - 11: Select the transmission mode

$$\begin{cases} \text{if } \frac{N_{\text{packets}}}{M_S} > LoL, \text{ then} & \text{" BC mode" and select the cluster,} \\ & \text{whose buffer is fullest.} \\ \text{elseif } \frac{\mathcal{A}_{\max SR}}{\mathcal{A}_{\max RS}} \geq G, \text{ then} & \text{" MA mode",} \\ \text{otherwise,} & \text{" BC mode".} \end{cases}$$
-

where $k \in \{1, \dots, K\}$. After finding $\mathcal{A}_{k_{\max} SR}$ for each cluster, we compute the ordering and find the largest metric:

$$\mathcal{A}_{\max SR} = \max(\mathcal{A}_{k_{\max} SR}). \quad (5-20)$$

Therefore, we choose the cluster and the relay R_i that fulfil (5-20) to receive M_s packets from the selected cluster. For each cluster, in the fourth step, we calculate the metrics $\mathcal{A}_{R_{ij}S_1}$ related to the RS_1 links of each sub-matrix $\mathbf{H}_{R_{ij},S_1}^{v,v'}$ associated with each pair R_i and R_j , for BC mode:

$$\mathcal{A}_{R_{ij}S_1}^{v,v'} = \begin{cases} \mathcal{C}^{BC} = |\det(\mathbf{H}_{R_{ij},S_1}^{v,v'})|, & \text{for CNB,} \\ \mathcal{B}_{min}^{BC}, & \text{for MMD,} \end{cases}$$

where $\mathbf{H}_{R_{ij},S_1}^{v,v'} = \mathbf{H}_{R_i,S_1}^v + \mathbf{H}_{R_j,S_1}^{v'}$, v and $v' \in \{1, \dots, V\}$, i and $j \in \{1, \dots, N\}$.

In the fifth step, this reasoning is also applied to calculate the metric $\mathcal{A}_{R_{ij}S_2}^{v,v'}$. In the sixth step, we compare the metrics $\mathcal{A}_{R_{ij}S_1}^{v,v'}$ and $\mathcal{A}_{R_{ij}S_2}^{v,v'}$ and store the smallest one:

$$\mathcal{A}_{R_{ij}S}^{v,v'} = \min(\mathcal{A}_{R_{ij}S_1}^{v,v'}, \mathcal{A}_{R_{ij}S_2}^{v,v'}). \quad (5-21)$$

After finding $\mathcal{A}_{R_{ij}S}^{v,v'}$ for each pair of sub-matrices $\mathbf{H}_{R_{ij},S_1}^{v,v'}$ e $\mathbf{H}_{R_{ij},S_2}^{v,v'}$, we compute the ordering and find the largest metric:

$$\mathcal{A}_{R_{ij}S} = \max(\mathcal{A}_{R_{ij}S}^{v,v'}). \quad (5-22)$$

In the seventh step, after finding $\mathcal{A}_{R_{ij}S}$ for each pair of relays, we compute the ordering and find the largest metric:

$$\mathcal{A}_{k_{\max RS}} = \max(\mathcal{A}_{R_{ij}S}), \quad (5-23)$$

where $k \in \{1, \dots, K\}$. After finding $\mathcal{A}_{k_{\max RS}}$ for each cluster, we compute the ordering and find the largest metric:

$$\mathcal{A}_{\max RS} = \max(\mathcal{A}_{k_{\max RS}}). \quad (5-24)$$

Therefore, we select the cluster and the relays R_i and R_j that fulfil (5-24) to send simultaneously M_S packets stored in the associated cloud buffer to the selected cluster. The estimated channel matrix $\hat{\mathbf{H}}$ is considered, instead of \mathbf{H} , if we consider imperfect CSI.

5.3.2 Choice of the transmission mode

After calculating the metrics related to the SR and RS links and finding $\mathcal{A}_{\max SR}$ and $\mathcal{A}_{\max RS}$, these metrics are compared and we select the transmission mode:

$$\left\{ \begin{array}{l} \text{if } \frac{N_{\text{packets}}}{M_S} > LoL, \text{ then " BC mode" and select the cluster,} \\ \hspace{10em} \text{whose buffer is fullest.} \\ \text{elseif } \frac{A_{\text{max } SR}}{A_{\text{max } RS}} \geq G, \text{ then " MA mode",} \\ \text{otherwise, " BC mode",} \end{array} \right.$$

where $G = \frac{E[A_{\text{max } SR}]}{E[A_{\text{max } RS}]}$, N_{packets} is the total number of packets stored in the cloud buffers, LoL is a parameter that when reduced increases the probability of the protocol to operate in BC mode and, consequently, to achieve a reduced average delay (low latency).

5.4 Analysis

In this section, the PEP of the proposed MWC-Best-User-Link protocol is analysed and expressions for the sum-rate and average delay of MWC-Best-User-Link are derived. Moreover, the cost of MWC-Best-User-Link and existing protocols is also examined.

5.4.1 Pairwise Error Probability

The PEP assumes an error event when \mathbf{x}_n is sent and the detector calculates an incorrect \mathbf{x}_l (where $l \neq n$), based on the received symbol [11–13]. Considering $\mathcal{D}' = \|\mathbf{H}(\mathbf{x}_n - \mathbf{x}_l)\|^2$, in the MA mode, and $\mathcal{D}' = \frac{1}{2} \|\mathbf{H}(\mathbf{x}_n - \mathbf{x}_l)\|^2$, in BC mode, the PEP is given by

$$\mathbf{P}(\mathbf{x}_n \rightarrow \mathbf{x}_l | \mathbf{H}) = Q \left(\sqrt{\frac{E_s}{2N_0M_S} \mathcal{D}'} \right). \quad (5-25)$$

We may consider that the worst value of the PEP occurs for the smallest value of \mathcal{D}' and then the PEP worst case (\mathcal{D}'_{\min}) is given by

$$\mathbf{P}(\mathbf{x}_n \rightarrow \mathbf{x}_l | \mathbf{H}) = Q \left(\sqrt{\frac{E_s}{2N_0M_S} \mathcal{D}'_{\min}} \right). \quad (5-26)$$

Assuming that the probability of having no error in the two phases of the system is approximately given by the square of $(1 - \mathbf{P}(\mathbf{x}_n \rightarrow \mathbf{x}_l | \mathbf{H}))$, an expression for calculating the worst case of the PEP for cooperative transmissions (CT), in each time slot is given by

$$\begin{aligned} \mathbf{P}^{CT}(\mathbf{x}_n \rightarrow \mathbf{x}_l | \mathbf{H}) &= 1 - (1 - \mathbf{P}(\mathbf{x}_n \rightarrow \mathbf{x}_l | \mathbf{H}))^2 \\ &= 1 - \left(1 - Q \left(\sqrt{\frac{E_s}{2N_0M_S} \mathcal{D}'_{\min}} \right) \right)^2. \end{aligned} \quad (5-27)$$

Note that this expression may be used for calculating the worst case of the PEP, for both symmetric and asymmetric channels.

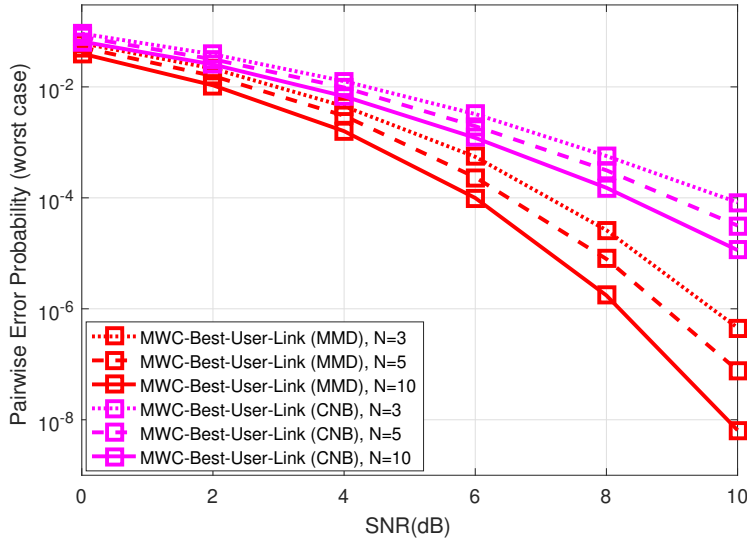


Figure 5.3: Theoretical PEP performance versus SNR.

Fig. 5.3 illustrates the theoretical PEP performance (computed by the algorithm based on the selected channel matrix \mathbf{H} , in each time slot) of MWC-Best-User-Link (MMD) and MWC-Best-User-Link (CNB) protocols, for $M_S = 2$, $M_{R_{rx}} = 4$ ($U = 1$), $M_{R_{tx}} = 2$ ($V = 1$), $K = 3$, $N = 3, 5$ and 10 , $LoL > KL$, perfect CSI, BPSK and unit power symmetric channels. By maximizing the metric \mathcal{D}'_{\min} , the extended MMD criterion minimizes the worst case of the PEP in the MWC-Best-User-Link protocol. Otherwise, while not taking into account \mathcal{D}'_{\min} , CNB maximizes the sum-rate in the MWC-Best-User-Link protocol and has low computational cost.

5.4.2 Sum-Rate

The system capacity upper bounds the sum-rate of a given system [35]. In MWC-Best-User-Link, as the relay selected for reception R_g may be different from the relay selected for transmission R_f , its capacity is given by [102]:

$$C_{DF} = \frac{1}{2} \min\{I_{DF}^{SR_g}, I_{DF}^{R_fS}\}, \quad (5-28)$$

where the terms in (5-28) are the maximum rate at which R_g can reliably decode the data sent by the selected cluster S_1 and S_2 and at which this selected cluster can reliably decode the estimated data sent by R_f , respectively. In [12], the relationship between mutual information and entropy is expanded for a

given channel matrix \mathbf{H}_{S,R_g} and the maximum mutual information is given by

$$I_{DF}^{SR_g} = \log_2 \det \left(\mathbf{H}_{S,R_g} (\mathbf{Q}_{S,R_g}/N_0) \mathbf{H}_{S,R_g}^H + \mathbf{I} \right), \quad (5-29)$$

where $\mathbf{Q}_{S,R_g} = E[\mathbf{x}(\mathbf{x})^H] = \mathbf{I} \frac{E_S}{M_S}$, and the vectors \mathbf{x} are structured by independent and identically distributed (i.i.d.) transmitted symbols. This also can be applied to $I_{DF}^{R_f S}$:

$$I_{DF}^{R_f S} = \log_2 \det \left(\mathbf{H}_{R_f,S} (\mathbf{Q}_{R_f,S}/N_0) \mathbf{H}_{R_f,S}^H + \mathbf{I} \right), \quad (5-30)$$

where $\mathbf{Q}_{R_f,S} = \mathbf{I} \frac{E_S}{2M_S}$. However, instead of considering the minimum of the terms in (5-28), to calculate the sum-rate of the proposed protocol, we employ an approximated expression given by the average of the values found in each time slot. Therefore, in the case of a time slot i selected for MA mode, the sum-rate is given by

$$\mathcal{R}_i^{SR} = \frac{1}{2} \log_2 \det \left(\mathbf{H}_{S,R_g} (\mathbf{Q}_{S,R_g}/N_0) \mathbf{H}_{S,R_g}^H + \mathbf{I} \right). \quad (5-31)$$

Furthermore, in the case of a time slot i selected for BC mode, the sum-rate is given by

$$\mathcal{R}_i^{RS_{1(2)}} = \frac{1}{2} \log_2 \det \left(\mathbf{H}_{R_f,S_{1(2)}} (\mathbf{Q}_{R_f,S_{1(2)}}/N_0) \mathbf{H}_{R_f,S_{1(2)}}^H + \mathbf{I} \right). \quad (5-32)$$

Therefore, by summing the sum-rate values found in each time slot and dividing this result by the total number of time slots, we have that the average sum-rate (\mathcal{R}) of the MWC-Best-User-Link scheme can be approximated by

$$\mathcal{R} \approx \frac{\sum_{i=1}^{n_{SR}} \mathcal{R}_i^{SR} + \sum_{i=1}^{n_{RS}} (\mathcal{R}_i^{RS_1} + \mathcal{R}_i^{RS_2})}{n_{SR} + n_{RS}}, \quad (5-33)$$

where n_{SR} and n_{RS} are the number of time slots selected for SR and RS transmissions, respectively.

5.4.3 Computational Cost

The number of operations of the relay selection algorithm of the proposed MWC-Best-User-Link is related to the complexity of the CNB or MMD [11–13] criterion. Table 5.2 shows the complexity of the relay selection algorithm in the proposed MWC-Best-User-Link (using the CNB criterion), and the existing MW-Max-Link [13], TW-Max-Link [14] and TW-Max-Min [82], here adapted for multiple-antenna systems (using the MMD criterion), for K clusters, N

Table 5.2: Computational Cost

Protocols	additions	multiplications
MWC-Best-User-Link	$2KN'V^2\mathcal{X} + KUN\mathcal{Y}$	$2KN'V^2\mathcal{Z} + KUN\mathcal{J}$
MW-Max-Link [13]	$KNM_S(\mathcal{U}^{total} - 3)$	$KNM_S(\mathcal{U}^{total})$
TW-Max-Link [14]	$NM_S(\mathcal{U}^{total} - 3)$	$NM_S(\mathcal{U}^{total})$
TW-Max-Min [82]	$\frac{NM_S}{2}(\mathcal{U}^{total} - 3)$	$\frac{NM_S}{2}(\mathcal{U}^{total})$

relays, M_S antennas at the users, $M_{R_{rx}} = 2UM_S$ antennas at the relays and $M_{R_{tx}} = M_S$ (selected among VM_S), considering $N' = N + C_2^N$, $\mathcal{X} = 0$, if $M_S = 1$, $\mathcal{X} = 1$, if $M_S = 2$, and $\mathcal{X} = 2M_S - 1$, if $M_S \geq 3$, $\mathcal{Y} = 1$, if $M_S = 1$, $\mathcal{Y} = 4M_S - 1$, if $M_S \geq 2$, $\mathcal{Z} = 0$, if $M_S = 1$, $\mathcal{Z} = 2$, if $M_S = 2$, and $\mathcal{Z} = 2(M_S^2 - M_S)$, if $M_S \geq 3$, $\mathcal{J} = 2$, if $M_S = 1$, $\mathcal{J} = 4M_S^2 - 2M_S$, if $M_S \geq 2$, and the number of calculations of the MMD metric for each relay is given by

$$\mathcal{U}^{total} = \sum_{i=1}^{2M_S} 2^{i-1}W^i C_i^{2M_S} + 2 \sum_{i=1}^{M_S} 2^{i-1}W^i C_i^{M_S}, \quad (5-34)$$

where W (quantity of distances between the constellation symbols) equals 1, for BPSK, and equals 3, for QPSK. Fig. 5.4 shows the complexity of the relay

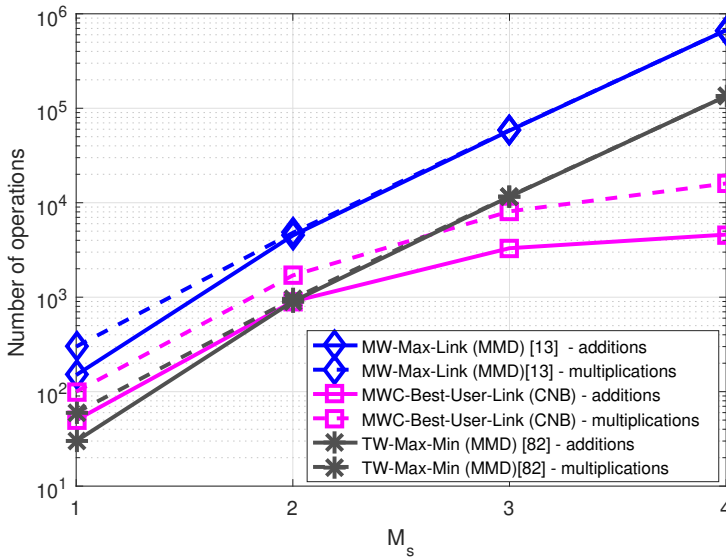


Figure 5.4: Computational cost.

selection algorithm in MWC-Best-User-Link (CNB), MW-Max-Link (MMD) and TW-Max-Min (MMD), for $M_{R_{rx}} = 2M_S$ ($U = 1$) and $M_{R_{tx}} = M_S$ ($V = 1$), $K = 5$, $N = 10$ and BPSK. From this result, we notice that the complexity of the relay selection algorithm in MWC-Best-User-Link (CNB) is smaller than the complexity of the relay selection algorithm in MW-Max-Link (MMD). If we increase the number of antennas to $M_S = 3$ (or more) the complexity of the MMD criterion is considerably greater than that of CNB.

5.4.4 Average Delay

In [39], a framework based on Discrete Time Markov Chains (DTMC) is proposed to analyze the traditional Max-Link algorithm, that considers single-antenna systems. This framework has been used in many subsequent works to analyze other buffer-aided relay selection protocols whose buffer is finite [45]. Moreover, in [45], this framework is used to analyze the average delay of an approach based on the Max-Link algorithm. In the following, we use this framework to analyze the average delay of the existing MW-Max-Link [13] and the proposed MWC-Best-User-Link protocols for multiple-antenna systems.

Similarly to Max-Link [39], MW-Max-Link [13] was originally considered for applications without critical delay constraints. In this work, by considering the importance of a short average delay in most modern applications, an expression for the average delay of the proposed MWC-Best-User-Link protocol is presented. The average delay is calculated by considering the time a packet needs to reach the destination once it has left the source (no delay is measured when the packet resides at the source [45]). So, the delay is the number of time slots the packet stays in the buffer of the relay [45]. In MW-Max-Link, each relay is equipped with a set of K buffers (each cluster has a particular buffer in the relays). For i.i.d. channels, the average delay is the same on all relays. Hence, it is sufficient to analyze the average delay on a single relay [45]. By Little's law, the average packet delay at relay's buffer R_j , denoted by $E[d_j]$ is given by

$$E[d_j] = \frac{E[L_j]}{E[T_j]}, \quad (5-35)$$

where $E[L_j]$ and $E[T_j]$ are the average queue length and average throughput, respectively [45]. The derivation for the average delay at the high SNR regime is given in [136]. As the selection of a relay's buffer is equiprobable, the average throughput at any relay's buffer R_j is $\frac{\rho}{NK}$, where ρ is the average data rate. Since we have half-duplex links $\rho = 1/2$ and therefore $E[T_j] = \frac{1}{2NK}$. Then, assuming an ideal balance between the operating modes (MA and BC), it can be shown that the average queue length at any relay is $E[L_j] = \frac{L}{2}$, where $L = \frac{J}{M_S}$. Thus, by Little's law, the average delay in the MW-Max-Link protocol is given by

$$E[d_j]^{BA} = E[d]^{BA} = NKL. \quad (5-36)$$

However, due to a possible unbalance between the operating modes, $E[L_j]$ may

be smaller or larger than $\frac{L}{2}$, ($E[L_j] < L$), and, consequently, $E[d_j]^{BA} < 2NKL$. So, as either the number of relays, the number of clusters or the buffer size increases, the average delay of MW-Max-Link increases. In contrast, in the Cloud-Driven MWC-Best-User-Link protocol, there is a unique set of K buffers that resides in the cloud. Consequently, as the number of relays increases, the average delay remains the same. Thus, by considering an ideal balance between the operating modes, the average delay in the proposed MWC-Best-User-Link is given by

$$E[d]^{CD} = KL. \quad (5-37)$$

However, with a possible unbalance between the operating modes, the same reasoning is applied and, consequently, $E[d_j]^{CD} < 2KL$. Nevertheless, the average delay can be further reduced by forcing the protocol to operate in BC mode and to select the cluster whose buffer is fullest, when the number of sets of M_S packets in the cloud buffers is greater than the low latency parameter LoL . By using LoL , considering an ideal balance between the operation modes, we have:

$$E[d]^{CD} = \begin{cases} 1, & \text{if } LoL = 0, \\ KL, & \text{if } LoL > KL. \end{cases} \quad (5-38)$$

or

$$E[d]^{CD} \approx LoL, \text{ if } 0 < LoL \leq KL, \quad (5-39)$$

and by considering a possible unbalance between the operating modes, the same reasoning applies.

5.5 Simulation Results

We assess via simulations the proposed MWC-Best-User-Link and the existing MW-Max-Link [13], using the CNB-based and the extended MMD-based relay selection algorithms. We employ BPSK signals and note that other constellations as QPSK and 16-QAM were not included but can be examined elsewhere. The performance of MWC-Best-User-Link and MW-Max-Link protocols was assessed for a set of L values. Then, we found that $L = \frac{J}{M_S} = 3$ sets of M_S packets is sufficient to ensure a good performance. We consider perfect and imperfect CSI and symmetric unit power channels ($\sigma_{S,R}^2 = \sigma_{R,S}^2 = 1$) and also asymmetric channels. We consider heterogeneous [88]

and homogeneous path-loss. As an example, in the simulated configuration with heterogeneous distances and path-loss, the distance between each source S_k (S_{1_k} or S_{2_k}) and each relay R_i is given by $d_{S_k,R_i} = \frac{d_{S_{k=1},R_i}}{1-0.1(k-1)}$ and the path-loss between each source S_k (S_{1_k} or S_{2_k}) and each relay R_i is given by $\xi_{S_k,R_i} = \xi_{S_{k=1},R_i} \times (1 + 0.25(k-1))$. In contrast, by considering homogeneous distances and path-loss, the source and relay nodes are distributed with different locations, but the relays have approximately equal distances and path-loss to the sources. Thus, the system model is simplified and given by $\mathbf{H}_{S_k,R_i} = \mathbf{G}_{S_k,R_i}$. Moreover, we consider time-uncorrelated and time-correlated channels. As an example, in the simulated configuration with time-correlated channels, the channel matrix in each time slot is given by $\mathbf{H}_{t+1} = \rho\mathbf{H}_t + \sqrt{1-\rho^2}\mathbf{H}_p$, where \mathbf{H}_t is the channel matrix in the previous time-slot, $-1 \leq \rho \leq 1$ and \mathbf{H}_p is also a zero mean complex Gaussian channel matrix ($\rho = 0$, for time-uncorrelated channels). The signal-to-noise ratio (SNR) given by E/N_0 ranges from 0 to 10 dB, where E is the energy transmitted from each source or the relay(s) and we consider $N_0 = 1$. The transmission protocols were simulated for $10000M_S$ packets, each with $T = 100$ symbols. We assumed perfect signaling between the cloud and the relays, but imperfect signaling can be considered in future works.

5.5.1 PEP and Sum-Rate performances

In this sub-section we present the theoretical PEP (computed by the algorithm based on the selected channel matrix \mathbf{H} , in each time slot) and the sum-rate performance obtained by simulation of the proposed MWC-Best-User-Link (using CNB and MMD) and the existing MW-Max-Link [13], TW-Max-Link [14] and TW-Max-Min [82] (using MMD).

Fig. 5.5 illustrates the Sum-Rate and the theoretical PEP performances, for homogeneous path-loss, Gaussian distributed signals and BPSK, respectively, of MWC-Best-User-Link (MMD), MWC-Best-User-Link (CNB), MW-Max-Link (MMD) [13], TW-Max-Link (MMD) [14] and TW-Max-Min (MMD) [82] protocols, for $M_S = 2$, $M_{R_{rx}} = 4$ ($U = 1$), $M_{R_{tx}} = 2$ ($V = 1$), $K = 5$, $N = 10$, $LoL > KL$, perfect CSI and unit power symmetric channels. The PEP performance of MWC-Best-User-Link (MMD) is considerably better than that of MWC-Best-User-Link (CNB), as MMD maximizes the metric \mathcal{D}'_{\min} , and the PEP performance of MWC-Best-User-Link (CNB) is close to the performance of MW-Max-Link. Nevertheless, the sum-rate performances of the MWC-Best-User-Link (MMD) and MWC-Best-User-Link (CNB) are considerably better than those of the other protocols for all the range of SNR values simulated.

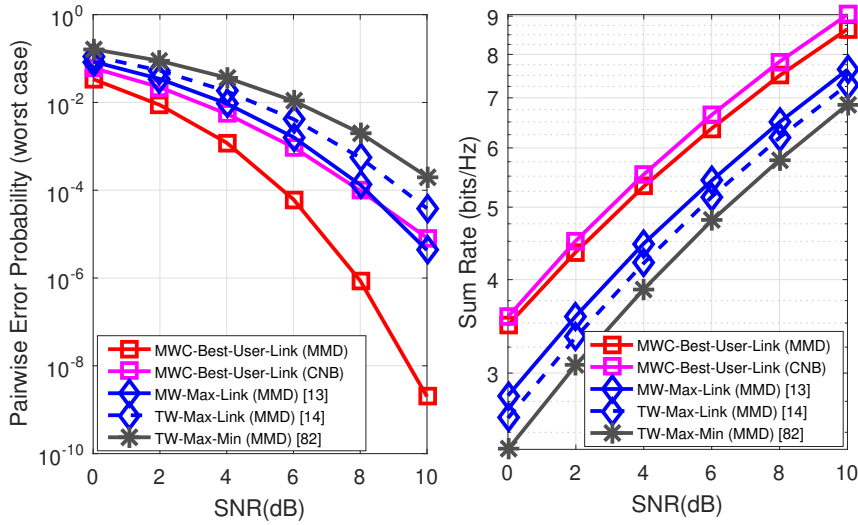


Figure 5.5: PEP and Sum-Rate performances versus SNR.

Moreover, the sum-rate performance of MWC-Best-User-Link (CNB) is superior to that of MWC-Best-User-Link (MMD), as CNB maximizes the sum-rate.

5.5.2 BER and Average Delay performances with the ML receiver

In this sub-section we present the BER and average delay performances of the proposed MWC-Best-User-Link (using the CNB-based and the extended MMD-based relay selection algorithms) and MW-Max-Link [13], using MMD, with the ML receiver, for homogeneous path-loss and time-uncorrelated channels.

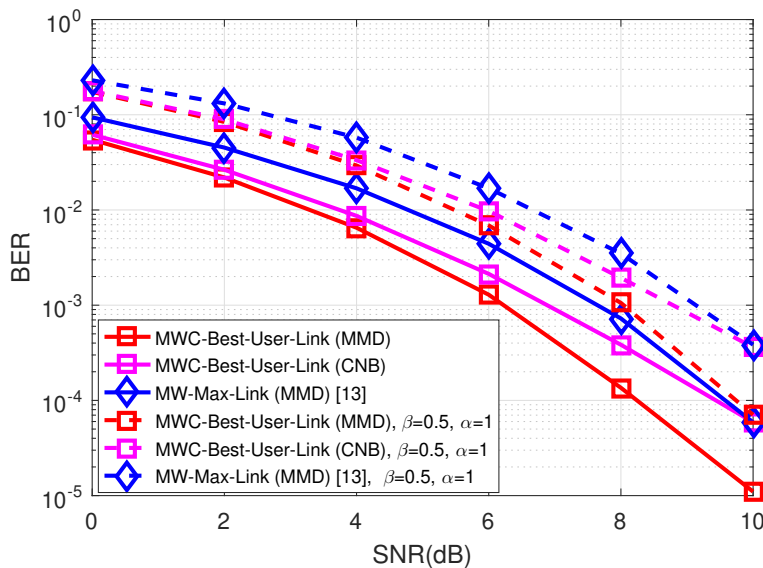


Figure 5.6: BER performance versus SNR, for perfect and imperfect CSI, with the ML receiver.

Fig. 5.6 depicts the BER performance of the MWC-Best-User-Link (MMD), MWC-Best-User-Link (CNB) and MW-Max-Link (MMD) protocols, for homogeneous path-loss, $M_S = 2$, $M_{R_{rx}} = 4$ ($U = 1$), $M_{R_{tx}} = 2$ ($V = 1$), $K = 5$, $N = 10$, BPSK, $LoL > KL$, perfect and imperfect CSI ($\beta = 0.5$ and $\alpha = 1$) and unit power symmetric channels. For both perfect and imperfect CSI (full and dashed curves, respectively), MWC-Best-User-Link (MMD) outperforms MWC-Best-User-Link (CNB), mainly for SNR values greater than 6dB, as MMD maximizes the metric \mathcal{D}'_{\min} . MWC-Best-User-Link (MMD) also outperforms MW-Max-Link for the range of SNR values simulated. Moreover, MWC-Best-User-Link (CNB) outperforms MW-Max-Link for SNR values less than 10dB. The results shown in Figs. 5.5 and 5.6 demonstrate the benefits of joint detection provided by the cloud-driven framework.

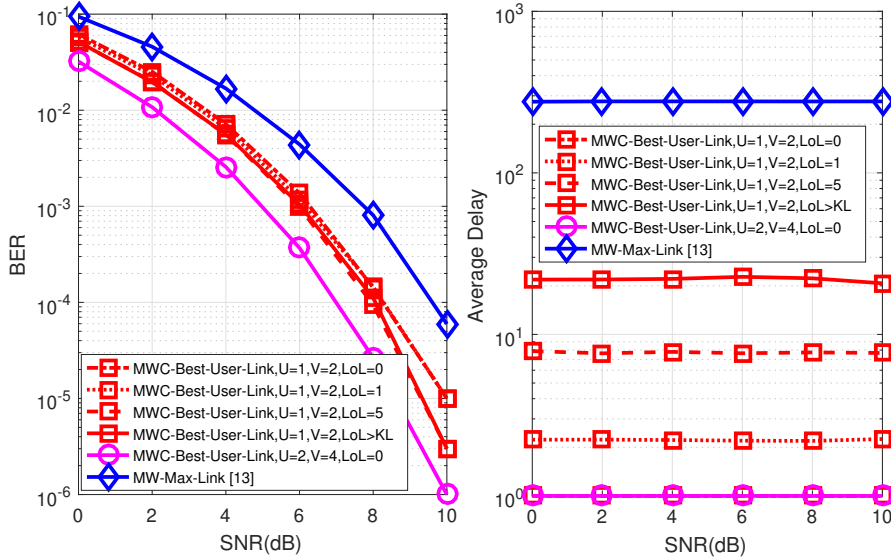


Figure 5.7: BER and Average Delay performances versus SNR, for perfect CSI and symmetric channels, with the ML receiver.

Fig. 5.7 illustrates the BER and the average delay performances of MWC-Best-User-Link (MMD) and MW-Max-Link (MMD) protocols, for homogeneous path-loss, BPSK, $M_S = 2$, $M_{R_{rx}} = 4$ and 8 ($U = 1$ and 2), $M_{R_{tx}} = 2$ ($V = 2$ and 4), $K = 5$, $N = 10$, $LoL = 0, 1, 5$ and $LoL > KL$, perfect CSI and unit power symmetric channels. The average delay performance of MWC-Best-User-Link is considerably better than that of MW-Max-Link, as MWC-Best-User-Link has a unique set of K cloud buffers. When we reduce the value of LoL to 0 in the MWC-Best-User-Link protocol, the average delay is reduced to 1 time slot, keeping almost the same BER performance. This result validates our analysis in Section 5.4. Moreover, the BER performance of MWC-Best-User-Link is considerably better than that of MW-Max-Link for $U = 1$ and $V = 2$. For higher values of U and V the BER performance of

MWC-Best-User-Link is considerably improved, due to a higher diversity gain in the uplink and the antenna selection in the downlink.

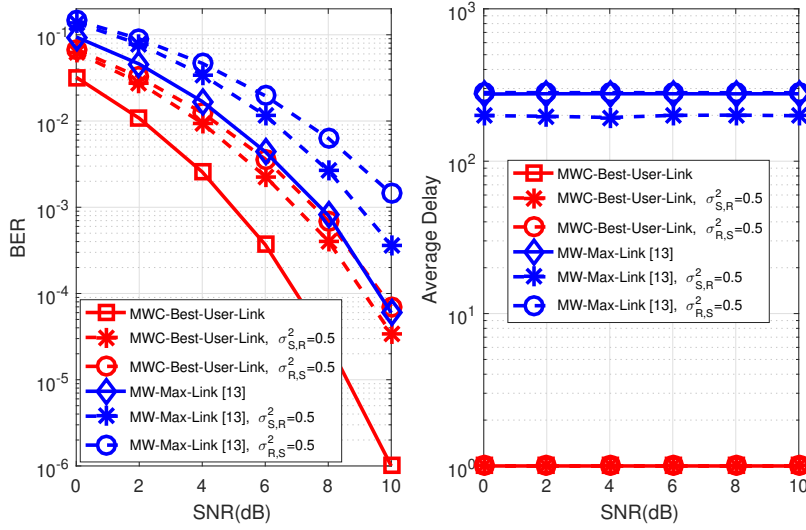


Figure 5.8: BER and Average Delay performances versus SNR, for perfect CSI, symmetric and asymmetric channels, with the ML receiver.

Fig. 5.8 illustrates the BER and the average delay performances of MWC-Best-User-Link (MMD) and MW-Max-Link (MMD) protocols, for homogeneous path-loss, BPSK, $M_S = 2$, $M_{R_{rx}} = 8$ ($U = 2$), $M_{R_{tx}} = 2$ ($V = 4$), $K = 5$, $N = 10$, $LoL = 0$, symmetric ($\sigma_{S,R}^2 = \sigma_{R,S}^2 = 1$) and asymmetric channels ($\sigma_{S,R}^2 = 1$ and $\sigma_{R,S}^2 = 0.5$ or $\sigma_{S,R}^2 = 0.5$ and $\sigma_{R,S}^2 = 1$) and perfect CSI. The average delay performance of MWC-Best-User-Link is considerably better than that of MW-Max-Link. When LoL equals 0 in the MWC-Best-User-Link protocol, the average delay equals 1 time slot and the BER performance of MWC-Best-User-Link is considerably better than that of MW-Max-Link, for both symmetric and asymmetric channels. If we consider higher values of U and V , the BER performance of MWC-Best-User-Link can be further improved.

5.5.3

BER and Average Delay performances with the MMSE receiver

In this sub-section we present the BER and average delay performances of the proposed MWC-Best-User-Link (using the CNB-based and the extended MMD-based relay selection algorithms) and MW-Max-Link [13], using CNB, with the linear MMSE receiver, for homogeneous path-loss and time-uncorrelated channels.

Fig. 5.9 depicts the BER performance of the MWC-Best-User-Link (MMD), MWC-Best-User-Link (CNB) and MW-Max-Link (CNB) protocols, for homogeneous path-loss, $M_S = 2$, $M_{R_{rx}} = 4$ ($U = 1$), $M_{R_{tx}} = 2$ ($V = 1$),

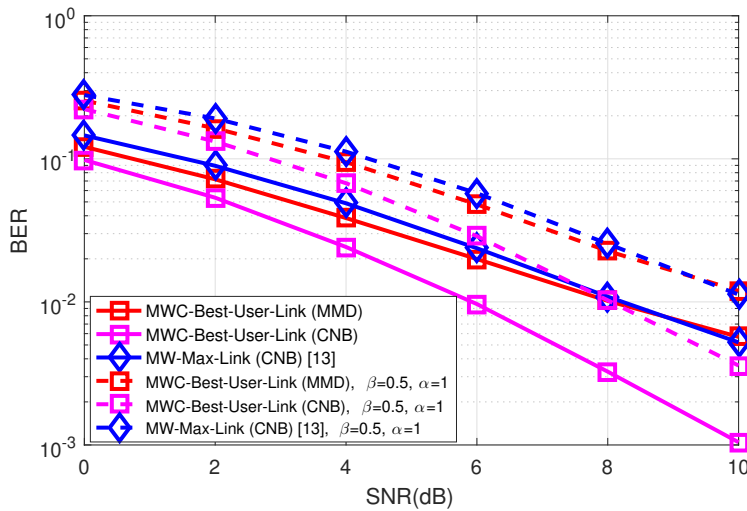


Figure 5.9: BER performance versus SNR, for perfect and imperfect CSI, with the linear MMSE receiver.

$K = 5$, $N = 10$, BPSK, $LoL > KL$, perfect and imperfect CSI ($\beta = 0.5$ and $\alpha = 1$) and unit power symmetric channels. For both perfect and imperfect CSI (full and dashed curves, respectively), the BER performance of MWC-Best-User-Link (CNB) is considerably better than that of MWC-Best-User-Link (MMD), as CNB minimizes the effects of the effective noise and, consequently, minimizes the BER in the MMSE receiver, and MMD is based on the ML principle and the PEP. Moreover, MWC-Best-User-Link (CNB) also outperforms MW-Max-Link (CNB) for all the range of SNR values simulated.

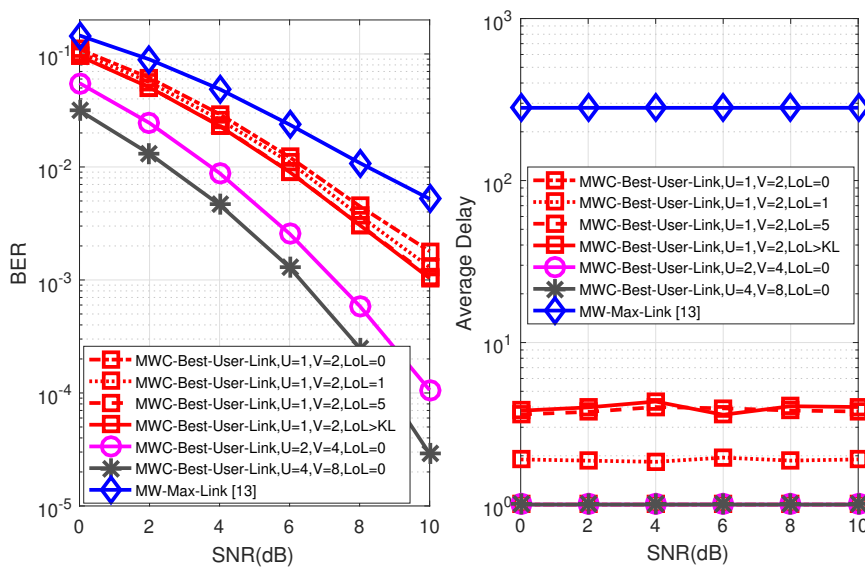


Figure 5.10: BER and Average Delay performances versus SNR, for perfect CSI and symmetric channels, with the linear MMSE receiver.

Fig. 5.10 illustrates the BER and the average delay performances of MWC-Best-User-Link (CNB) and MW-Max-Link (CNB), for homogeneous path-loss, BPSK, $M_S = 2$, $M_{R_{rx}} = 4, 8$ and 16 ($U = 1, 2$ and 4), $M_{R_{tx}} = 2$ ($V = 2, 4$ and 8), $K = 5$, $N = 10$, $LoL = 0, 1, 5$ and $LoL > KL$, perfect CSI and unit power symmetric channels. The average delay performance of MWC-Best-User-Link is considerably better than that of MW-Max-Link, as MWC-Best-User-Link has a unique set of K cloud buffers. When we reduce the value of LoL to 0 in the MWC-Best-User-Link protocol, the average delay is reduced to 1 time slot, keeping almost the same BER performance. Moreover, the BER performance of MWC-Best-User-Link is considerably better than that of MW-Max-Link for $U = 1$ and $V = 2$. For higher values of U and V the BER performance of MWC-Best-User-Link is considerably improved, due to a higher diversity gain in the uplink and the antenna selection in the downlink.

PUC-Rio - Certificação Digital N° 1712525/CA

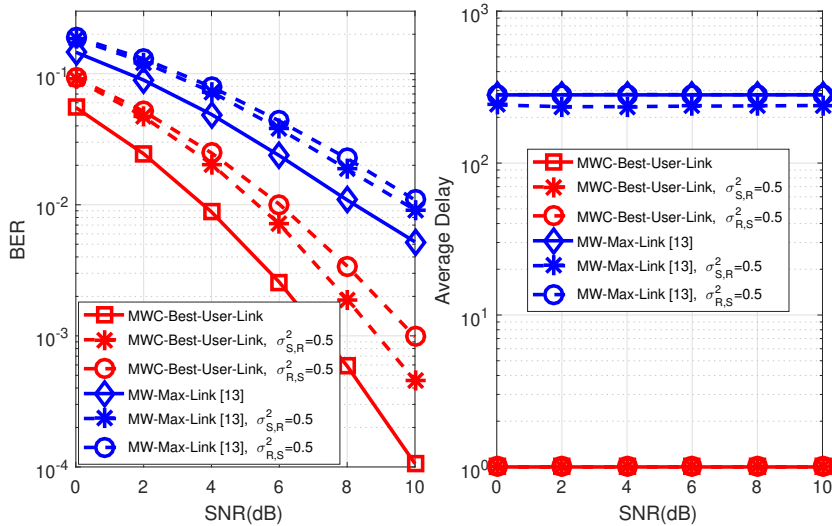


Figure 5.11: BER and Average Delay performances versus SNR, for perfect CSI, symmetric and asymmetric channels, with the linear MMSE receiver.

Fig. 5.11 illustrates the BER and the average delay performances of MWC-Best-User-Link (CNB) and MW-Max-Link (CNB) protocols, for homogeneous path-loss, BPSK, $M_S = 2$, $M_{R_{rx}} = 8$ ($U = 2$), $M_{R_{tx}} = 2$ ($V = 4$), $K = 5$, $N = 10$, $LoL = 0$, symmetric ($\sigma_{S,R}^2 = \sigma_{R,S}^2 = 1$) and asymmetric channels ($\sigma_{S,R}^2 = 1$ and $\sigma_{R,S}^2 = 0.5$ or $\sigma_{S,R}^2 = 0.5$ and $\sigma_{R,S}^2 = 1$) and perfect CSI. The average delay performance of MWC-Best-User-Link is considerably better than that of MW-Max-Link. When LoL equals 0 in the MWC-Best-User-Link protocol, the average delay equals 1 time slot and the BER performance of MWC-Best-User-Link is considerably better than that of MW-Max-Link, for both symmetric and asymmetric channels. If we consider higher values of U and V , the BER performance of MWC-Best-User-Link can be further improved.

5.5.4

BER and Sum-Rate performances, for heterogeneous path-loss and time-correlated channels

In this section we present the BER and sum-rate performances of the proposed MWC-Best-User-Link and the existing MW-Max-Link [13] (using the extended MMD-based relay selection algorithm with the linear ML receiver and the CNB-based relay selection algorithm with the linear MMSE receiver), for heterogeneous path-loss and time-correlated channels.

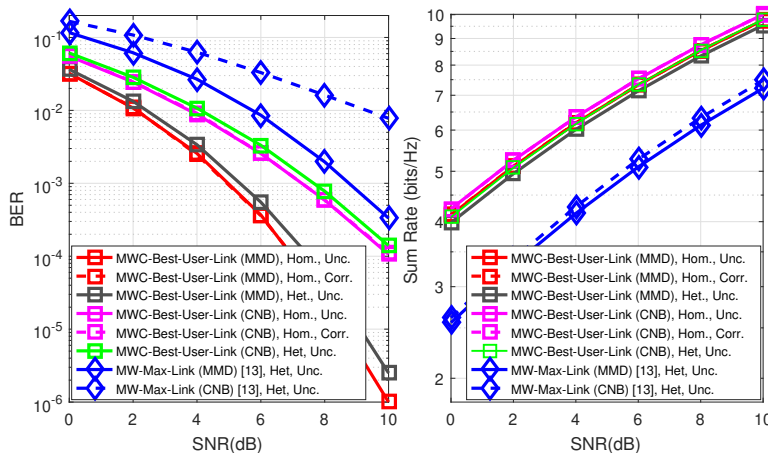


Figure 5.12: BER and Sum-Rate performances versus SNR, for homogeneous and heterogeneous path-loss, time-correlated and time-uncorrelated channels.

Fig. 5.12 illustrates the BER and the sum-rate performances of MWC-Best-User-Link (MMD) and MWC-Best-User-Link (CNB) protocols, considering 3 different configurations: a) homogeneous path-loss and time-uncorrelated channels, b) homogeneous path-loss and time-correlated channels ($\rho^2 = 0.9$), c) heterogeneous path-loss and time-uncorrelated channels, for BPSK, $M_S = 2$, $M_{R_{rx}} = 8$ ($U = 2$), $M_{R_{tx}} = 2$ ($V = 4$), $K = 5$, $N = 10$, $LoL = 0$ and perfect CSI. The BER and sum-rate performances of MWC-Best-User-Link are the same for time-uncorrelated or time-correlated channels, as these protocols select the best links in each time slot. Moreover, the BER and sum-rate performances of MWC-Best-User-Link considering heterogeneous path-loss are almost equal to that for homogeneous path-loss, as the links selected by the proposed protocol tends to be associated with the cluster of users which is closest to the cluster of relays. Furthermore, the BER and sum-rate performances of MWC-Best-User-Link considering heterogeneous path-loss are considerably better than those of MW-Max-Link.

5.6 Summary

A novel framework using a cloud as a central node with buffers has been introduced and investigated as a favorable relay selection strategy for multi-way protocols. We have examined relay-selection techniques for multi-way cooperative MIMO systems that are driven by a cloud central node, where a cluster with two sources is selected to simultaneously transmit to each other aided by relays. In order to perform signal detection at the cloud and the nodes, we have presented ML and linear MMSE detectors. Moreover, we have considered the ideal case where the fronthaul links have unconstrained capacities and the relays can convey their exact received signals to the cloud processor. Practical systems, however, have capacity-constrained fronthaul links [93], which can be considered in future works and the performance achieved by the proposed protocol may be considered as an upper bound. Simulations illustrate the excellent performance of the proposed MWC-Best-User-Link protocol, that by using the novel CNB-based or the extended MMD-based relay selection algorithm outperformed the existing MW-Max-Link scheme in terms of PEP, sum-rate, average delay and computational cost. In particular, this novel protocol has a considerably reduced average delay, keeping the high diversity gain, both for MMSE and ML detection. Moreover, MWC-Best-User-Link (MMD) has the best performance when ML detection is used, as the MMD criterion minimizes the error in the ML receiver. In contrast, MWC-Best-User-Link (CNB) has the best performance when MMSE detection is present, as the CNB criterion minimizes the error in the MMSE receiver. Thus, by comparing the complexity and the performance of these relay selection algorithms and receivers, we recommend the use of MMD and ML detection, for $M_S \leq 2$ antennas, and CNB and linear MMSE detection, otherwise.

6

Conclusions and Future Work

6.1

Conclusions

In this work, we have presented the novel MMD relay selection criterion and novel protocols based on the MMD for Cooperative Multi-Antenna Systems:

- Switched Max-Link Relay Selection for One-Way Cooperative Multi-Antenna Systems;
- Buffer-Aided Max-Link Relay Selection for Two-Way and Multi-Way Cooperative Multi-Antenna Systems;

We have investigated the benefits of using Switched Max-Link with the MMD relay selection criterion for MIMO systems. Switched Max-Link was evaluated experimentally and outperformed the conventional direct transmission and the existing QN Max-Link scheme. Despite the higher complexity of the proposed Switched Max-Link with the MMD relay selection criterion, it is an attractive solution for relaying systems with source and destination nodes equipped with a small number of antennas and relay nodes equipped with a small or large number of antennas due to its high performance and reduced delay.

We have also examined a relay-selection strategy for multi-way cooperative multi-antenna systems that is aided by a central processor node denoted MW-Max-Link, where a cluster formed by two users is selected to simultaneously transmit to each other with the help of relays. In particular, the MW-Max-Link multi-way relay selection strategy selects the best link, exploiting the use of buffers and PLNC. The proposed MW-Max-Link was evaluated experimentally and outperformed the TW-Max-Link and the existing TW-Max-Min scheme. The use of a central processor node and buffers in the relays is advocated as a promising relay selection technique and a framework for multi-way protocols (where each cluster has a particular buffer established on demand in the relays).

Moreover, a novel framework configured by a cloud as a central node with buffers has been introduced and investigated as a favorable relay selection

strategy for multi-way protocols. We have examined relay-selection techniques for multi-way cooperative MIMO systems that are driven by a cloud central node, where a cluster with two sources is selected to simultaneously transmit to each other aided by relays. In order to perform signal detection at the cloud and the nodes, we have developed ML and linear MMSE detectors. Simulations illustrate the excellent performance of the proposed MWC-Best-User-Link protocol, that by using the novel CNB-based or the extended MMD-based relay selection algorithm outperformed the existing MW-Max-Link scheme in terms of PEP, sum-rate, average delay and computational cost. In particular, this novel protocol has a considerably reduced average delay, keeping the high diversity gain, both for MMSE and ML detection. Moreover, MWC-Best-User-Link (MMD) has the best performance when ML detection is used, as the MMD criterion minimizes the error in the ML receiver. In contrast, MWC-Best-User-Link (CNB) has the best performance when MMSE detection is present, as the CNB criterion minimizes the effects of the effective noise and, consequently, minimizes the BER in the MMSE receiver. Thus, by comparing the complexity and the performance of these relay selection algorithms and receivers, we recommend the use of MMD and ML detection, for $M_s \leq 2$ antennas, and CNB and linear MMSE detection, otherwise.

6.2 Future Work

In this section we discuss about possible future work: a) Use of capacity-constrained fronthaul links in the presented MWC-Best-User-Link protocol; b) Design of a novel Cloud-Driven Best-User-Link Relay Selection protocol for Multi-Way Cooperative Multi-Antenna Systems, in which multiple clusters are selected to establish communication simultaneously and exploiting different kinds of PLNC (XOR, linear and non-linear); c) Investigation of channel estimation techniques for the proposed protocols; and d) Use of the presented protocols in Unmanned Aerial Vehicles (UAVs).

6.2.1 Capacity-Constrained Fronthaul Links

In this Thesis, in chapter 5, we focused on the ideal case where the fronthaul links have unconstrained capacities, and the relays can convey their exact received signals to the cloud processor. This could happen only if the relays were near the cloud and experiencing high signal-to-noise and low interference conditions. Practical systems, however, have capacity-constrained fronthaul links [93] and this limits the amount of information that the relays

can retransmit. Thus, capacity-constrained fronthaul links can be considered in future works and the performance achieved by the presented MWC-Best-User-Link protocol may be considered as an upper bound.

6.2.2 Physical-Layer Network Coding

We are working on the design of a novel Cloud-Driven Best-User-Link Relay Selection protocol for Multi-Way Cooperative Multiple-Antenna Systems, in which multiple clusters are selected to establish communication simultaneously, named Multi-Clusters Cloud-Driven Best-User-Link (MCC-Best-User-Link). All the processing including detection will be done in the cloud processor. We will test the performance of this protocol, exploiting different kinds of PLNC (XOR, linear and non-linear). Our intention is to develop a new approach in PLNC and apply it in this protocol. Fig 6.1 shows the system model of a cloud-driven multi-clusters relay system.

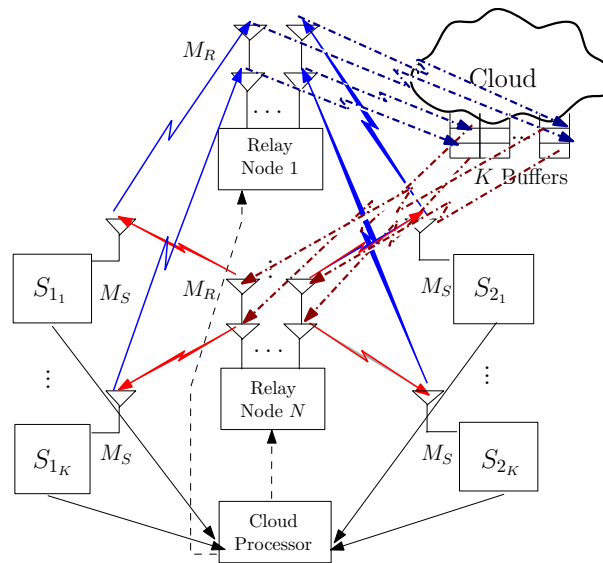


Figure 6.1: System model of a cloud-driven multi-clusters relay system.

6.2.3 Channel Estimation

Cooperative diversity schemes have been proposed for cellular networks that permit a base station (or a mobile station) to relay signals to a destination receiver [138]. This increases the network coverage and reliability. The mobile relays usually decode and forward (DF) or amplify and forward (AF) the received signal. Most existing analyses of cooperation diversity assumes perfect channel information at the receiver. A realistic assessment should consider the

effects of practical channel estimation schemes [138]. Thus, future works may consider pilot symbol aided channel estimation for the presented MWC-Best-User-Link cooperation diversity system with buffers and cloud, using the DF protocol or modified to use the AF protocol. Since the overall channel in AF systems is different from conventional cellular channels, the channel estimation problem is interesting and challenging and therefore the works may be also on AF systems [138]. Thus, future works may address issues such as the estimator design, pilot symbol spacing based upon realistic channel models, and BER analysis that accounts for imperfect channel estimation.

6.2.4

Unmanned Aerial Vehicles and time-correlated channels

Unmanned Aerial Vehicles (UAVs) and their networks are becoming increasingly important in a number of practical applications in a variety of communication and information systems [139, 140]. In the context of wireless communications, UAVs can be used to establish a temporary communication infrastructure during a natural disaster [139, 141], military battles, or to provide coverage to remote areas by acting as drone cells [139, 142], among other uses. The presented protocols (Switched Max-Link, MW-Max-Link and MWC-Best-User-Link) could be adapted and used in UAVs networks, in which the UAVs would be used as relays in scenarios with heterogeneous distances and path-loss between the UAV relay nodes and the mobile users. Moreover, in this context, time-correlated channels could be considered in the design of the UAV relay-selection algorithms, leading to lower computational complexity than those of the presented CNB-based and MMD-based relay selection algorithms, that were designed considering time-uncorrelated channels.

As an example, in UAVs networks using the Switched-Max-Link protocol we could consider a multiple-antenna UAV relay scheme with one source node, one destination node and N half-duplex (HD) decode-and-forward (DF) relays. The source and destination nodes (mobile users) would have M_S antennas for transmission and reception, respectively, and each UAV relay $M_R = UM_S$ antennas, where $U \in \{1, 2, 3, \dots\}$. All the M_R antennas would be used for reception ($M_{R_{rx}} = M_R$) and a set of M_S antennas would be selected among M_R to be used for transmission ($M_{R_{tx}} = M_S$).

Moreover, in UAVs networks using the MW-Max-Link protocol we could consider a multiple-antenna multi-way MABC UAV relay scheme with $Z \in \{1, 2, 3, \dots\}$ pairs of mobile users and N HD DF UAV relays. The users would be equipped with M_S antennas and each UAV relay with $2M_S$ antennas (or more, in a MW-Max-Link modified protocol). A total of Z buffers would be

accessed by the selected UAV relays for storing or extracting (each pair of users would have a particular buffer established on demand in the UAV relays). In the multiple-access phase, a UAV relay would be selected to receive simultaneously M_S packets from a selected cluster (pair of mobile users) and decode the data. Then, XOR type PLNC would be employed on the decoded data and the resulting packets would be stored in their particular buffers. In the broadcast-channel phase, a UAV relay would be selected to transmit M_S packets from the particular buffer to the selected cluster.

Furthermore, in UAVs networks using the MWC-Best-User-Link protocol we could consider a multiple-antenna multi-way MABC UAV relay scheme formed by K clusters and N HD DF UAV relays. In a C-RAN, the UAV relays would represent RRHs. The users would have M_S antennas for transmission or reception and each UAV relay $M_R = 2UM_s$ antennas, where $U \in \{1, 2, 3 \dots\}$, all of them used by the selected UAV relay for reception ($M_{R_{rx}} = M_R$) and M_S out of VM_S antennas would be selected of each UAV relay used for transmission ($M_{R_{tx}} = M_S$), where $V \in \{1, 2, 3 \dots\}$ and $VM_S \leq M_R$. The selected UAV relays would access a number of K cloud buffers for extracting or storing M_S packets in each time slot. Each cluster would have a particular cloud buffer established on demand. In the multiple-access phase, a cluster would be selected to send M_S packets simultaneously to a selected UAV relay for reception. Then, the data would be decoded by the cloud processor and XOR type PLNC would be applied to combine the decoded vectors (inputs of the XOR) and generate a codeword (output of the XOR) that is stored in their particular cloud buffers. In the broadcast-channel phase, two UAV relays would be selected to broadcast M_S packets from the particular cloud buffer to the selected cluster.

Bibliography

- [1] LANEMAN, J. N.; TSE, D. N. C.; WORNELL, G. W.. **Cooperative Diversity in Wireless Networks: Efficient Protocols and Outage Behavior**. IEEE Transactions on Information Theory, 50(12):3062-3080, Dec. 2004.
- [2] SENDONARIS, A.; ERKIP, E.; AAZHANG, B.. **User cooperation diversity - parts I and II**. IEEE Transactions on Communications, 51(11):1927–1948, Nov. 2003.
- [3] COVER, T.; GAMAL, A.E.. **Capacity Theorems for the Relay Channel**. IEEE Transactions on Information Theory, 25(5):572-584, Sept. 1979.
- [4] IKHLEF, A.; MICHALOPOULOS, D. S.; SCHOBER, R.. **Max-Max Relay Selection for Relays with Buffers**. IEEE Transactions on Wireless Communications, 11(3):1124-1135, March 2012.
- [5] HESKETH, T.; DE LAMARE, R. C.; WALES, S.. **Joint maximum likelihood detection and link selection for cooperative MIMO relay systems**. IET Communications, 8(4):2489-2499, Sept. 2014.
- [6] CLARKE, P.; DE LAMARE, R. C.. **Transmit Diversity and Relay Selection Algorithms for Multirelay Cooperative MIMO Systems**. IEEE Transactions on Vehicular Technology, 61(3):1084-1098, March 2012.
- [7] LIU, K. J. R.; SADEK, A. K.; SU, W.; KWASINSKI, A.. **Cooperative Communications and Networking**. Cambridge University Press, 1st edition, 2009.
- [8] ZEMLIANOV, A.; DE VECIANA, G.. **Capacity of ad hoc wireless networks with infrastructure support**. IEEE Journal on Selected Areas in Communications, 23(3): 657-667, March 2005.
- [9] BIGLIERI, E.; CALDERBANK, R.; CONSTANTINIDES, A.; GOLDSMITH, A.; PAULRAJ, A.; POOR, H. V.. **MIMO Wireless Communications**. Cambridge University Press, 1st edition, Cambridge, U.K, 2007.
- [10] CUNHA T. E. B.. **Joint Automatic Gain Control and Receiver Design for Quantized Large-Scale MU-MIMO Systems**. Master Thesis. Pontif-

- ical Catholic University of Rio de Janeiro (PUC-Rio), March 2019. [Online]. Available at: <https://www.maxwell.vrac.puc-rio.br/45629/45629.PDF>
- [11] DUARTE, F. L.; DE LAMARE, R. C.. **Switched Max-Link Buffer-Aided Relay Selection for Cooperative Multiple-Antenna Systems**. In: SCC 2019; 12TH INTERNATIONAL ITG CONFERENCE ON SYSTEMS, COMMUNICATIONS AND CODING, Rostock, Germany, 2019, pp. 1-6.
- [12] DUARTE, F. L.; DE LAMARE, R. C.. **Switched Max-Link Relay Selection Based on Maximum Minimum Distance for Cooperative MIMO Systems**. IEEE Transactions on Vehicular Technology, 69(2):1928-1941, Feb. 2020.
- [13] DUARTE, F. L.; DE LAMARE, R. C.. **Buffer-Aided Max-Link Relay Selection for Multi-Way Cooperative Multi-Antenna Systems**. IEEE Communications Letters, 23(8):1423-1426, Aug. 2019.
- [14] DUARTE, F. L.; DE LAMARE, R. C.. **Buffer-Aided Max-Link Relay Selection for Two-Way Cooperative Multi-Antenna Systems**. In: 2019 16TH INTERNATIONAL SYMPOSIUM ON WIRELESS COMMUNICATION SYSTEMS (ISWCS), Oulu, Finland, 2019, pp. 288-292.
- [15] NOMIKOS, N. ET AL. **A Survey on Buffer-Aided Relay Selection** IEEE Communications Surveys & Tutorials, 18(2):1073-1097, Secondquarter 2016.
- [16] CHEN, Z.; FAN, P. ; WU, D. O.. **Joint Power Allocation and Strategy Selection for Half-Duplex Relay System**. IEEE Transactions on Vehicular Technology, 66(3):2144-2157, March 2017.
- [17] ZLATANOV, N.; IKHLEF, A.; ISLAM, T.; SCHOBER, R.. **Buffer-aided cooperative communications: opportunities and challenges**. IEEE Communications Magazine, 52(4):146-153, April 2014.
- [18] HOYMANN, C. **Relaying in 3GPP LTE**, ITG Fachtagung – IMT Advanced, Ericsson Research – AACHEN. July 2010. [Online]. Available at: <https://www.slideshare.net/allabout4g/relaying-in-3gpp-lteadvanced>
- [19] ERICSSON. **5 G Radio Access**. White Paper 1, 10p, Ericsson, Uen 284 23-3204 Rev C | April 2016. [Online]. Available at: <https://www.ericsson.com/assets/local/publications/white-papers/wp-5g.pdf>
- [20] BLETSAS, A.; KHISTI A.; REED, D. P.; LIPPMAN, A., **A simple cooperative diversity method based on network path selection**. IEEE Journal on Selected Areas in Communications, 24(3):659-672, March 2006.

- [21] BLETSAS, A.; SHIN, H.; WIN, M. Z.. **Cooperative communications with outage-optimal opportunistic relaying**. IEEE Transactions on Wireless Communications, 6(9):3450-3460, Sept. 2007.
- [22] MICHALOPOULOS, D. S.; KARAGIANNIDIS, G. K.. **Performance analysis of single relay selection in Rayleigh fading**. IEEE Transactions on Wireless Communications, 7(10):3718-3724, Oct. 2008.
- [23] MICHALOPOULOS, D. S.; KARAGIANNIDIS, G. K.. **Two relay distributed switch and stay combining**. IEEE Transactions on Communications, 56(11):1790-1794, Nov. 2008.
- [24] KRIKIDIS, I.; THOMPSON, J.; MCLAUGHLIN, S.; GOERTZ, N.. **Amplify-and-forward with partial relay selection**. IEEE Communications Letters, 12(4):235-237, April 2008.
- [25] MICHALOPOULOS, D. S.; LIOUMPAS, A. S.; KARAGIANNIDIS, G. K.; SCHOBBER, R.. **Selective Cooperative Relaying over Time-Varying Channels**. IEEE Transactions on Communications, 58(8):2402-2412, Aug. 2010.
- [26] MICHALOPOULOS, D. S.; SURAWEERA, H. A.; KARAGIANNIDIS, G. K.; SCHOBBER, R.. **Amplify-and-Forward Relay Selection with Outdated Channel Estimates**. IEEE Transactions on Communications, 60(5):1278-1290, May 2012.
- [27] MICHALOPOULOS, D. S.; NG, J.; SCHOBBER, R.. **Optimal Relay Selection for Outdated CSI**. IEEE Communications Letters, 17(3):503-506, March 2013.
- [28] RIIHONEN, T.; WERNER, S.; WICHMAN, R.. **Hybrid Full-Duplex/Half-Duplex Relaying with Transmit Power Adaptation**. IEEE Transactions on Wireless Communications, 10(9):3074-3085, Sept. 2011.
- [29] RIIHONEN, T.; WERNER, S.; WICHMAN, R.. **Mitigation of Loopback Self-Interference in Full-Duplex MIMO Relays**. IEEE Transactions on Signal Processing, 59(12), 5983-5993, Dec. 2011.
- [30] KRIKIDIS, I.; SURAWEERA, H. A.; SMITH, P. J.; YUEN, C.. **Full-Duplex Relay Selection for Amplify-and-Forward Cooperative Networks**. IEEE Transactions on Wireless Communications, 11(12):4381-4393, Dec. 2012.
- [31] RANKOV, B.; WITTNEBEN, A.. **Spectral efficient protocols for half-duplex fading relay channels**. IEEE Journal on Selected Areas in Communications, 25(2):379-389, Feb. 2007.

- [32] FAN, Y.; WANG, C.; THOMPSON, J.; POOR, H. V.. **Recovering Multiplexing Loss through Successive Relaying Using Repetition Coding**. IEEE Transactions on Wireless Communications, 6(12):4484-4493, Dec. 2007.
- [33] WICAKSANA, H.; TING, S. H.; GUAN, Y. L.; XIA, X.. **Decode-and-Forward Two-Path Half-Duplex Relaying: Diversity-Multiplexing Tradeoff Analysis**. IEEE Transactions on Communications, 59(7):1985-1994, July 2011.
- [34] DING, Z.; KRIKIDIS, I.; RONG, B.; THOMPSON, J. S.; WANG, C.; YANG, S.. **On combating the half-duplex constraint in modern cooperative networks: protocols and techniques**. IEEE Wireless Communications, 19(6):20-27, Dec. 2012.
- [35] GU, J.; DE LAMARE, R. C.; HUEMER, M.. **Buffer-Aided Physical-Layer Network Coding With Optimal Linear Code Designs for Cooperative Networks**. IEEE Transactions on Communications, 66(6):2560-2575, June 2018.
- [36] MEHTA, N. B.; SHARMA, V.; BANSAL, G.. **Performance Analysis of a Cooperative System with Rateless Codes and Buffered Relays**. IEEE Transactions on Wireless Communications, 10(4):1069-1081, April 2011.
- [37] WANG, R.; LAU, V. K. N.; HUANG, H.. **Opportunistic Buffered Decode-Wait-and-Forward (OBDWF) Protocol for Mobile Wireless Relay Networks**. IEEE Transactions on Wireless Communications, 10(4):1224-1231, April 2011.
- [38] NOMIKOS, N.; CHARALAMBOUS, T.; KRIKIDIS, I.; SKOUTAS, D. N.; VOUYIOUKAS, D.; JOHANSSON, M.. **A Buffer-Aided Successive Opportunistic Relay Selection Scheme With Power Adaptation and Inter-Relay Interference Cancellation for Cooperative Diversity Systems**. IEEE Transactions on Communications, 63(5):1623-1634, May 2015.
- [39] KRIKIDIS, I.; CHARALAMBOUS, T.; THOMPSON, J. S.. **Buffer-Aided Relay Selection for Cooperative Diversity Systems without Delay Constraints**. IEEE Transactions on Wireless Communications, 11(5): 1957-1967, May 2012.
- [40] CHARALAMBOUS, T.; NOMIKOS, N.; KRIKIDIS, I.; VOUYIOUKAS, D.; JOHANSSON, M.. **Modeling Buffer-Aided Relay Selection in Networks With Direct Transmission Capability**. IEEE Communications Letters, 19(4):649-652, April 2015.

- [41] TIAN, Z.; CHEN, G.; GONG, Y.; CHEN, Z.; CHAMBERS, J. A.. **Buffer-Aided Max-Link Relay Selection in Amplify-and-Forward Cooperative Networks**. IEEE Transactions on Vehicular Technology, 64(2):553-565, Feb. 2015.
- [42] LUO, S.; TEH, K. C.. **Buffer State Based Relay Selection for Buffer-Aided Cooperative Relaying Systems**. IEEE Transactions on Wireless Communications, 14(10):5430-5439, Oct. 2015.
- [43] XU, P.; DING, Z.; KRIKIDIS, I.; DAI, X.. **Achieving Optimal Diversity Gain in Buffer-Aided Relay Networks With Small Buffer Size**. IEEE Transactions on Vehicular Technology, 65(10): 8788-8794, Oct. 2016.
- [44] OIWA, M.; TOSA, C.; SUGIURA, S.. **Theoretical Analysis of Hybrid Buffer-Aided Cooperative Protocol Based on Max-Max and Max-Link Relay Selections**. IEEE Transactions on Vehicular Technology, 65(11): 9236-9246, Nov. 2016.
- [45] POULIMENEAS, D.; CHARALAMBOUS, T.; NOMIKOS, N.; KRIKIDIS, I.; VOUYIOUKAS, D.; JOHANSSON, M.. **Delay-and diversity-aware buffer-aided relay selection policies in cooperative networks**. In: 2016 IEEE WIRELESS COMMUNICATIONS AND NETWORKING CONFERENCE, Doha, 2016, pp. 1-6.
- [46] SIDDIG, A. A. M.; SALLEH, M. F. M.. **Balancing Buffer-Aided Relay Selection for Cooperative Relaying Systems**. IEEE Transactions on Vehicular Technology, 66(9):8276-8290, Sept. 2017.
- [47] MANOJ, B. R.; MALLIK, R. K.; BHATNAGAR, M. R.. **Performance Analysis of Buffer-Aided Priority-Based Max-Link Relay Selection in DF Cooperative Networks**. IEEE Transactions on Communications, 66(7): 2826-2839, July 2018.
- [48] ZLATANOV, N.; SCHOBBER, R.; POPOVSKI, P.. **Buffer-Aided Relaying with Adaptive Link Selection**. IEEE Journal on Selected Areas in Communications, 31(8):1530-1542, Aug. 2013.
- [49] ZLATANOV, N.; SCHOBBER, R.. **Buffer-Aided Relaying With Adaptive Link Selection-Fixed and Mixed Rate Transmission**. IEEE Transactions on Information Theory, 59(5):2816-2840, May 2013.
- [50] IKHLEF, A.; JUNSU, K.; SCHOBBER, R.. **Mimicking Full-Duplex Relaying Using Half-Duplex Relays With Buffers**. IEEE Transactions on Vehicular Technology, 61(7):3025-3037, Sept. 2012.

- [51] NOMIKOS, N. ET AL., **Joint relay-pair selection for buffer-aided successive opportunistic relaying**. Wiley-Blackwell Transactions on Emerging Telecommunications Technologies, 25(8): 823-834, Aug. 2014.
- [52] NOMIKOS, N.; MAKRIS, P.; VOUYIOUKAS, D.; SKOUTAS, D. N.; SKIANNIS, C.. **Distributed joint relay-pair selection for buffer-aided successive opportunistic relaying**. In: 2013 IEEE 18TH INTERNATIONAL WORKSHOP ON COMPUTER AIDED MODELING AND DESIGN OF COMMUNICATION LINKS AND NETWORKS (CAMAD), Berlin, 2013, pp. 185-189.
- [53] NOMIKOS, N.; CHARALAMBOUS, T.; KRIKIDIS, I.; SKOUTAS, D. N.; VOUYIOUKAS, D.; JOHANSSON, M.. **Buffer-aided successive opportunistic relaying with inter-relay interference cancellation**. In: 2013 IEEE 24TH ANNUAL INTERNATIONAL SYMPOSIUM ON PERSONAL, INDOOR, AND MOBILE RADIO COMMUNICATIONS (PIMRC), London, 2013, pp. 1316-1320.
- [54] NOMIKOS, N.; CHARALAMBOUS, T.; KRIKIDIS, I. ; SKOUTAS, D. N.; VOUYIOUKAS, D.; JOHANSSON, M.. **A Buffer-Aided Successive Opportunistic Relay Selection Scheme With Power Adaptation and Inter-Relay Interference Cancellation for Cooperative Diversity Systems**. IEEE Transactions on Communications, 63(5):1623–1634, May 2015.
- [55] ZLATANOV, N.; SCHOBER, R.. **Buffer-Aided Half-Duplex Relaying Can Outperform Ideal Full-Duplex Relaying**. IEEE Communications Letters, 17(3):479-482, March 2013.
- [56] NOMIKOS, N.; CHARALAMBOUS, T.; KRIKIDIS, I.; VOUYIOUKAS, D.; JOHANSSON, M.. **Hybrid cooperation through full-duplex opportunistic relaying and max-link relay selection with transmit power adaptation**. In: 2014 IEEE INTERNATIONAL CONFERENCE ON COMMUNICATIONS (ICC), Sydney, NSW, 2014, pp. 5706-5711.
- [57] ZHANG, Q.; JIA, J.; ZHANG, J.. **Cooperative relay to improve diversity in cognitive radio networks**. IEEE Communications Magazine, 47(2):111-117, Feb. 2009.
- [58] ZHANG, X.; YAN, Z.; GAO, Y.; WANG, W.. **On the Study of Outage Performance for Cognitive Relay Networks (CRN) with the Nth Best-Relay Selection in Rayleigh-fading Channels**. IEEE Wireless Communications Letters, 2(1):110-113, Feb. 2013.

- [59] BANG, J.; LEE, J.; KIM, S.; HONG, D.. **An Efficient Relay Selection Strategy for Random Cognitive Relay Networks**. IEEE Transactions on Wireless Communications, 14(3):1555-1566, March 2015.
- [60] DARABI, M.; MAHAM, B.; ZHOU, X.; SAAD, W.. **Buffer-aided relay selection with interference cancellation and secondary power minimization for cognitive radio networks**. In: 2014 IEEE INTERNATIONAL SYMPOSIUM ON DYNAMIC SPECTRUM ACCESS NETWORKS (DYSPAN), McLean, VA, 2014, pp. 137-140.
- [61] CHEN, G.; TIAN, Z.; GONG, Y.; CHAMBERS, J.. **Decode-and-Forward Buffer-Aided Relay Selection in Cognitive Relay Networks**. IEEE Transactions on Vehicular Technology, 63(9): 4723-4728, Nov. 2014.
- [62] KRIKIDIS, I.; THOMPSON, J. S.; MCLAUGHLIN, S.. **Relay selection for secure cooperative networks with jamming**. IEEE Transactions on Wireless Communications, 8(10):5003-5011, Oct. 2009.
- [63] BASSILY, R.; ULUKUS, S.. **Deaf Cooperation and Relay Selection Strategies for Secure Communication in Multiple Relay Networks**. IEEE Transactions on Signal Processing, 61(6): 1544-1554, March 2013.
- [64] ZOU, Y.; WANG, X.; SHEN, W.. **Optimal Relay Selection for Physical-Layer Security in Cooperative Wireless Networks**. IEEE Journal on Selected Areas in Communications, 31(10):2099-2111, Oct. 2013.
- [65] CHEN, G.; DWYER, V.; KRIKIDIS, I.; THOMPSON, J. S.; MCLAUGHLIN, S.; CHAMBERS, J.. **Comment on "Relay Selection for Secure Cooperative Networks with Jamming"**. IEEE Transactions on Wireless Communications, 11(6):2351-2351, June 2012.
- [66] CHEN, G. ; TIAN, Z.; GONG, Y.; CHEN, Z.; CHAMBERS, J. A.. **Max-Ratio Relay Selection in Secure Buffer-Aided Cooperative Wireless Networks**. IEEE Transactions on Information Forensics and Security, 9(4):719-729, April 2014.
- [67] KIM, S. M.; BENGTTSSON, M.. **Virtual full-duplex buffer-aided relaying in the presence of inter-relay interference**. IEEE Transactions on Wireless Communications, 15(4): 2966-2980, April 2016.
- [68] CHARALAMBOUS, T.; KIM, S. M.; NOMIKOS, N.; BENGTTSSON, M.; JOHANSSON, M.. **Relay-pair selection in buffer-aided successive opportunistic relaying using a multi-antenna source**. Ad Hoc Networks, 84(1): 29-41, March 2019.

- [69] GU, J.; DE LAMARE, R. C.; HUEMER, M.. **Buffer-Aided Physical-Layer Network Coding Techniques for Cooperative Networks**. [Online]. Available at: http://delamare.cetuc.puc-rio.br/ba_plnc_arxiv.pdf
- [70] ZHANG, S.; LIEW, S. C.; LAM, P. P. **Hot topic: Physical-layer network coding**. In: PROC. ANNUAL INTERNATIONAL CONFERENCE ON MOBILE COMPUTING AND NETWORKING (MOBICOM 2006), LA, CA, USA, Sept. 2006.
- [71] SANNA, M.; IZQUIERDO, E.. **A Survey of Linear Network Coding and Network Error Correction Code Constructions and Algorithms**. International Journal of Digital Multimedia Broadcasting, vol. 2011, 2011.
- [72] HE, J.; LIEW, S.. **Building Blocks of Physical-Layer Network Coding**. IEEE Transactions on Wireless Communications, 14(5):2711-2728, May 2015.
- [73] UCHOA, A. G. D.; HEALY, C.; DE LAMARE, R. C.; SOUZA, R. D.. **Design of LDPC Codes Based on Progressive Edge Growth Techniques for Block Fading Channels**. IEEE Communications Letters, 15(11):1221-1223, Nov. 2011.
- [74] YANG, L.; YANG, T.; XIE, Y.; YUAN, J.; AN, J.. **Linear Physical-Layer Network Coding and Information Combining for the K -User Fading Multiple-Access Relay Network**. IEEE Transactions on Wireless Communications, 15(8):5637-5650, Aug. 2016.
- [75] NOKLEBY, M.; AZHANG, B.. **Cooperative Compute-and-Forward**. IEEE Transactions on Wireless Communications, 15(1):14-27, Jan. 2016.
- [76] ZHANG, H.; ZHENG, L.; CAI, L.. **Design and Analysis of Heterogeneous Physical Layer Network Coding**. IEEE Transactions on Wireless Communications, 15(4):2484-2497, April 2016.
- [77] HEALY, C. T.; DE LAMARE, R. C.. **Design of LDPC Codes Based on Multipath EMD Strategies for Progressive Edge Growth**. IEEE Transactions on Communications, 64(8):3208-3219, Aug. 2016.
- [78] BURR, A. ; FANG, D.. **Linear physical layer network coding for multihop wireless networks**. In: 2014 22ND EUROPEAN SIGNAL PROCESSING CONFERENCE (EUSIPCO), Lisbon, 2014, pp. 1153-1157.
- [79] BURR, A.; FANG, D.. **Linear physical-layer network coding for 5G radio access networks**. In: 1ST INTERNATIONAL CONFERENCE ON 5G FOR UBIQUITOUS CONNECTIVITY, Akaslompolo, 2014, pp. 116-121.

- [80] AHLWEDE, R.; CAI N.; LI S. R.; YEUNG R. W.. **Network information flow**. IEEE Transactions on Information Theory, 46(4):1204-1216, July 2000.
- [81] LI, S. R.; SUN, Q. T.; SHAO, Z.. **Linear Network Coding: Theory and Algorithms**. In: PROCEEDINGS OF THE IEEE, 99(3):372-387, March 2011.
- [82] KRIKIDIS, I.. **Relay Selection for Two-Way Relay Channels With MABC DF: A Diversity Perspective**. IEEE Transactions on Vehicular Technology, 59(9):4620-4628, Nov. 2010.
- [83] XIA, X.; ZHANG, D.; XU, K.; XU, Y.. **Interference-Limited Two-Way DF Relaying: Symbol-Error-Rate Analysis and Comparison**. IEEE Transactions on Vehicular Technology, 63(7):3474-3480, Sept. 2014.
- [84] ZHANG, Z.; MA, Z. ; XIAO, M.; KARAGIANNIDIS, G. K.; DING, Z.; FAN, P.. **Two-Timeslot Two-Way Full-Duplex Relaying for 5G Wireless Communication Networks**. IEEE Transactions on Communications, 64(7):2873-2887, July 2016.
- [85] LIU, H.; POPOVSKI, P.; CARVALHO, E. D.; ZHAO, Y.. **Sum-Rate Optimization in a Two-Way Relay Network with Buffering**. IEEE Communications Letters, 17(1):95-98, Jan. 2013.
- [86] ZHANG S.; LIEW S. C.. **Applying Physical-layer Network Coding in Wireless Networks**. Eurasip Journal of Wireless Communications and Networking, 2010.
- [87] AHADORMEY, R. K.; ANOKYE, P.; JO, H.; LEE, K.. **Performance Analysis of Two-Way Relaying in Cooperative Power Line Communications**. IEEE Access, 7: 97264-97280, 2019.
- [88] ENGEL, F.; ABRÃO, T.; HANZO, L.. **Relay selection methods for maximizing the lifetime of wireless sensor networks**. In: 2013 IEEE WIRELESS COMMUNICATIONS AND NETWORKING CONFERENCE (WCNC), Shanghai, 2013, pp. 2339-2344.
- [89] CHEN, Z.; LIU, H.; WANG, W.. **A Novel Decoding-and-Forward Scheme with Joint Modulation for Two-Way Relay Channel**. IEEE Communications Letters, 14(12):1149-1151, Dec. 2010.
- [90] DO, T. P.; WANG, J. S.; SONG, I.; KIM, Y. H.. **Joint Relay Selection and Power Allocation for Two-Way Relaying with Physical Layer Network Coding**. IEEE Communications Letters, 17(2):301-304, Feb. 2013.

- [91] ANYUGU FRANCIS LIN, B. , YE, X.; HAO, S.. **Adaptive protocol for full-duplex two-way systems with the buffer-aided relaying**. IET Communications, 13(1):54-58, 4 1 2019.
- [92] GUNDUZ, D.; YENER, A.; GOLDSMITH, A.; POOR, H. V.. **The Multiway Relay Channel**. IEEE Transactions on Information Theory, 59(1):51-63, Jan. 2013.
- [93] QUEK, T. Q. S. ; PENG, M.; SIMEONE, O.; YU, W.; EDS. **Cloud Radio Access Networks: Principles, Technologies, and Applications**. Cambridge University Press. April 2017.
- [94] JAMALI, V.; ZLATANOV, N.; SCHOBBER, R.. **Bidirectional Buffer-Aided Relay Networks With Fixed Rate Transmission - Part I: Delay-Unconstrained Case**. IEEE Transactions on Wireless Communications, 14(3):1323-1338, March 2015.
- [95] JAMALI, V.; ZLATANOV, N.; SCHOBBER, R.. **Bidirectional Buffer-Aided Relay Networks With Fixed Rate Transmission - Part II: Delay-Constrained Case**. IEEE Transactions on Wireless Communications, 14(3):1339-1355, March 2015.
- [96] WEI, C.; YIN, Z.; YANG, W.; CAI, Y.. **Enhancing Physical Layer Security of DF Buffer-Aided Relay Networks With Small Buffer Sizes**. IEEE Access, 7: 128684-128693, 2019.
- [97] SHABBIR, G. ET AL.. **Buffer-Aided Successive Relay Selection Scheme for Energy Harvesting IoT Networks**. IEEE Access, 7: 36246-36258, 2019.
- [98] ATTARKASHANI, A.; HAMOUDA, W.; MOUALEU, J. M.; HAGHIGHAT, J.. **Performance Analysis of Turbo Codes and Distributed Turbo Codes in Buffer-Aided Relay Systems**. IEEE Transactions on Communications, 67(7):4620-4633, July 2019.
- [99] LIU, G.; LI, L.; CIMINI, L. J.; SHEN, C.. **Extending Proportional Fair Scheduling to Buffer-Aided Relay Access Networks**. IEEE Transactions on Vehicular Technology, 68(1):1041-1044, Jan. 2019.
- [100] WEI, C.; YANG, W.; CAI, Y.; TANG, X.; KANG, G.. **Secrecy Outage Performance for DF Buffer-Aided Relaying Networks With a Multi-Antenna Destination**. IEEE Access, 7: 41349-41364, 2019.
- [101] WOLNIANSKY P. W.; FOSCHINI G. J.; GOLDEN G. D.; VALENZUELA R. A. **V-BLAST: an architecture for realizing very high data rates over**

- the rich-scattering wireless channel.** In: 1998 URSI INTERNATIONAL SYMPOSIUM ON SIGNALS, SYSTEMS, AND ELECTRONICS. Conference Proceedings (Cat. No.98EX167), Pisa, Italy, 1998, pp. 295-300.
- [102] TELATAR, I. E.. **Capacity of multi-antenna gaussian channels.** AT&T Bell Laboratories, Internal Tech. Memo, June 1995.
- [103] ALAMOUTI, S. M.. **A simple transmit diversity technique for wireless communications.** IEEE Journal on Selected Areas in Communications, 16(8):1451-1458, Oct. 1998.
- [104] COVER, T. M.; THOMAS, J. A.. **Elements of Information Theory.** John Wiley and Sons, 2nd edition, Hoboken, New Jersey, USA, 2006.
- [105] KÜHN, V.. **Wireless Communications over MIMO Channels: Applications to CDMA and Multiple Antenna Systems.** John Wiley and Sons, 1st edition, Chichester, West Sussex, England, 2006.
- [106] BROWN T.; KYRITSI P.; DE CARVALHO E.. **Practical Guide to MIMO Radio Channel: with MATLAB Examples.** John Wiley and Sons, 1st edition, 2012.
- [107] TSE, D.; VISWANATH, P.. **Fundamentals of Wireless Communications.** Cambridge University Press, 1st edition, Cambridge, 2005.
- [108] LI P.. **Low-Complexity Iterative Detection Algorithms for Multi-Antenna Systems.** PhD Thesis. University of York. York. UK. Dec. 2011. [Online]. Available at: <http://delamare.cetuc.puc-rio.br/Peng Li PhD thesis.pdf>
- [109] SMITH, D. R.. **Digital Transmission Systems.** Cambridge University Press, 3rd edition, Springer, 2004.
- [110] DE LAMARE, R. C.. **Massive MIMO systems: Signal processing challenges and future trends.** URSI Radio Science Bulletin, 2013(347): 8-20, Dec. 2013.
- [111] RUSEK, F. ET AL. **Scaling Up MIMO: Opportunities and Challenges with Very Large Arrays.** IEEE Signal Processing Magazine, 30(1):40-60, Jan. 2013.
- [112] JOHAM, M.; UTSCHICK, W.; NOSSEK J. A.. **Linear transmit processing in MIMO communications systems.** IEEE Transactions on Signal Processing, 53(8):2700-2712, Aug. 2005.

- [113] SPENCER, Q. H.; SWINDLEHURST, A. L.; HAARDT, M.. **Zero-forcing methods for downlink spatial multiplexing in multiuser MIMO channels**. IEEE Transactions on Signal Processing, 52(2):461-471, Feb. 2004.
- [114] CAIRE, G.; SHAMAI, S.. **On the achievable throughput of a multi-antenna Gaussian broadcast channel**. IEEE Transactions on Information Theory, 49(7):1691-1706, July 2003.
- [115] WINDPASSINGER, C.; LAMPE, L.; FISCHER, R. F. H.; HEHN, T.. **A performance study of MIMO detectors**. IEEE Transactions on Wireless Communications, 5(8):2004-2008, Aug. 2006.
- [116] PEEL, C. B.; HOCHWALD, B. M.; SWINDLEHURST, A. L.. **A vector perturbation technique for near capacity multiantenna multiuser communication - part I: channel inversion and regularization**. IEEE Transactions on Communications, 53(1):195-202, Jan. 2005.
- [117] MARZETTA, T. L.. **Noncooperative Cellular Wireless with Unlimited Numbers of Base Station Antennas**. IEEE Transactions on Wireless Communications, 9(11):3590-3600, Nov. 2010.
- [118] PROAKIS, J. G.; SALEHI, M.. **Digital Communications**. McGraw-Hill, 5th edition, New York, EUA, 2008.
- [119] CLERCKX, B.; OESTGES, C.. **MIMO Wireless Networks: Channels, Techniques and Standards for Multi-Antenna, Multi-User and Multi-Cell Systems**. Cambridge University Press, 2nd edition, Waltham, MA, USA, 2013.
- [120] TREES, H. L. V.. **Optimum Array Processing: Part IV of Detection, Estimation, and Modulation Theory**, John Wiley & Sons, 1st edition, Nova Jersey, USA, 2002.
- [121] DINIZ, P. S. R.. **Adaptive Filtering: Algorithms and Practical Implementation**, Springer US, 4th edition, New York, USA.
- [122] LI, P.; DE LAMARE, R. C.; FA, R.. **Multiple Feedback Successive Interference Cancellation Detection for Multiuser MIMO Systems**. IEEE Transactions on Wireless Communications, 10(8):2434-2439, Aug. 2011.
- [123] CHOI, J. H.; YU, H.; LEE, Y. H.. **Adaptive MIMO decision feedback equalization for receivers with time-varying channels**. IEEE Transactions on Signal Processing, 53(11):4295-4303, Nov. 2005.

- [124] VARANASI, M. K.. **Decision feedback multiuser detection: A systematic approach**. IEEE Transactions on Information Theory, 45(1): 219-240, Jan. 1999.
- [125] WOODWARD, G.; RATASUK, R.; HONIG, M. L.; RAPAJIC P. B.. **Minimum mean-squared error multiuser decision-feedback detectors for DS-CDMA**. IEEE Transactions on Communications, 50(12): 2104-2112, Dec. 2002.
- [126] DE LAMARE, R.C.; SAMPAIO-NETO, R.. **Adaptive MBER decision feedback multiuser receivers in frequency selective fading channels**. IEEE Communications Letters, 7(2):73-75, Feb. 2003.
- [127] DE LAMARE, R.C.; SAMPAIO-NETO, R.. **Minimum Mean-Squared Error Iterative Successive Parallel Arbitrated Decision Feedback Detectors for DS-CDMA Systems**. IEEE Transactions on Communications, 56(5):778-789, May 2008.
- [128] LI, P.; DE LAMARE, R. C.. **Adaptive Decision-Feedback Detection With Constellation Constraints for MIMO Systems**. IEEE Transactions on Vehicular Technology, 61(2):853-859, Feb. 2012.
- [129] REUTER, M.; ALLEN, J.C.; ZEIDLER, J. R.; NORTH, R. C.. **Mitigating error propagation effects in a decision feedback equalizer**. IEEE Transactions on Communications, 49(11):2028-2041, Nov. 2001.
- [130] DE LAMARE, R. C.; SAMPAIO-NETO, R.; HJORUNGNES, A.. **Joint iterative interference cancellation and parameter estimation for cdma systems**. IEEE Communications Letters, 11(12):916-918, Dec. 2007.
- [131] JOUDEH ,H.; CLERCKX, B.. **Sum-Rate Maximization for Linearly Precoded Downlink Multiuser MISO Systems With Partial CSIT: A Rate-Splitting Approach**. IEEE Transactions on Communications, 64(11):4847-4861, Nov. 2016.
- [132] LU, X.; DE LAMARE, R. C.. **Buffer-Aided Relay Selection for Physical-Layer Security in Wireless Networks**. In: WSA 2015; 19TH INTERNATIONAL ITG WORKSHOP ON SMART ANTENNAS, Ilmenau, Germany, 2015, pp. 1-5.
- [133] SHANKAR, R.; KUMAR, I.; KUMARI, A.; PANDEY, K. N.; MISHRA, R. K.. **Pairwise error probability analysis and optimal power allocation for selective decode-forward protocol over Nakagami-m fading channels**.

- In: 2017 INTERNATIONAL CONFERENCE ON ALGORITHMS, METHODOLOGY, MODELS AND APPLICATIONS IN EMERGING TECHNOLOGIES (ICAMMAET), Chennai, 2017, pp. 1-6.
- [134] PENG, T.; DE LAMARE, R. C.. **Adaptive Buffer-Aided Distributed Space-Time Coding for Cooperative Wireless Networks**. IEEE Transactions on Communications, 64(5):1888-1900, May 2016.
- [135] HOLTER, B.. **On the Capacity of the MIMO Channel - A Tutorial Introduction**. [Online]. Available at: <http://citeseerx.ist.psu.edu/viewdoc/download?doi=10.1.1.503.3015&rep=rep1&type=pdf>.
- [136] TIAN, Z.; CHEN, G.; GONG, Y.; CHEN, Z. ; CHAMBERS, J. A.. **Buffer-Aided Max-Link Relay Selection in Amplify-and-Forward Cooperative Networks**. IEEE Transactions on Vehicular Technology, 64(2):553-565, Feb. 2015.
- [137] DUARTE, F. L.; DE LAMARE, R. C.; **Cloud-Aided Multi-Way Multiple-Antenna Relaying with Best-User Link Selection and Joint ML Detection**. In: 24TH INTERNATIONAL ITG WORKSHOP ON SMART ANTENNAS (WSA 2020), Hamburg, Germany, 2020.
- [138] PATEL, C. S.; STUBER, G. L.. **Channel Estimation for Amplify and Forward Relay Based Cooperation Diversity Systems**. IEEE Transactions on Wireless Communications, 6(6):2348-2356, June 2007.
- [139] KOYUNCU, E.. **Power-Efficient Deployment of UAVs as Relays**. In: 2018 IEEE 19TH INTERNATIONAL WORKSHOP ON SIGNAL PROCESSING ADVANCES IN WIRELESS COMMUNICATIONS (SPAWC), Kalamata, 2018, pp. 1-5.
- [140] ZENG, Y.; ZHANG, R.; LIM, T. J.. **Wireless communications with unmanned aerial vehicles: opportunities and challenges**. IEEE Communications Magazine, 54(5): 36-42, May 2016.
- [141] TUNA, G.; NEFZI, B.; CONTE, G.. **Unmanned aerial vehicle-aided communications system for disaster recovery**. Journal of Network and Computer Applications., 41(1): 27-36, May 2014.
- [142] BOR-YALINIZ, I.; YANIKOMEROGLU, H.. **The New Frontier in RAN Heterogeneity: Multi-Tier Drone-Cells**. IEEE Communications Magazine, 54(11):48-55, Nov. 2016.

- [143] **MIMO Detection Algorithms**, Nov. 2017. [Online]. Available at:
<https://web.stanford.edu/class/ee359/pdfs/mimo-detection-algorithms.pdf>

A

Proof of $\mathcal{D}'_{\min}^{MMD} \geq \mathcal{D}'_{\min}^{QN}$

The selected matrix by the MMD criterion, that maximizes the minimum distances \mathcal{D} , is given by

$$\mathbf{H}^{MMD} = \arg \max_{\mathbf{H}} \min (\mathcal{D}_j, \mathcal{D}_{j,k}, \dots, \mathcal{D}_{1,\dots,M_S}) \quad (\text{A-1})$$

$$j, k = 1, \dots, M_S, j \neq k,$$

where $\mathbf{H} \in \{\mathbf{H}_{S,R_1}, \dots, \mathbf{H}_{S,R_N}, \mathbf{H}_{R_1,D}, \dots, \mathbf{H}_{R_N,D}, \mathbf{H}_{S,D}\}$ and $H_{i,j} \in \mathbb{C}(0, \sigma^2)$.

As $\mathcal{D} = \frac{E}{M_S} \mathcal{D}'$, where $\mathcal{D}' = \|\mathbf{H}^u(\mathbf{x}_n - \mathbf{x}_l)\|^2$, for $\mathcal{D}_{SR_i}^u$ and $\mathcal{D}_{R_i,D}^u$, or $\mathcal{D}' = 2\|\mathbf{H}^u(\mathbf{x}_n - \mathbf{x}_l)\|^2$, for \mathcal{D}_{SD} , we have

$$\mathbf{H}^{MMD} = \arg \max_{\mathbf{H}} \min (\mathcal{D}'_j, \mathcal{D}'_{j,k}, \dots, \mathcal{D}'_{1,\dots,M_S})$$

$$j, k = 1, \dots, M_S, j \neq k,$$

where the PEP arguments \mathcal{D}' are given by

$$\mathcal{D}'_j = |d_{c_w}|^2 \sum_{i=1}^{M_S} |H_{i,j}^u|^2$$

$$w = 1, \dots, W, \quad (\text{A-2})$$

$$\mathcal{D}'_{j,k} = \sum_{i=1}^{M_S} \left| \pm d_{c_w} H_{i,j}^u \pm d_{c_h} H_{i,k}^u \right|^2$$

$$w, h = 1, \dots, W,$$

$$\mathcal{D}'_{1,\dots,M_S} = \sum_{i=1}^{M_S} \left| \pm d_{c_w} H_{i,1}^u \dots \pm d_{c_v} H_{i,M_S}^u \right|^2$$

$$w, v = 1, \dots, W.$$

So, the maximized minimum value of the PEP argument associated to \mathbf{H}^{MMD} is given by

$$\mathcal{D}'_{\min}{}^{MMD} = \min(\mathcal{D}'_j{}^{MMD}, \mathcal{D}'_{j,k}{}^{MMD}, \dots, \mathcal{D}'_{1,\dots,M_S}{}^{MMD}) \quad (\text{A-3})$$

$$j, k = 1, \dots, M_S, j \neq k.$$

However, the selected matrix by the QN criterion is given by

$$\mathbf{H}^{QN} = \arg \max_{\mathbf{H}} \sum_{j=1}^{M_S} \sum_{i=1}^{M_R} |H_{i,j}|^2 \quad (\text{A-4})$$

$$= \arg \max_{\mathbf{H}} \left(\sum_{i=1}^{M_R} |H_{i,1}|^2 + \dots + \sum_{i=1}^{M_R} |H_{i,M_S}|^2 \right),$$

where $\mathbf{H} \in \{\mathbf{H}_{S,R_1}, \dots, \mathbf{H}_{S,R_N}, \mathbf{H}_{R_1,D}, \dots, \mathbf{H}_{R_N,D}\}$ and $H_{i,j} \in \mathbb{C}(0, \sigma^2)$.

The minimum value of the PEP argument associated to \mathbf{H}^{QN} is given by

$$\mathcal{D}'_{\min}{}^{QN} = \min(\mathcal{D}'_j{}^{QN}, \mathcal{D}'_{j,k}{}^{QN}, \dots, \mathcal{D}'_{1,\dots,M_S}{}^{QN}) \quad (\text{A-5})$$

$$j, k = 1, \dots, M_S, j \neq k.$$

If the sum of the powers of the coefficients of one of the columns (or the combination of 2 or more columns by addition or subtraction) of a selected submatrix and/or matrix \mathbf{H}^{QN} is very small or tends to zero, we have

$$\mathcal{D}'_j{}^{QN} \rightarrow 0, \mathcal{D}'_{j,k}{}^{QN} \rightarrow 0, \dots, \text{or } \mathcal{D}'_{1,\dots,M_S}{}^{QN} \rightarrow 0, \quad (\text{A-6})$$

and, consequently: $\mathcal{D}'_{\min}{}^{QN} \rightarrow 0$.

As MMD maximizes \mathcal{D}'_{\min} , the submatrix and/or matrix selected by QN will be different from the selected by MMD:

$$\mathbf{H}^{QN} \neq \mathbf{H}^{MMD} \text{ and } \mathcal{D}'_{\min}{}^{QN} \neq \mathcal{D}'_{\min}{}^{MMD}.$$

We have seen that the MMD criterion computes all the values of \mathcal{D}' and stores its minimum value (\mathcal{D}'_{\min}), for each submatrix \mathbf{H}^u . Then, this criterion selects the matrix \mathbf{H} (\mathbf{H}^{MMD}) that is associated to the maximum \mathcal{D}'_{\min} ($\mathcal{D}'_{\min}{}^{MMD}$) and the associated relay. As the goal of this criterion is to maximize the argument of the PEP in its worst case (\mathcal{D}'_{\min}), another criterion such as QN can not outperform MMD but only equalize its performance, resulting in the same \mathcal{D}'_{\min} , if the matrix selected by QN (\mathbf{H}^{QN}) is equal

to \mathbf{H}^{MMD} . Therefore, if we have $\mathbf{H}^{QN} \neq \mathbf{H}^{MMD}$, this implies that the \mathcal{D}'_{\min} associated to \mathbf{H}^{MMD} ($\mathcal{D}'_{\min}{}^{MMD}$) is greater than the \mathcal{D}'_{\min} associated to \mathbf{H}^{QN} ($\mathcal{D}'_{\min}{}^{QN}$). As there are cases where $\mathbf{H}^{QN} \neq \mathbf{H}^{MMD}$, we may conclude that:

$$\mathcal{D}'_{\min}{}^{MMD} \geq \mathcal{D}'_{\min}{}^{QN}. \quad (\text{A-7})$$

B

Proof of the minimization of the PEP and of the error in the ML receiver - MMD

We have seen in Chapter 5, Section II, that the ML detector is the optimal detector from the point of view of minimizing the probability of error (assuming equiprobable \mathbf{x}) and the solution is given by

$$\begin{aligned}\hat{\mathbf{x}}[i] &= \arg \min_{\mathbf{x}'[i]} \left(\left\| \mathbf{y}[i] - \sqrt{\frac{E_s}{M}} \mathbf{H} \mathbf{x}'[i] \right\|^2 \right), \\ &= \arg \min_{\mathbf{x}'[i]} \left(\left\| \sqrt{\frac{E_s}{M}} \mathbf{H} \mathbf{x}[i] + \mathbf{n}[i] - \sqrt{\frac{E_s}{M}} \mathbf{H} \mathbf{x}'[i] \right\|^2 \right).\end{aligned}\tag{B-1}$$

We have seen in Chapter 5, Section IV, that the PEP worst case is given by

$$\mathbf{P}(\mathbf{x}_n \rightarrow \mathbf{x}_l | \mathbf{H}) = Q \left(\sqrt{\frac{E_s}{2N_0 M} \mathcal{D}'_{min}} \right).\tag{B-2}$$

where $\mathcal{D}' = \|\mathbf{H}(\mathbf{x}_n - \mathbf{x}_l)\|^2$, in MA mode, and $\mathcal{D}' = \frac{1}{2} \|\mathbf{H}(\mathbf{x}_n - \mathbf{x}_l)\|^2$, in BC mode, and $l \neq n$.

The proposed MWC-Best-User-Link, using the MMD relay selection criterion, selects the channel matrix \mathbf{H}^{MMD} , minimizing the PEP worst case, as shown by

$$\begin{aligned}\mathbf{H}^{MMD} &= \arg \min_{\mathbf{H}} \mathbf{P}(\mathbf{x}_n \rightarrow \mathbf{x}_l | \mathbf{H}) \\ &= \arg \min_{\mathbf{H}} Q \left(\sqrt{\frac{E_s}{2N_0 M} \mathcal{D}'_{min}} \right) \\ &= \arg \max_{\mathbf{H}} \left(\sqrt{\frac{E_s}{2N_0 M} \mathcal{D}'_{min}} \right) \\ &= \arg \max_{\mathbf{H}} \mathcal{D}'_{min} \\ &= \arg \max_{\mathbf{H}} \min \|\mathbf{H}(\mathbf{x}_n - \mathbf{x}_l)\|^2\end{aligned}\tag{B-3}$$

Consequently, the MMD relay selection criterion, by maximizing the minimum Euclidian distance between different vectors of transmitted symbols, minimizes

the error in the ML receiver, as shown by

$$\begin{aligned}
 \mathbf{H}^{MMD} &= \arg \max_{\mathbf{H}} \min \left(\left\| \sqrt{\frac{E_s}{M}} \mathbf{H} \mathbf{x}_n + \mathbf{n}[i] - \sqrt{\frac{E_s}{M}} \mathbf{H} \mathbf{x}_l \right\|^2 \right) \\
 &= \arg \max_{\mathbf{H}} \min \left(\frac{E_s}{M} \|\mathbf{H} \mathbf{x}_n - \mathbf{H} \mathbf{x}_l\|^2 \right) \\
 &= \arg \max_{\mathbf{H}} \min \|\mathbf{H}(\mathbf{x}_n - \mathbf{x}_l)\|^2
 \end{aligned} \tag{B-4}$$

This reasoning may be applied also for each of the square sub-matrices \mathbf{H}^u in a non square matrix \mathbf{H} (formed by multiple square sub-matrices). Thus, it is proven that the MMD relay selection criterion minimizes the error in the ML receiver, in the proposed MWC-Best-User-Link protocol.

C

Proof of the Sum-Rate Maximization - CNB

We have shown in Chapter 5, Section IV, that the sum-rate of a cooperative system in each time slot for a given channel matrix \mathbf{H} is given by

$$R = \frac{1}{2} \log_2 \det (\mathbf{H}(\mathbf{Q}/N_0)\mathbf{H}^H + \mathbf{I}). \quad (\text{C-1})$$

where $\mathbf{Q} = E[\mathbf{x}(\mathbf{x})^H] = \mathbf{I} \frac{E_s}{M_s}$, in the MA mode, and $\mathbf{Q} = \mathbf{I} \frac{E_s}{2M_s}$, in BC mode. By considering a square channel matrix \mathbf{H} , the proposed MWC-Best-User-Link, using the CNB relay selection criterion, selects the channel matrix \mathbf{H}^{CNB} , maximizing the sum-rate, as shown by

$$\begin{aligned} \mathbf{H}^{CNB} &= \arg \max_{\mathbf{H}} \frac{1}{2} \log_2 \det (\mathbf{H}(\mathbf{Q}/N_0)\mathbf{H}^H + \mathbf{I}) \\ &= \arg \max_{\mathbf{H}} \det (\mathbf{H}(\mathbf{Q}/N_0)\mathbf{H}^H + \mathbf{I}) \\ &= \arg \max_{\mathbf{H}} \det (\mathbf{H}\mathbf{H}^H + \mathbf{I}) \\ &= \arg \max_{\mathbf{H}} \det (\mathbf{H}\mathbf{H}^H) \\ &= \arg \max_{\mathbf{H}} \det (\mathbf{H}) \det (\mathbf{H}^H) \\ &= \arg \max_{\mathbf{H}} \det (\mathbf{H}) (\det (\mathbf{H}))' \\ &= \arg \max_{\mathbf{H}} |\det (\mathbf{H})|^2 \\ &= \arg \max_{\mathbf{H}} |\det (\mathbf{H})|. \end{aligned} \quad (\text{C-2})$$

This reasoning may be applied also for each of the square sub-matrices \mathbf{H}^u in a non square matrix \mathbf{H} (formed by multiple square sub-matrices). Thus, it is proven that the CNB relay selection criterion maximizes the sum-rate in the proposed MWC-Best-User-Link protocol.

D

Proof of minimization of the error in the MMSE receiver - CNB

We have seen in Chapter 5, Section II, that in the linear MMSE receiver the estimate of the transmitted vector of symbols is given by

$$\begin{aligned}\tilde{\mathbf{x}}[i] &= \mathbf{W}_{\text{MMSE}}\mathbf{y}[i] \\ &= \left(\mathbf{H}^H\mathbf{H} + \frac{\sigma_n^2}{\sigma_x^2}\mathbf{I} \right)^{-1} \mathbf{H}^H\mathbf{y}[i].\end{aligned}\quad (\text{D-1})$$

Since $\mathbf{y}[i] = \mathbf{H}\mathbf{x}[i] + \mathbf{n}[i]$, from the above equation we can conclude that the performance of linear detection is directly related to the power of the MMSE effective noise [108] which is calculated as

$$E\left(\|\mathbf{n}_{\text{MMSE}}\|^2\right) = E\left(\left\|\left(\mathbf{H}^H\mathbf{H} + \frac{\sigma_n^2}{\sigma_x^2}\mathbf{I}\right)^{-1} \mathbf{H}^H\mathbf{n}[i]\right\|^2\right).\quad (\text{D-2})$$

The effects of the effective noise in MMSE can be minimized if the power of the coefficients of the pseudo inverse channel matrix $\mathbf{W}_{ZF} = (\mathbf{H}^H\mathbf{H})^{-1}\mathbf{H}^H$ are small. Note that \mathbf{W}_{ZF} corresponds to the equalization matrix in the Zero Forcing receiver.

We know that the relation between \mathbf{W}_{ZF} and its determinant ($\det(\mathbf{W}_{ZF})$) is given by

$$\begin{aligned}\mathbf{W}_{ZF} &= (1/\det(\mathbf{W}_{ZF}^{-1}))\text{Adj}\left(\mathbf{W}_{ZF}^{-1}\right) \\ &= \det(\mathbf{W}_{ZF})\text{Adj}\left(\mathbf{W}_{ZF}^{-1}\right).\end{aligned}\quad (\text{D-3})$$

By considering a square channel matrix \mathbf{H} , the proposed MWC-Best-User-Link, using the CNB relay selection criterion, selects the channel matrix \mathbf{H}^{CNB} , minimizing the effects of the effective noise in ZF and MMSE receivers,

as shown by

$$\begin{aligned}
\mathbf{H}^{CNB} &= \arg \min_{\mathbf{H}} \det(\mathbf{W}_{ZF}) \\
&= \arg \min_{\mathbf{H}} \det((\mathbf{H}^H \mathbf{H})^{-1} \mathbf{H}^H) \\
&= \arg \min_{\mathbf{H}} \left(\frac{\det(\mathbf{H}^H)}{\det(\mathbf{H}^H \mathbf{H})} \right) \\
&= \arg \min_{\mathbf{H}} \left(\frac{\det(\mathbf{H}^H)}{\det(\mathbf{H}^H) \det(\mathbf{H})} \right) \tag{D-4} \\
&= \arg \min_{\mathbf{H}} \left(\frac{1}{\det(\mathbf{H})} \right) \\
&= \arg \max_{\mathbf{H}} \det(\mathbf{H}) \\
&= \arg \max_{\mathbf{H}} |\det(\mathbf{H})|.
\end{aligned}$$

This reasoning may be applied also for each of the square sub-matrices \mathbf{H}^u in a non square matrix \mathbf{H} (formed by multiple square sub-matrices). Thus, it is proven that the CNB relay selection criterion minimizes the error in the Zero Forcing and, consequently, in the linear MMSE receiver, in the proposed MWC-Best-User-Link protocol.